A novel family of fatty acyl thioesterases from *Arabidopsis thaliana*

By: Christine Lowe

B.Sc. Honours, Carleton University, 2008.

A thesis submitted to the Faculty of Graduate Studies and Research in partial fulfillment of the requirements for the degree of

Master of Science

in

Biology

Carleton University

Ottawa ON, Canada

Your file Votre référence
ISBN: 978-0-494-79608-5
Our file Notre référence
ISBN: 978-0-494-79608-5

Abstract

Extracellular lipid based barriers, such as the cuticle, suberin, and sporopollenin, protect plants from the environment. Despite the importance of these barriers, many aspects of extracellular lipid biosynthesis remain uncharacterized. I have identified a four member family of thioesterases from *Arabidopsis thaliana* termed MODIFIERS OF EXTRACELLULAR LIPIDS (MEL1-4). The gene expression patterns of three members of this family, *MEL1*, *MEL2*, and *MEL4*, were found to correlate with the deposition of cuticle, suberin, and sporopollenin, respectively. Artificial microRNA silenced and over-expression lines were created to determine if MEL1 influences cuticle composition. The cuticular wax and cutin composition were analyzed, but no effect on the load or composition was apparent. This may be due to gene redundancy or insufficient silencing or over-expression of *MEL1*. It is also possible that the effects on extracellular compounds are not detectable using common methods. MEL1 was shown *in vitro* to hydrolyze palmitoyl-CoA (16:0) into a free fatty acid and CoA. Members of the MEL family were also shown in *E. coli* to have acyl-ACP thioesterase activity toward β-ketoacyl-ACP and non-oxygenated acyl-ACP substrates. These results confirm that MEL proteins possess fatty acyl thioesterase activity and likely fulfill a role in extracellular lipid biosynthesis. I discuss several potential roles for thioesterases in extracellular lipid biosynthesis, such as in termination of fatty acid synthesis in the plastid, synthesis of β-ketoacids leading to the production of methylketones and/or alkanes, production of long-chain or very-long-chain free fatty acids found in cutin and cuticular wax, respectively, and in regulation of extracellular lipid metabolism. The MEL enzymes are expected to fulfill one or more of these roles.

Acknowledgements

I would like to thank my supervisor, Dr. Owen Rowland, for providing me with the opportunity to undertake this research project, and for his support and supervision during the last two years. I would also like to thank my M.Sc. graduate committee members, Dr. John Vierula and Dr. Gopal Subramaniam of Carleton University, for their suggestions through out the course of this work. I would like to express my appreciation to Dr. Ashkan Golshani for the use of his experimental equipment. I am also thankful for the support I have received from the members of the Rowland and Hepworth labs, and for their input and ideas that have proved invaluable throughout the course of this work. Finally, I am extremely grateful for the support I have received from my friends and family.

Statement of Contribution

I would like to acknowledge the work of Dr. Owen Rowland, Swara Narayanan, Carlos Canez, Sollapura Vishwanath, and Xiaoxue Wen for their contributions to this thesis. I acknowledge Swara Narayanan for the creation of the promoter:GUS constructs for MEL1, MEL2, MEL3, and MEL4 and the transformation of *Arabidopsis* with these constructs, under my supervision. I also acknowledge Swara Narayanan, Carlos Canez, and Sollapura Vishwanath for analyzing and photographing the promoter:GUS transgenic plants. Dr. Owen Rowland and Xiaoxue Wen also contributed to this thesis by generating the constructs for the expression of MEL2 and MEL3 in *E. coli.* I would also like to express my appreciation to Dr. Frédéric Domergue (Centre National de la Recherché Scientifique, Laboratoire de Biogenèse Membranaire, Université Victor Ségalen Bordeaux, Bordeaux, France), for analyzing the cutin monomer composition, by GC-MS, of stem and leaf samples that I provided to him.

Table of Contents

List of Tables

List of Figures

List of appendices

List of Abbreviations

1-OH: primary alcohol

2-OH: secondary alcohol

2OH: 2-hydroxy fatty acid

4HBT: 4-hydroxybenzoyl-CoA thioesterase

ACP: acyl carrier protein

ALD: aldehyde

ALK: alkane

amiRNA: artificial microRNA

ATT1: aberrant induction of type three genes

BSTFA+TMCS: bis(trimethylsilyl)trifluoroacetamide:trimethylchlorosilane

CER: eceriferum

CoA: coenzyme A

Col-WT: Columbia-0 wild-type *Arabidopsis thaliana*

DCA: dicarboxylic acid

DEPC: diethylpyrocarbonate

diOH: 9,10 dihydroxy fatty acid

DTNB: 5,5'-dithiobis-(2-nitrobenzoic acid)

DW: dry weight

ER: endoplasmic reticulum

FAE: fatty acid elongase

FAR: fatty acyl-CoA reductase

FAS: fatty acid synthase

FAT: fatty acyl-ACP thioesterase

FFA: free fatty acid

FFA: free fatty acids

GAPC: glyceraldehyde – 3 – phosphate dehydrogenase

GC-FID: gas chromatography-flame ionization detector

GC-MS: gas chromatography-mass spectrophotometry

GPAT: glycerol-3-phosphate acyltransferase

GUS: glucuronidase

HNF: human nuclear factor

IPTG: isopropyl β-D-1-thiogalactopyranoside

KET: ketone

LACS: long-chain acyl-CoA synthetase

LCR: lacerata

Lf: rosette leaf

MAH: mid-chain alkane hydroxylase

MEL: modifier of extracellular lipids

MKS: methylketone synthase

MS: male sterility

OH: alcohol

PBS: phosphate buffered saline

PPAR: peroxisome proliferator-activated receptor

RT-PCR: reverse transcription PCR

Rt: roots

St: stem

TBS-T: TRIS buffered saline with tween

TNB: 5-thio-2-nitrobenzoate

VLCFA: very-long-chain fatty acids

wOH: ω-hydroxy fatty acid

WSD: wax synthase/diacylglycerol acyltransferase

Chapter 1: Introduction

1.1 Surface lipid barriers in plants

Plants have three major extracellular lipid barriers for protection against various biotic and abiotic stresses: (1) the cuticle, which coats aerial surfaces, (2) suberin, found associated with the cell wall of various external and internal tissue layers including the root endodermis and peridermis, and (3) sporopollenin, found in the outer wall of pollen. The cuticle functions to protect plants from stresses such as UV radiation and non-stomatal water loss (Krauss *et al.*, 1997; Riederer and Schreiber, 2001). The cuticle also functions to mediate plant-insect interactions and to inhibit infection by some pathogens (Kolattukudy, 1987; Jenks *et al*, 1994; Markstädter *et al.*, 2000). In addition, the cuticle influences plant development by preventing organs from fusing (Sieber, *et al.*, 2000). Suberin functions primarily to prevent uncontrolled water transport and to limit the uptake of solutes from the soil (Franke and Schreiber, 2007; Bernards, 2002). Sporopollenin makes up the protective exine layer that protects pollen grains from desiccation and makes them extremely resistant to degradation (Piffanelli *et al.*, 1998). While the synthesis of each of these polymers begins with the *de novo* synthesis of fatty acids in the plastid, specific modifications occur in the endoplasmic reticulum (ER). The various lipids are then secreted to the outside of the cell.

1.2 Cuticle

The cuticle is a highly hydrophobic barrier synthesized and secreted by the epidermal cells of vascular plants. The mature cuticle is composed of two distinct components: (1) a lipid-based cutin layer embedded with various waxes, and (2) an outer

layer composed primarily of wax (Figure 1). Cutin is a polyester matrix containing glycerol and esterified hydroxylated and dicarboxylic acids fatty acids of 16 or 18 carbons in length (Figure 2). Cutin also contains other minor components such as unsubstituted fatty acids and primary alcohols. This layer is highly resistant to mechanical damage and provides structure to the cuticle (Heredia, 2003). Cuticular wax is typically comprised of very-long-chain fatty acids (VLCFA) consisting of 20 to 32 carbons and a variety of derivatives including alkanes, primary and secondary alcohols, ketones, aldehydes, and wax esters (Figure 3) (Samuels, *et al.* 2008). The specific chemical make up is dependent on the organ and plant type. For example, while all of the above described compounds are found in *Arabidopsis* stem cuticle, the leaf cuticle lacks secondary alcohols and ketones (Jenks *et al.*, 1995). In addition to forming epicuticular wax crystals, waxes are also embedded within the cutin matrix.

The synthesis of all lipid polymers begins with the *de novo* biosynthesis of acyl-acyl carrier protein (ACP) chains within the plastid by the fatty acid synthase (FAS) complex. This process begins with a condensation reaction between acetyl-coenzyme A (CoA) and malonyl-ACP. Following this condensation, the fatty acyl chain undergoes two separate reduction reactions and a dehydration step, resulting in a fatty acyl chain that is two carbons longer. Subsequent rounds of C2 additions from malonyl-ACP yield fatty acyl chains that are C16 and C18 in length (Ohlrogge and Jaworski, 1997). Once these molecules reach either C16 or C18 in length, the fatty acids are hydrolyzed from the ACP by acyl-ACP thioesterases (e.g. FATB and FATA) and exported from the plastid (Bonaventure *et al.* 2003; Salas and Ohlrogge, 2002). Free fatty acids at the outer envelope of the plastid are activated through the addition of CoA by a long-chain acyl-

CoA synthase (LACS) (Schnurr, *et al.*, 2002). A portion of the C16/C18 fatty acyl pool is used for plastidial membrane lipid synthesis within the plastid, while the majority is relocated to the ER for modifications (e.g. desaturation, oxidation) to synthesize the cutin and cuticular waxes that make up the cuticle, as well as other membrane and storage lipids (Ohlrogge and Jaworski, 1997). Many enzymes involved in the biosynthesis of the cuticle have been investigated and identified (Appendix 3). In spite of recent progress, several aspects of the cuticle biosynthetic pathways remain unknown.

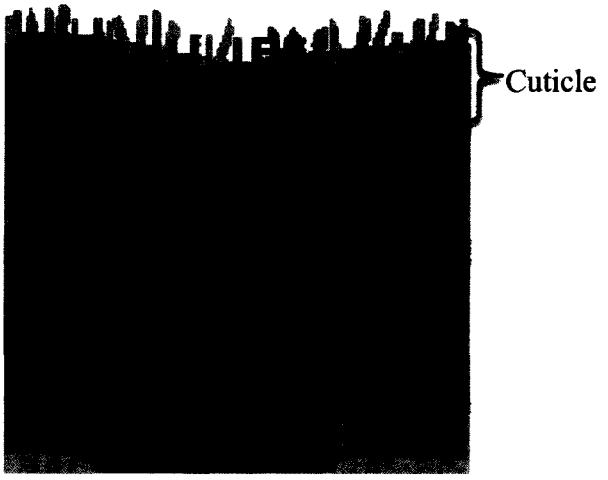

Figure 1: Schematic representation of the cuticle.

The cuticle is deposited outside of the plant cell wall (PW). This representation of a leaf cross-section illustrates the two distinct layers of the cuticle proper, the cutin layer (C), and the epicuticular wax layer (EW). This model also shows the cuticular layer (CL), which is composed of cutin and polysaccharides from the cell wall. Adapted from Pollard *et al.,* 2008.

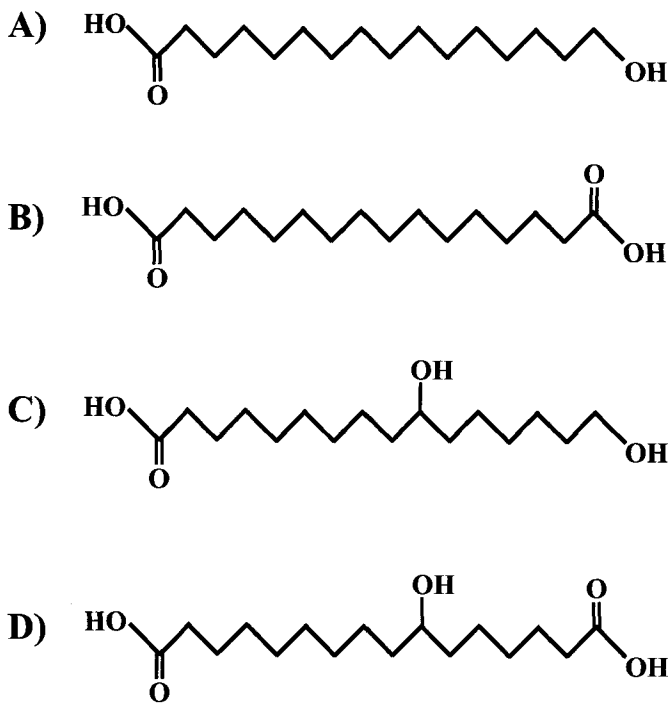

Figure 2: Major compounds found in the cutin matrix.

The *Arabidopsis* cutin matrix is primarily made up of hydroxylated (**A**), α,ω-dicarboxylic acids (**B**), mid-chain hydroxylated fatty acids (**C**), and mid-chain hydroxylated dicarboxylic acids (**D**).

Compound	Structure
Fatty acid	
Primary alcohol	
Wax ester	
Aldehyde	
Alkane	
Secondary Alcohol	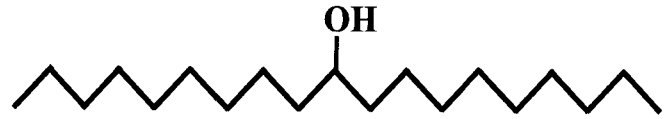
Ketone	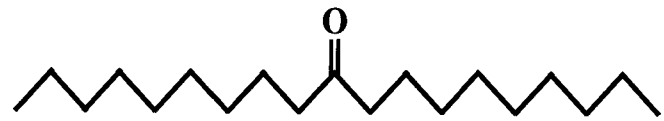

Figure 3: Major compounds found in the stem cuticular wax of *Arabidopsis.*

The cuticular waxes of *Arabidopsis* are made up of various aliphatic compounds such as fatty acids, primary alcohols, wax esters, aldehydes, alkanes, secondary alcohols, and ketones. These compounds are typically found in other plant cuticles, but in varying proportions.

1.2.1 Cutin synthesis

Cutin accounts for a large portion of the cuticle (40 to 80% depending on the plant and tissue type) and is primarily composed of hydroxylated C16 and C18 fatty acids and glycerol (Heredia, 2003; Pollard *et al.*, 2008). Detailed analysis of the cutin component of the cuticle has thus far been challenging due to its insolubility in organic solvents. Cutin must be chemically depolymerized before analysis and therefore only the levels of the monomeric building blocks can be detected (Bonaventure *et al.*, 2004, Kolattukudy, 2001). To build cutin, the fatty acid carboxyl groups esterify with glycerol as well as with the mid-chain hydroxyl groups from the various fatty acids to generate a three-dimensional matrix (Ray *et al.*, 1998a, b; Graça and Lamosa, 2010).

The enzymes involved in cutin synthesis have only recently begun to be identified and characterized, largely in *Arabidopsis* (Appendix 3). LACS1 and LACS2 are long chain acyl-CoA synthetases required for cutin synthesis. Plants lacking *LACS2* transcript have a thinner cuticle layer than wild-type and exhibit typical features of cutin defects, such as increased chlorophyll leaching (Schnurr *et al.*, 2004). *LACS1* mutants have a less dramatic cutin defect, but are deficient in C16 monomer derivatives (Lü *et al.*, 2009). The double *lacs1 lacs2* mutant has a major cutin defect, showing a dramatic increase in non-stomatal water loss (Lü *et al.*, 2009; Weng *et al.*, 2010). Two hydroxylases, LCR and ATT1, have been implicated in cutin biosynthesis (Xiao *et al.*, 2004; Wellesen *et al.*, 2001). Both of these enzymes are cytochrome P450 monooxygenases from the CYP86 family of cytochromes. Plants with mutations in these genes show characteristics of cutin defects, such as increased susceptibility to disease in the case of *att1* and organ fusions in the case of *lcr* (Xiao *et al.*, 2004; Wellesen *et al.*, 2001). Both of these genes are thought

to hydroxylate free fatty acids into ω-hydroxy fatty acid or α,ω-dihydroxycarboxylic acid cutin monomers. It is known that hydroxylated fatty acids in cutin are esterified to glycerol, an activity that can be attributed to a glycerol-3-phosphate acyltransferase (GPAT), which joins hydroxy fatty acyl-CoAs to glycerol to form mono and diacylglycerolipids in cutin. This activity has been attributed to GPAT4 and GPAT8. These genes act redundantly and the *gpat4 gpat8* double mutant displays major physiological changes indicative of cuticular defects, such as increased non-stomatal water loss (Li *et al.*, 2007). GPAT4 and GPAT8 are not the only acyltransferase enzymes responsible for the polymerization of the cutin compounds. Recently a cytosolic acyltransferase, DCR, has been identified. DCR plays a role in the incorporation of 9,10,16-hydroxy-hexadecanedioic acid into the cutin matrix as the *dcr* mutant has a marked decrease in this compound following cutin depolymerization (Panikashvili *et al.*, 2009). However, the specific role of this acyltransferase in the overall pathway is currently unknown.

A mystery in cutin monomer biosynthesis is the order in which these events occur. One model has a thioesterase releasing a free fatty acid, which is subsequently oxidized to a hydroxy fatty acid, which then is reactivated to a hydroxy fatty acyl-CoA before being transferred to glycerol (Figure 4A). The hydroxylases ATT1 and LCR from *Arabidopsis* show activity toward free fatty acids *in vitro*, while ATT1 does not appear to have any activity toward the activated acyl-CoA (Benveniste *et al.*, 2006; Wellesen *et al.*, 2001). In *Petunia hybrida*, however, a fatty acyl-CoA ω-hydroxylase has been identified that preferentially hydroxylates fatty acyl-CoA substrates over free fatty acids (Han *et al.*, 2010). Nevertheless, the current evidence in *Arabidopsis* indicates that the activated

acyl-CoA substrates imported into the ER are likely converted to a free fatty acid prior to hydroxylation. These free hydroxy-fatty acids would need to be reactivated by a LACS, such as LACS1 or LACS2, for the GPAT to form the mono and diacylglycerolipids (Lü *et al.*, 2009). It has been reported that LACS2 has a higher *in vitro* activity with hydroxylated fatty acids over non-hydroxylated fatty acids (Schnurr *et al.*, 2004). No enzyme has yet to be identified fulfilling the role of an acyl-CoA thioesterase responsible for the synthesis of the free fatty acids in the cutin biosynthetic pathway (Figure 4B). In addition to the mystery surrounding the order of the events in cutin biosynthesis, the mechanism for cutin polymerization outside of the cell wall remains uncharacterized.

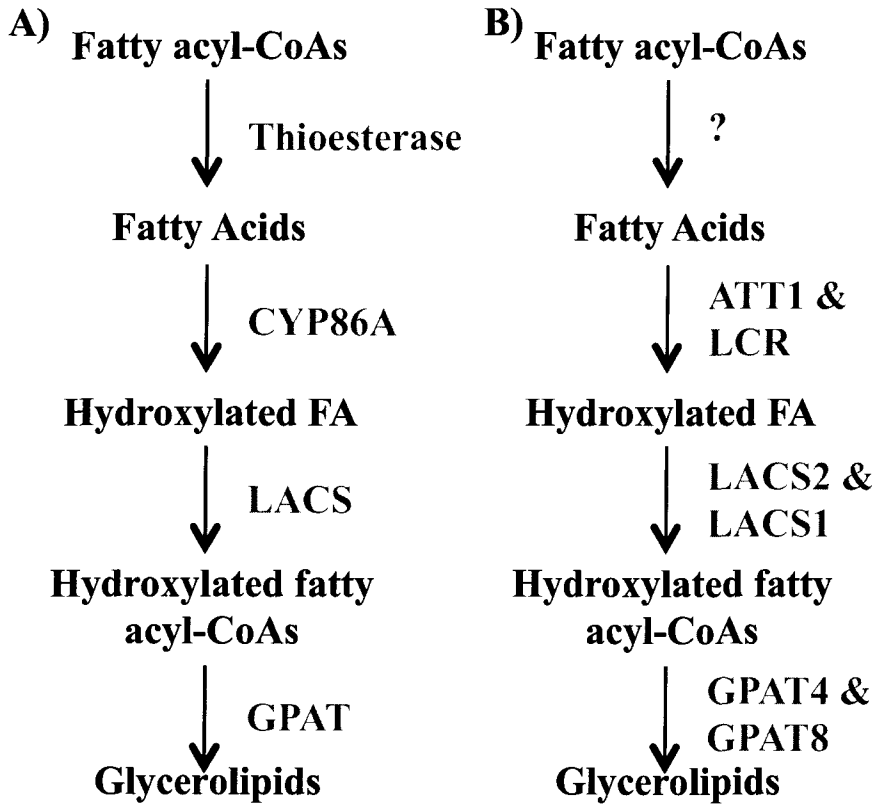

Figure 4: A model for cutin biosynthesis.

The understanding of the cutin biosynthetic pathway is in its infancy in comparison with the study of cuticular wax biosynthesis. (**A**) Some of the activities that occur in cutin synthesis are characterized, such as hydroxylation of fatty acids by cytochrome P450s and the transfer of these hydroxylated fatty acyl-CoAs to glycerol (Pollard *et al.*, 2008). (**B**) Gene products from *Arabidopsis* that carry out some of these functions have recently been identified (Appendix 3). ATT1, ABERRANT INDUCTION OF TYPE THREE GENES; LCR, LACERATA; LACS, LONG-CHAIN ACYL-COA SYNTHASE; GPAT, GLYCEROL-3-PHOSPHATE ACYLTRANSFERASE.

1.2.2 Cuticular wax synthesis

Cuticle biosynthesis occurs almost exclusively within the ER. Some of the C16/C18 fatty acyl-CoAs in the ER are modified to form cutin monomers as previously described, while others are elongated to lengths between 20 and 32 carbons to generate the compounds in the cuticular wax. Elongation of fatty acyl-CoAs is carried out by the fatty acid elongase (FAE) complex at the ER membrane by a mechanism similar to that found during fatty acid synthesis (von Wettstein-Knowles, 1982; Post – Beittenmiller, 1996). The FAE complex catalyzes the elongation of the imported fatty acyl-CoAs through the addition of C2 units from malonyl-CoA instead of from malonyl-ACP, as is found in fatty acid synthesis (Fehling and Mukherjee, 1991). The elongation of the long-chain fatty acyl-CoAs is controlled by the β-ketoacyl-CoA synthase, the first enzyme in the FAE complex. To date, four β-ketoacyl-CoA synthases have been reported to be associated with cuticle biosynthesis, each with its own specific substrate specificity (Miller and Kunst, 1997) (Appendix 3).

Following synthesis, very-long-chain fatty acyl-CoAs can be directed toward one of two major pathways: (1) the primary alcohol-forming pathway, or (2) the alkane-forming pathway (Figure 5) (Samuels *et al.*, 2008). Very-long-chain fatty acyl-CoAs in the alcohol-forming pathway are reduced to primary fatty alcohols by CER4 and a subset of these primary alcohols are further esterified to form wax esters by WSD1 (Rowland *et al.*, 2006; Li *et al.*, 2008). In the alkane-forming pathway it is predicted that very-long-chain fatty acyl-CoAs are reduced to form aldehydes, and subsequently decarbonylated to form alkanes (Cheesborough and Kolattukudy, 1984). CER1, CER3, and CER22 have been implicated in the biosynthesis of aldehydes and alkanes, but none of these predicted

enzymes have been characterized sufficiently to elucidate the mechanism surrounding this step of the pathway (Rashotte et al., 2004; Rowland *et al.*, 2007; Samuels et al., 2008). Within this pathway, the odd chain alkanes serve as substrates for MAH1. MAH1 is a mid-chain hydroxylase responsible for not only the synthesis of secondary alcohols, but also the synthesis of ketones (Greer *et al.*, 2007). A portion of very-long-chain fatty acyl-CoAs enter neither of these two pathways and are cleaved to form free fatty acids, which make-up approximately 3.2% of the total cuticular wax (Figure 5) (Jenks et al., 1995; Pollard *et al.*, 2008). While no enzyme responsible for the synthesis of very-long-chain free fatty acids has been identified, the recently characterized CER8/LACS1 carries out the reverse reaction (Lü *et al.*, 2009). CER8/LACS1 activates very-long-chain fatty acids with CoA to form very-long-chain fatty acyl-CoAs and is highly active for C30 acyl chains. These very-long-chain fatty acyl-CoAs can then be either further elongated or modified by one of the two primary wax biosynthetic pathways into other cuticular wax compounds (Lü *et al.*, 2009; Weng *et al.*, 2010).

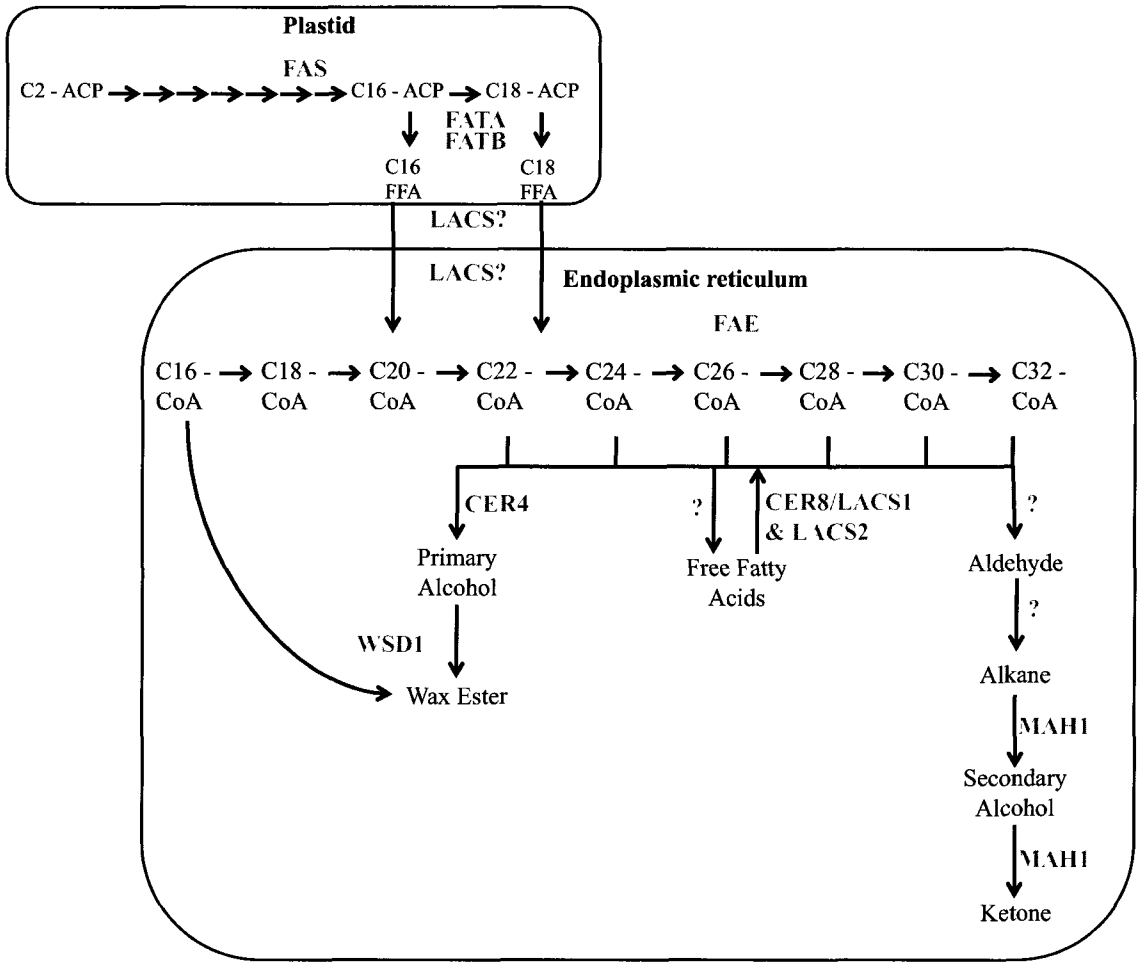

Figure 5: A simplified pathway for wax biosynthesis in *Arabidopsis*.

Enzymes functioning in several parts of the pathway have been well characterized such as CER4 (Rowland *et al.*, 2006), WSD1 (Li *et al.*, 2008), and MAH1 (Greer *et al.*, 2007) (Appendix 3). In spite of this recent progress, our understanding of some aspects of the wax biosynthetic pathway remain limited. FAS, fatty acid synthase; FAT, fatty acyl-ACP thioesterase; FFA, free fatty acid; LACS, long-chain acyl-CoA synthetase; FAE, fatty acid elongase; CER, ECERIFERUM; WSD, wax synthase/diacylglycerol acyltransferase; MAH, mid-chain alkane hydroxylase.

1.3 Roles for thioesterases in lipid biosynthesis.

In spite of recent progress in the identification of cuticle biosynthetic genes (Appendix 3), several aspects have yet to be characterized such as alkane synthesis, aldehyde synthesis, and the production of free fatty acids. The cuticle contains very-long-chain free fatty acids and therefore fatty acyl-CoAs in the ER must be converted to free fatty acids (Figure 5). Cutin synthesis may also require the conversion of fatty acyl-CoAs to free fatty acids in order for hydroxylation to occur (Figure 4). For free fatty acids to be released from the fatty acyl-CoA substrates, the thioester bond between the CoA and the fatty acyl group must be hydrolyzed. This activity is typically carried out by a thioesterase (Figure 6). Two known plant acyl-ACP thioesterases, FATA and FATB, terminate fatty acid synthesis in the plastid (Salas and Ohlrogge, 2002). The FATB enzyme appears to be responsible for approximately 50% of cuticular wax precursors, while thioesterases contributing to the other 50% of precursors have not been identified (Bonaventure *et al.*, 2003). The action of these additional thioesterases may be especially important in cells where lipid synthesis is high, such as in epidermal cells secreting large amounts of cuticular lipids. There are several potential roles for thioesterases in lipid biosynthesis including terminating fatty acid synthesis in the plastid, the formation of free fatty acids for the cuticular wax, the biosynthesis of cutin, and possibly as an indirect mechanism to regulate gene expression (also see Discussion). It is also possible that thioesterases are functioning in the biosynthesis of compounds that have yet to be identified within the cuticle. Only thioesterases functioning in fatty acid synthesis have thus far been identified.

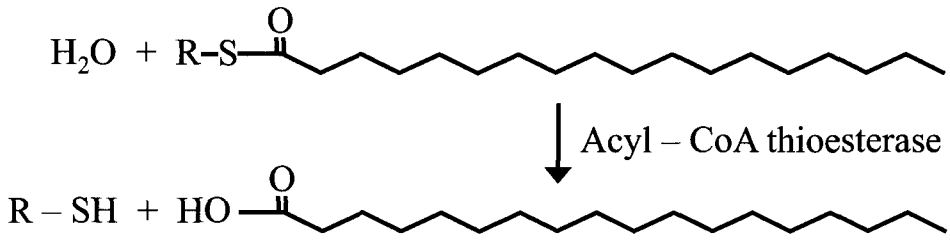

Figure 6: The fatty acyl thioesterase reaction.

Thioesterases cleave the thioester bond through the hydrolysis of a water molecule. R can represent a CoA or ACP moiety. It can also represent a protein in the case of degrading acylated proteins.

1.4 Families of thioesterases

Thioesterases are involved in a wide range of physiological roles such as lipid metabolism, aromatic compound degradation, acylated protein degradation, and signal transduction (Hunt and Alexson, 2002; Salas and Ohlrogge, 2002; Zhuang *et al.*, 2003; Lu *et al.*, 1996; Schujman *et al.*, 2006; Hertz *et al.*, 1998). There are two major superfamilies of thioesterases characterized to date, the α/β hydrolase and the Hotdog fold superfamilies. A recently developed database of enzymes that modify thioester bonds, ThYme, identifies 23 families of thioesterases based on the primary amino acid sequence (Cantu *et al.*, 2010a). Of these 23 families, 8 belong to the α/β hydrolase superfamily and 12 belong to the Hotdog fold superfamily; accounting for approximately 87% of known thioesterases. While members of both superfamilies are capable of hydrolyzing the thioester bond, the three-dimensional structures of the two superfamilies are different (Cantu *et al.*, 2010b).

1.4.1 α/β hydrolase superfamily

The α/β hydrolase superfamily was initially identified by Ollis *et al.* (1992), who recognized that several unrelated proteins possess the same tertiary structure and conserved catalytic residues. Many of the members of this superfamily do not share primary sequence similarity, but the tertiary structure and arrangement of the catalytic site is remarkably similar (Ollis *et al.*, 1992, Nardini and Dijkstra, 1999). Members of the α/β hydrolase superfamily carry out a variety of hydrolysis activities such as esterase and peroxidase reactions (Nardini and Dijkstra, 1999). The substrates of these enzymes are equally variable. Members of this superfamily can hydrolyze the thioester bond

between long chain fatty acids and CoA in humans, while others function in the degradation of aromatic secondary metabolites, such as nicotine (Jones and Gould, 2000; Schleberger *et al.*, 2007). The α/β hydrolase fold consists of a series of 8 parallel β-sheets surrounded by α-helices, and typically exists as a monomer or dimer (Figure 7A). Between the various α/β hydrolase members, the number and position of the α-helices can vary provided that the catalytic triad is unaltered and the parallel β-sheet conformation is conserved (Cantu *et al*, 2010b; Nardini and Dijkstra, 1999). This catalytic trio consists of a nucleophile, an acidic residue, and a histidine, all found on the loops between β-sheets (Figure 7B) (Ollis *et al.*, 1992) (Nardini and Dijkstra, 1999). The majority of α/β hydrolase fold thioesterases characterized to date hydrolyze the thioester bond between an acyl chain and a protein, such as a fatty acid and an acyl carrier protein, or in the degradation of acylated proteins. Only 1 of the 8 α/β hydrolase fold subfamilies that have thioesterase activity use CoA activated acyl chains as substrates (Cantu *et al.*, 2010b). While this superfamily accounts for a significant portion of known thioesterases, acyl-CoA thioesterases appear to only account for a small portion of the α/β hydrolase fold superfamily.

Figure 7: The α/β hydrolase fold is one of two major superfamilies with thioesterase activity.

This superfamily is characterized by series of 8 parallel β-sheets surrounded by loops and α-helices (**A**). All types of hydrolases belonging to this family contain a conserved catalytic triad typically found on the loops between β-sheets consisting of a nucleophile (N), an acidic residue (A), followed by a histidine (H) (**A**). Between individual proteins, the number and position of the α-helices may vary provided the parallel series of sheets and catalytic residues are conserved (**B**). Arrows represent β-sheets and rectangles represent α-helices in this model. Domains labeled in black illustrate some of the variations that have been identified from the typical α/β hydrolase model. Adapted from Nardini and Dijkstra (1999).

A)

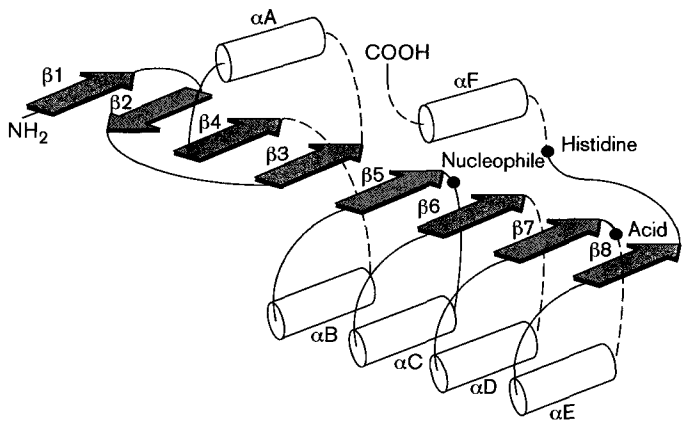
αA
COOH
αF
β1
β2
β4
β3
NH2
Histidine
Nucleophile
β5
β6
β7
Acid
β8
αB
αC
αD
αE

B)

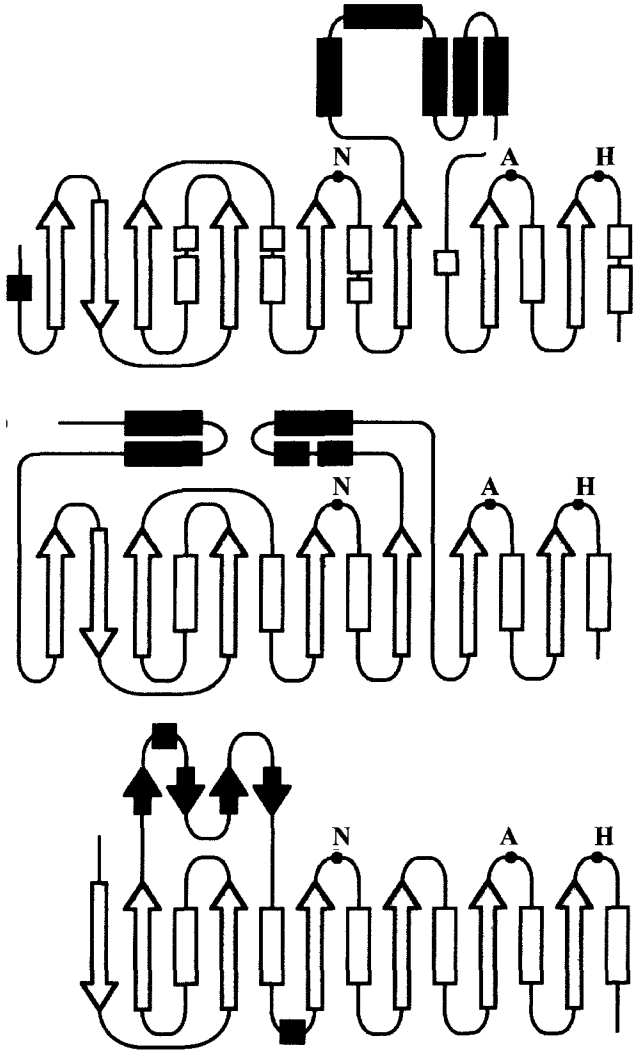
N
A
H
N
A
H
N
A
H

1.4.2 Hotdog fold superfamily

The Hotdog fold superfamily accounts for approximately half of known thioesterases. Unlike the α/β hydrolase fold, 83% of Hotdog fold thioesterases hydrolyze CoA thioester bonds (Cantu *et al.*, 2010b). The Hotdog fold is characterized by a single α-helix surrounded by a series of approximately 5 β-sheets (Dillon and Bateman, 2004) (Figure 8A). In contrast to the multitude of activities observed in the α/β hydrolase fold superfamily, thus far all known Hotdog fold superfamily members catalyze only either thioesterase or dehydration reactions. The Hotdog fold was first described in the structure of the *E. coli* dehydratase FABA and the first Hotdog fold member identified with thioesterase activity was the 4-hydroxybenzoyl-CoA thioesterase 4HBT from *Pseudomonas* sp. Strain CBS-3 (Leesong *et al.*, 1996; Benning *et al.*, 1998). While the definition of an α/β hydrolase fold was dependent both on the location of specific catalytic residues and the tertiary structure, the Hotdog fold is defined only by tertiary structure. Each Hotdog fold subfamily possesses its own catalytic residues depending on the quaternary structure and substrate specificity of that specific subfamily (Pidugu *et al.*, 2009). However, the catalytic residues of many of the Hotdog fold thioesterases involve an acidic residue (Pidugu *et al.* 2009; Zhuang *et al.*, 2008; Kotaka *et al.*, 2009). Hotdog fold proteins always involve the association of more than one Hotdog domain. This association can be through the interaction of two or more Hotdog domains within a single amino acid sequence or by the interaction of 2 monomeric subunits (Pidugu *et al.*, 2009). Dimers typically form between two Hotdog domains in an anti-parallel manner such that one continuous β- sheet is formed, while the α- helices run opposite of one another (Figure 8B) (Pidugu *et al.*, 2009). If these dimers associate as tetramers, they do so in

either a back-to-back orientation or through the central helix interaction (Figure 8 C and D). Hexamers can form, but the associations between the subunits are more complex (Pidugu *et al.*, 2009). The association of multiple Hotdog domains is important for the correct formation of the active site and binding pocket, and this is what provides the Hotdog fold superfamily the flexibility to hydrolyze a wide variety of substrates. The varying quaternary associations and variation within the superfamily contribute to the differences between the 1,4-dihydroxy-2-naphthoate-CoA thioesterase in the vitamin K biosynthetic pathway and FATA/FATB, which terminate *Arabidopsis* fatty acid synthesis (Widhalm *et al.*, 2009; Salas and Ohlrogge, 2002). In spite of the lack of sequence identity, Hotdog fold proteins have a conserved structure and can have either thioesterase or dehydratase activity, accommodating a wide variety of substrates.

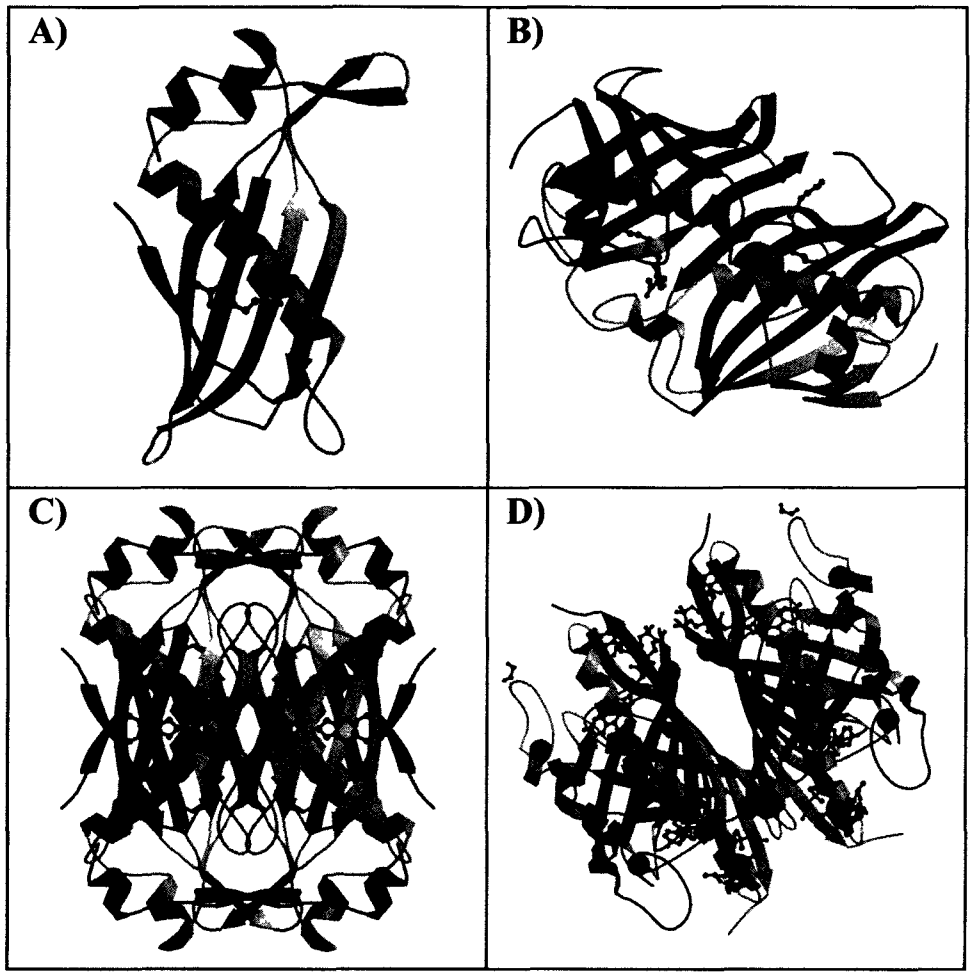

Figure 8: Conformations of the Hotdog fold superfamily.

The non-functional monomeric conformation of a Hotdog fold domain is an α-helix surrounded by approximately 5 β- sheets (**A**) (Benning *et al.*, 1998). The FABA *E. coli* dehydratase was the first identified Hotdog fold protein and assumes a dimeric conformation (**B**) (Leesong *et al.*, 1996). Dimers commonly associate with one another to form tetramers through interactions between α-helices, as is the case with the *Pseudomonas* sp. Strain CBS-3 4HBT (**C**) or in a back-to-back conformation found in the 4-hydroxybenzoyl-CoA thioesterase from *Arthrobacter* (**D**) (Benning *et al.*, 1998; Thoden *et al*, 2003).

1.5 Thesis rationale

The purpose of this Masters thesis was to identify genes that encode thioesterases involved in cuticle biosynthesis in *Arabidopsis thaliana*. There are several potential roles for thioesterases in cuticle biosynthesis. Thioesterases could function in the release of very-long-chain fatty acids found in cuticular waxes. There is also a role for a thioesterase in one model of cutin monomer biosynthesis, in releasing long-chain free fatty acids for hydroxylation by cytochrome P450 enzymes. It is also possible that a novel thioesterase is working in parallel with FATB in terminating saturated fatty acid synthesis. There are also other putative roles for thioesterases in the regulation of lipid biosynthetic genes or in the production of lipid-associated secondary metabolites. I have identified a four member gene family that I have termed *MODIFIERS OF EXTRACELLULAR LIPIDS* (*MEL*) encoding thioesterases whose expression patterns are consistent with roles in extracellular lipid biosynthesis. I demonstrate that MEL1 has thioesterase activity *in vitro* toward palmitoyl-CoA. I also determine that in *E. coli,* MEL1, MEL2, and MEL3 are able to synthesize long-chain free fatty acids and medium-chain β-ketoacids.

Chapter 2: Materials and Methods

2.1 Plant materials and growth conditions

All *Arabidopsis thaliana* plants were in the Columbia-0 background. Seeds were surface sterilized by incubation in 100% ethanol for 1 minute, followed by a 1 minute incubation in 50% bleach (approximately 6% sodium hypochlorite) containing 0.5% SDS. Seeds were rinsed several times with sterile distilled water. Sterile seeds were sown on minimal media containing 5 mM KNO_3, 2.5 mM KH_2PO_4, 2 mM $MgSO_4$, 2 mM $Ca(NO_3)_2$, 50 μM Fe(EDTA), 70 μM H_3BO_3, 14 μM $MnCl_2 \cdot 4H_20$, 0.5 μM $CuSO_4$, 1 μM $ZnSO_4 \cdot 7H_20$, 0.2 μM $NaMoO_4 \cdot 2H_20$, 10 μM NaCl, 0.01 μM $CoCl_2 \cdot 6H_20$, and 0.7% agar (Somerville and Ogren, 1982). Seeds were then stratified in the dark for 3 to 5 days at 4°C and transferred to long-day conditions, 16 hours of light and 8 hours of dark, at 21°C (Conviron, Winnipeg MB) or to continuous-light conditions at room temperature. After approximately 14 days, seedlings were transferred to a soil-vermiculite mixture (ProMix-MVP), fertilized with 1 g/L 20-20-20 fertilizer (Plant-Prod, Brampton ON), and grown under long-day conditions at 22°C in a controlled growth chamber (Conviron or Percival chamber) or under continuous light in Nesbitt room 113A.

2.2 Gene expression analysis by RT-PCR

To determine in which tissues the *MEL* genes were expressed, reverse transcription PCR (RT-PCR) was performed. Approximately 100 mg each of flower, stem, and leaf was harvested from 4-week-old *Arabidopsis* and frozen in liquid nitrogen. Roots from 15-day-old seedlings was also harvested and frozen in liquid nitrogen. RNA was isolated from the tissues using TRIzol reagent (Invitrogen, Burlington ON) as per

the manufacturer's instructions. All solutions prepared in house were treated for 24 hours with diethylpyrocarbonate (DEPC) (Bioshop, Burlington ON) and autoclaved before use. First strand cDNA synthesis was carried out with 1 μg of RNA and SuperScript III RT (Invitrogen) as per the manufacturer's specifications. A 0.4 μL aliquot of cDNA from the various tissues was used as a template for PCR with pairs of gene specific primers: MEL1_RT_Fwd with, MEL1 RT_Rev, MEL2_RT_Fwd with MEL2_RT_Rev, and MEL3_RT_Fwd with MEL3_RT_Rev (Appendix 1). *GLYCERALDEHYDE-3-PHOSPHATE DEHYDROGENASE* (*GAPC*) levels were measured as a constitutive control using primers GAPC_Fwd and GAPC_Rev (Appendix 1). The PCR products were separated on a 1% agarose gel containing ethidium bromide and visualized using an AlphaImager 2200 (Alpha Innotech, Santa Clara CA).

2.3 Cuticular wax analysis of *Arabidopsis* stems

The cuticular wax composition of stem tissues was analyzed by gas chromatography and using a flame ionization detector (GC-FID). Approximately 8 cm of stem from 6-week-old plants grown under long day conditions was harvested just above the first internode. Samples were immersed in spectro grade chloroform (Caledon, Georgetown ON) containing 1 μg of methyl heptadecanoate (Sigma-Aldrich) for 30 seconds. The chloroform was evaporated to dryness at 37°C under a gentle stream of nitrogen. The samples were dissolved in *N, O* – bis(trimethylsilyl)trifluoroacetamide:trimethylchlorosilane (BSTFA+TMCS; 99:1) (Sigma Aldrich), and derivatized at 80°C for 90 minutes. A 1 μL aliquot was then analyzed by gas chromatography on a Varian 450-GC equipped with a HP-1 capillary

column (15m x 250μm i.d., 0.25um film thickness, Varian, Santa Clara, CA) using helium as the carrier gas. The injector was held at 250°C and the oven held at a temperature of 150°C for 1 minute. The oven temperature was then raised at a rate of 4°C per minute to a final temperature of 300°C. Finally, the oven was held at 300°C for 15 minutes.

2.4 Cutin analysis of *Arabidopsis thaliana*

About three mature rosette leaves and a comparable amount of stem tissue were harvested into chloroform rinsed glass vials for delipidation. The vials were filled with hot isopropanol and incubated at 80°C for 10 minutes. Once cooled, the isopropanol was replaced with a 2:1 (v/v) solution of chloroform:methanol for 24 hours. The samples were then incubated in 1:1 (v/v) chloroform:methanol, 1:2 (v/v) chloroform:methanol, and 100% methanol for 24 hours each with changes twice a day. Samples were dried in the fumehood for 2 days and in a dessicator for a further 2 days (Domergue *et al.*, 2010).

The dilipidated samples were sent to our collaborator, Dr. Frédéric Domergue, and the following procedure carried out in his laboratory. The dried tissues were depolymerized by incubation in 1 M sulfuric acid in methanol and 2% (v/v) dimethoxypropane for 3 hours at 85°C. The samples were spiked with 10 μg heptadecanoic acid, 10 μg ω - pentalactone, and 10 μg pentadecanol as internal standards. Once cooled, 3 mL of 2.5% NaCl was added to each sample and the lipids extracted with hexane. The hexane fraction was washed with 3 mL of saline solution (200 mM NaCl and 200 mM Tris, pH8) and then transferred to a fresh vial and dried under nitrogen. Samples were derivatized in 150 μL of BSTFA+TMCS at 110°C for 30 minutes. The

BSTFA+TMCS was evaporated under nitrogen and then the sample was dissolved in hexane for gas chromatography-mass spectrophotometry (GC-MS). GC-MS was carried out using an Agilent 6850 gas chromatograph with a HP-5MS column (30m X 0.25 mm X 0.25 μm) and an Agilent 5975 mass spectrometric detector (70 eV, mass-to-charge ratio 50-750). The oven temperature was held at 50°C for 1 minute, increased at 25°C per minute to 150°C, held at 150°C for 1 minute, increased by 10°C per minute to 320°C, and held at 320°C for 8 minutes (method from Domergue *et al.* 2010).

2.5 Ectopic expression of MEL1 in *Arabidopsis.*

To ectopically express *MEL1,* the cDNA sequence was cloned into a vector downstream of the cauliflower mosaic virus 35S promoter. The *MEL1* cDNA sequence was amplified from the clone U14921 (ABRC, Columbus OH) with primers MEL1_OE_XbaI_Fwd and MEL1_OE_SacI_Rev (Appendix 1) and iProof High-Fidelity DNA polymerase (Bio-Rad, Mississauga ON). The PCR product was digested with the restriction enzymes *Xba*I and *Sac*I (Invitrogen) and ligated with T4 DNA ligase (Invitrogen) into the vector pBAR containing the 35S promoter to generate pBAR::35S-MEL1 (Appendix 2). The product was also inserted between the *Xba*I and *Sac*I sites in the pVKH18 vector containing a 35S promoter with six enhancer sequences (Batoko *et al.*, 2000). The pVKH18::35S-GFPN vector was digested with *Xba*I and *Sac*I, excising the green fluorescent protein (GFP) coding sequence. The digested pVKH18::35S vector fragment was gel purified by the following phenol extraction procedure. Following electrophoresis, a UV box was used to image the DNA fragments and the large fragment associated with the pVKH18::35S vector was excised with a razor. The gel fragment was

crushed with a syringe into a microcentrifuge tube and TE saturated phenol (Bioshop) added in a 1 µl/mg of gel ratio. The mixture was vortexed for 1 minute before being frozen in liquid nitrogen. The aqueous layer was separated by centrifugation at 13,000 rpm for 15 minutes and the top layer transferred to a fresh microcentrifuge tube. Further purification of the DNA occurred by the addition of an equal volume of 25:24:1 (v/v) phenol:chloroform:isoamyl alcohol (Bioshop). After 1 minute of mixing, the sample was centrifuged at 13,000 rpm for 5 minutes. The aqueous layer was transferred to a fresh vial and the DNA ethanol precipitated with 3M sodium acetate. The *MEL1* coding sequence was ligated into pVKH18::35S between the corresponding restriction sites to generate pVKH18::35S-MEL1 (Appendix 2).

The vectors were transformed into chemically competent *E. coli* DH5α cells. Five µL of each ligation was incubated with 50 µL of thawed cells on ice for 30 minutes and heat shocked for 45 seconds at 45°C. The cells were incubated at 37°C in 1 mL of LB media for 1 hour and plated on LB media with 1.5% agar containing 50 µg/mL kanamycin. *E. coli* colonies containing the plasmid with an insert were identified through colony PCR. Plasmids were then purified from 5 mL of overnight culture using a standard miniprep procedure, and the *MEL1* insert verified by DNA sequencing (Eurofin MWG Operon, Huntsville AL). Plasmids were transformed into GV3101 *Agrobacterium tumefaciens* cells by electroporation using a MicroPulser Electroporator (BioRad, Mississauga ON). The *Agrobacterium* was used to introduce the T-DNA regions of the binary plasmids into wild-type plants by the floral dip method (Zhang *et al.*, 2006). Successful *Arabidopsis* transformants containing the T-DNA harbouring 35S-MEL1 were selected on minimal media containing 30 µg/mL hygromycin (Bioshop).

Arabidopsis containing the T-DNA harbouring 35S-MEL1 were selected with a 1:1000 dilution of Finale (Farnam Companies Inc, Phoenix AZ), which was sprayed on seedlings 4, 7, and 10 days after sowing. Positive transformants were transplanted to soil and after approximately 4 weeks of growth stem samples were harvested for cuticular wax as described above.

2.6 Generation of artificial microRNA lines

To decrease the transcript levels of *MEL1,* artificial microRNAs (amiRNAs) were generated using the *miR319a Arabidopsis* microRNA backbone and overlapping PCR to selectively change nucleotide residues (Figure 9) (Ossowski *et al.*, 2008). MEL1 specific amiRNA sequences were identified with WMD2-Web MicroRNA Designer to generate amiRNA lines A and B (Ossowski *et al.*, 2005) (Ossowski *et al.*, 2008). Based on these amiRNA sequences, the WMD2 tool provided the amiRNA specific primers MEL1_ami-A_I, MEL1_ami-A_II, MEL1_ami-A_III, and MEL1_ami-A_IV in the case of MEL1_amiRNA-A, and MEL_ami-B_I, MEL_ami-B_II, MEL_ami-B_III, and MEL_ami-B_IV in the case of MEL1_amiRNA-B (Appendix 1). In addition to these amiRNA specific primers, the general primers pRS300_A and pRS300_B (Appendix 1) were used to complete the overlap PCR reactions outlined in Table 1 (Figure 9) with iProof High Fidelity Polymerase to generate MEL1_amiRNA-A and MEL1_amiRNA-B.

Each of the first 3 reactions was gel-purified from a 1% agarose gel using the phenol extraction procedure described above, and these were used as a template for reaction 4. The reaction 4 amplified product was digested with the restriction enzymes *Eco*RI and *Bam*HI (Invitrogen) and ligated between the corresponding sites in the

pBluescript vector to generate pBluescript-MEL1_amiRNA-A and pBluescript-MEL1_amiRNA-B. The ligation mixtures were transformed into chemically competent DH5α and clones containing inserts were identified. The inserts were sequenced to make sure there were no unintended mutations. Adapter primers, Ami_adapterA_XbaI and Ami_adapterB_SacI (Appendix 1), were used to amplify by PCR the amiRNAs from pBluescript appending *Xba*I to the 5' end and *Sac*I to the 3' end of the amiRNAs with iProof High Fidelity polymerase. The products were then cloned into the corresponding sites of pBAR::35S and pVKH18::35S to create the constructs pBAR::35S-MEL1_amiRNA-A, pVKH18::35S-MEL1_amiRNA-A, pBAR::35S-MEL1_amiRNA-B, and pVKH18::35S-MEL1_amiRNA-B (Appendix 2). Following verification of the DNA sequence, the vectors were transformed into GV3101 *Agrobacterium tumefaciens* cells by electroporation and wild-type *Arabidopsis* were transformed by the floral dip method (Zhang *et al.*, 2006). Selection and analysis of transformants was carried out as previously described for the MEL1 over-expression plants.

Table 1: PCR strategy to synthesize amiRNA sequences specific for *MEL1*

Summary of the PCR strategy showing the primers and template used for each of the amplifications to form the full-length amiRNA sequences (Adapted from Ossowski *et al.*, personal communication, 2005). The X is used in place of A or B in the primer names as this strategy applies to the synthesis of both MEL1_amiRNA-A and MEL1_amiRNA-B.

Reaction	Primers	Template
Reaction 1	pRS300_A MEL1_ami-X_IV	pRS300
Reaction 2	MEL1_ami-X_III MEL1_ami-X_II	pRS300
Reaction 3	MEL1_ami-X_I pRS300_B	pRS300
Reaction 4	pRS300_A pRS300_B	Reactions 1, 2, and 3

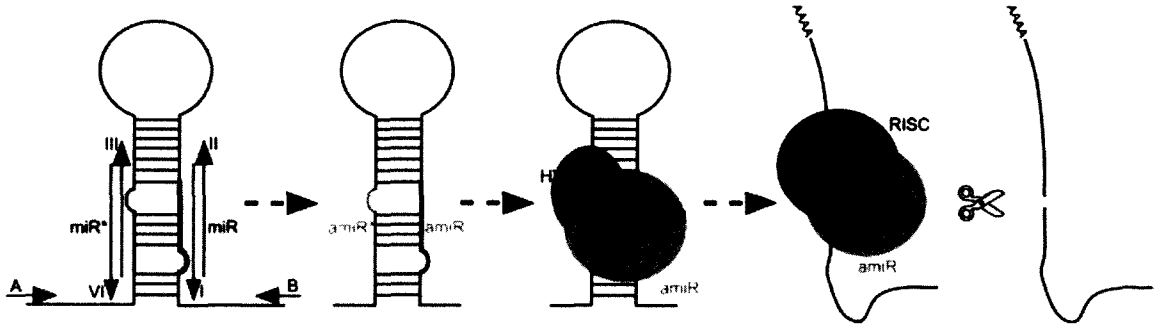

Figure 9: A model for artificial amiRNA synthesis and how amiRNAs silence genes of interest.

Following overlapping PCR, a hairpin RNA sequence is synthesized with specific mutations which may the artificial microRNA specific for the gene of interest. RNA processing machinery within the plant recognizes the double-stranded RNA within the hairpin structure and cleaves the RNA. The small fragments of RNA are then free to anneal to the targeted transcipt. This again induces RNA processing to cleave the double-stranded RNA including the mRNA template (Ossowski *et al.*, 2005).

2.7 *In situ* hybridization for the detection of *MEL1* transcript

An antisense probe specific for *MEL1* was amplified from the clone U14921 (ABRC) containing the cDNA sequence for *MEL1* using the primers MEL1_Antisense_Fwd and MEL1_Antisense_Rev (Appendix 1) that appends the T7 polymerase binding site to the 5' end of the template strand. As a negative control, a sense probe was also amplified from the same clone using the primers MEL1_sense_Fwd and MEL1_sense_Rev (Appendix 1). Amplification was carried out with Taq polymerase and the resulting PCR product purified using the Wizard SV Gel and PCR Clean up kit (Promega, Madison WI). Transcription of digoxigenin labeled RNA probes was carried out with DIG RNA Labeling Kit (SP6/T7) (Roche, Mannheim Germany) using the sense and antisense templates. The probe was then ethanol precipitated with 4M LiCl and resuspended in 100 μL of DEPC treated water. The full-length RNA probe was subject to carbonate-mediated hydrolysis by incubating the probe with 60mM $NaHCO_3$ and 40mM Na_2CO_3 for 27 minutes at 60°C, followed by ethanol precipitation with 3M sodium acetate. The probe was resuspended in 50% deionized formamide and quantified as outlined by the manufacturer's instructions in the DIG RNA Labeling Kit (SP6/T7) and the DIG Nucleic Acid Detection Kit (Roche). The probe was quantified by spotting the probe onto a nylon membrane and then imaged using an AlphaImager 2200 (Alpha Innotech).

Stem tissue for *in situ* hybridization was harvested from 6-week-old wild-type plants and fixed in formol-acetic-alcohol (50% ethanol, 5% acetic acid, 3.7% paraformaldehyde) (Canemco, Lakefield QC), in a glass scintillation vial (Huijzer *et al.*, 1992). The tissues immersed in fixative were repeatedly placed in a vacuum at 15

minutes intervals until all tissue had sunk to the bottom of the vial, after which the fixation was allowed to proceed for 2 hours at room temperature. The samples were washed with 50% ethanol and incubated in fresh 50% ethanol for 30 minutes. Samples were dehydrated through 30-minute incubations in each of 50%, 60%, 70%, 85%, and 95% ethanol, and then incubated in 95% ethanol with 0.1% eosin overnight. Samples were incubated in 100% ethanol for 2 hours with changes for fresh 100% ethanol after 60 and 90 minutes. The tissue was infiltrated with xylene (Fisher Scientific, Pittsburgh PA) through 30-minute incubations in increasing concentrations (25%, 50%, and 75%) of xylene in ethanol followed by a 1-hour incubation in 100% xylene with a change to fresh xylene after 30 minutes. Approximately 20 paraplast (Sigma-Aldrich) chips were added to the vial and the samples incubated overnight at room temperature. The vial was placed in a 42°C waterbath for 1 hour to melt the paraplast chips, and moved to the 60°C oven for 4 hours. The paraplast- xylene mix was changed for 100% melted paraplast chips. The paraplast was replaced with fresh melted chips twice daily for 3 days. Following 6 wax changes, the infiltrated tissues and wax was poured into a petri dish floating in a 60°C water bath. Samples were arranged with dissecting needles and the temperature lowered allowing the paraplast to solidify. The samples were cut from the paraplast block and mounted onto small wooden blocks and 8 μm cross sections of stem were sectioned with a rotary microtome (ThermoFisher Scientific, Waltham MA) and placed on frosted slides (Superfrost Plus, Fisher Scientific). The sections were bonded to the slides by incubating the slides at 42°C overnight on a slide warmer.

Slide preparations were dewaxed by 2 incubations of 10 minutes in 100% xylene. Rehydration was performed by incubating the slides twice in 100% ethanol for 2 minutes,

followed by incubations in 95% and 90% ethanol, and 80%, 60%, and 30% ethanol containing 0.85% NaCl for 1 minute per solution. Slides were incubated in 0.85% NaCl and phosphate buffered saline (PBS) for 2 minutes. Slides were then subjected to proteinase K digestion by incubation in 1 μg/mL proteinase K (Sigma-Aldrich), 100 mM TRIS ph 7.5, and 50 mM EDTA for 30 min and incubated for 2 minutes each in 0.5 g/L glycine in PBS and PBS. Slides were postfixed in 4% paraformaldehyde in PBS for 2 minutes followed by a 2 min rinse in PBS. Samples were acetylated by incubating slides for 2 minutes in approximately 100 mM triethanolamine and 30 mM acetic anhydride, followed by 2- 5 minute washes in PBS and a 5 minute wash in 0.85% NaCl. Slides were dehydrated by dipping slides in each of 0.85% NaCl, 30% ethanol, 60% ethanol, 80% ethanol, and 90% ethanol containing 0.85% NaCl, and 95% ethanol, and 2 rinses in 100% ethanol for 30 seconds each.

Hybridization with the probe was performed with 150 μL of hybridization buffer (50% formamide, 10% dextran sulfate (Sigma-Aldrich), 1X Denhardt's (Sigma-Aldrich), 20 mg/mL tRNA(Roche), 10 mM Tris pH 7.5, 1 mM EDTA, and 300 mM NaCl) combined with 5, 10 and 20 ng of antisense probe, 5 ng of sense probe for a negative control, and 5 ng of CER6 probe for a positive control (CER6 probe synthesized and provided by Mingli Xu, Ph.D candidate, Dr. Hepworth lab; described in Hooker *et al.*, 2002). Probes were diluted in 50% formamide to a final volume of 50 μL, such that the final ratio of hybridization buffer to probe was 3:1 (Samach *et al.*, 1997). The probe hybridization solution was heated to 80°C for 2 minutes and then placed on ice. All the sample slides were placed on the slide warmer at 52°C, and 150 μL of the hybridization buffer containing the probe was applied to each slide and a cover slip lowered to cover all

samples without causing air bubbles. The slides were placed on risers in a box pre-warmed to 55°C with Whatman paper soaked in 2X SSC (300 mM NaCl and 30 mM sodium citrate dihydrate) in 50% formamide. The box was sealed in a plastic bag with water soaked paper towels and left at 55°C overnight. To wash excess probe from the slides, samples were transferred to 2x SSC for 5 minutes at 55°C dipping slides up and down until cover slips were removed. Slides were incubated in 0.2X SSC at 55°C for 2 hours with a change of solution every 30 minutes. They were then transferred to 0.2X SSC at 37°C for 5 minutes and finally 0.2X SSC at room temperature for 5 min. The slides were stored in a plastic container containing PBS over night at 4°C. Each slide was incubated for 1 hour in 1 mL of 1% blocking solution (Roche) in maleic acid. Slides were washed with 2 mL of wash solution (1% BSA, 0.3% Triton-X100, 100 mM Tris HCl pH 7.5, and 150 mM NaCl) per slide, for 1 hour. The anti-digoxigenin-AP, Fab – fragments (Roche) were diluted 1:1250 in the wash solution and 250 µL of the diluted antibody solution was added to each slide under a cover slip and incubated for 90 minutes at room temperature (Coen *et al.*, 1990). The excess antibody was removed by rinsing the slides 3 times in wash solution for intervals of 20 minutes each. Slides were placed in 100 mM TRIS-HCl (pH 9.5), 500 mM NaCl, and 100 mM $MgCl_2$ for 30 minutes changing solutions after 15 minutes. The colourimetric reaction was carried out by the addition of 250 µL of 18% BCIP/NBT in 100 mM TRIS-HCl pH 9.5, 500 mM NaCl, and 100 mM $MgCl_2$ to each slide. The reaction proceeded overnight in the dark and was stopped by placing the slides in 10 mM TRIS-HCl pH 8 and 10 mM EDTA, and imaged under 50% glycerol using an Axio Imager M2 (Zeiss, Thornwood NY). All solutions

used for *in situ* hybridization except for the ones containing TRIS were treated with DEPC for 24 hours and autoclaved before use.

2.8 Promoter-glucuronidase (GUS) fusions and the GUS histochemical assay

The expression patterns of *MEL1*, *MEL2*, *MEL3*, and *MEL4* were examined using the β- glucuronidase (GUS) reporter system. Approximately 1.8 Kb of sequence upstream of the start codon of each of each gene was amplified from the BAC clones containing genomic DNA. The BACs T9I1, containing *MEL1* and *MEL2*, and T22E19 containing, *MEL3* and *MEL4*, (ABRC), were used as templates with the following primers: MEL1_Prom_SalI_Fwd with MEL1_Prom_BamHI_Rev, MEL2_Prom_SalI_Fwd with MEL2_Prom_BamHI_Rev, MEL3_Prom_SalI_Fwd with MEL3_Prom_BamHI_Rev, and MEL4_Prom_SalI_Fwd with MEL4_Prom_BamHI_Rev (Appendix 1) using iProof High-Fidelity DNA polymerase. The PCR products were digested with the restriction enzyme *Sal*I (Invitrogen) and *Bam*HI and ligated between the corresponding sites in the pBI101.1 vector and in frame with the GUS coding region to generate pBI101-MEL1 promoter GUS, pBI101-MEL2 promoter GUS, pBI101-MEL3 promoter GUS, and pBI101-MEL4 promoter GUS. These vectors were transformed into DH5α cells as previously described, and the amplified region sequenced to confirm that there were no PCR-induced errors. The plasmids were then transformed into GV3101 *Agrobacterium* cells by electroporation. *Agrobacterium* was then used to transform wild-type plants by the floral dip method (Zhang *et al.*, 2006). I acknowledge Swara Narayanan for the construction of these plasmids. Successful transformants were identified by selection on minimal media containing 50 μg/mL kanamycin, as described

previously. These were transplanted to soil and at about 4 weeks of age various aerial tissues were stained to identify lines with appropriate staining patterns. GUS staining of aerial tissues was carried out by immersing tissue in heptane for a few minutes and then rinsing with pre-chilled staining buffer, 50 mM NaH_2PO_4, 100 mM $KFe(CN)_6$, and 0.1% Triton X-100. Samples were incubated in staining solution, which is staining buffer plus 1 mM X-Glucuronide (Gold Biotechnologies, St. Louis MO), at 37°C for 2-18 hours depending on the individual line and tissue type. The staining solution was then replaced with 70% ethanol and samples imaged with a Zeiss SteREO Discovery V20 (Zeiss). Seeds from transgenic lines showing consistent staining patterns were harvested and sown on selectable media. Following transplantation, samples from these plants were harvested at various ages and stained to further characterize the expression pattern of the reporter genes driven by the upstream regions of the *MEL* genes. Positive transgenics were also transplanted to non-selectable media and grown vertically on plates for several days. Root tissue was stained by incubating samples GUS staining solution for approximately 2 hours at 37°C and stored in 70% ethanol.

Stained tissues were embedded in paraffin and cross-sectioned using a rotary microtome as described in section 2.7. The slides were prepared as described previously, except following rehydration samples were mounted under 50% glycerol. A cover slip was applied and samples imaged with an Axio Imager.M2. Slides were sealed with nail polish for long-term storage. I acknowledge Swara Narayanan, Carlos Canez, and Sollapura Vishwanath for analyzing and photographing the MEL promoter:GUS lines.

2.9 Plasmid constructs for expression of MELs in *E. coli*

The cDNA sequences for *MEL1*, *MEL2*, and *MEL3* were amplified from clones U14921 (*MEL1*), U84163 (*MEL2*), and U14083 (*MEL3*) obtained from ABRC using iProof High-Fidelity DNA polymerase and primers: MEL1_BamHI_Fwd with MEL1_EcoRI_Rev, MEL2_BamHI_Fwd with MEL2_EcoR1_Rev, and MEL3_BamHI_Fwd with MEL3_EcoRI_Rev (Appendix 1). PCR products were digested with *Bam*HI and *Eco*RI restriction enzymes and ligated between the corresponding sites of the pET28a vector (Novagen, Darmstadt Germany), which contains a region encoding an N-terminal His 6X tag and a T7 epitope tag, to generate pET28a-MEL1, pET28a-MEL2, and pET28a-MEL3 (Appendix 2). I acknowledge Xiaoxue Wen and Dr. Owen Rowland for building the pET28a-MEL2 and pET28a-MEL3 constructs. To generate a non-active version of MEL1, the codon for aspartic acid residue at position 64 was mutated to a codon encoding an alanine. For this, the cDNA sequence for MEL1 was amplified with mutagenic primers in 2 segments with iProof High-Fidelity DNA polymerase from the clone U14921 (ABRC). The first reaction contained primers MEL1_BamHI_Fwd and MEL1_D64A_Rev and the second reaction contained MEL1_D64A_Fwd and MEL1_EcoR1_Rev (Appendix 1). The resulting fragments were gel purified by the phenol extraction procedure, as described in section 2.5, and used as the template for overlapping PCR with the primers MEL1_BamHI_Fwd and MEL1_EcoRI_Rev (Heckman and Pease, 2007). The resulting product was then digested with *Bam*HI and *Eco*RI and ligated between the corresponding sites of pET28a to generate pET28a-MEL1(D64A) (Appendix 2).

The FATB open reading frame lacking the region coding for the chloroplast transit sequence was amplified from flower cDNA using iProof High-Fidelity DNA polymerase with the primers FatB_Trunc_SacI_Fwd and FatB_HindIII_Rev (Appendix 1) (Mayer and Shanklin, 2007). This was then digested with *Sac*I and *Hind*III restriction enzymes and ligated into the pET28a vector to generate pET28a-FATB (Appendix 2).

Plasmids containing *MEL1*, *MEL1 (D64A)*, *MEL2*, *MEL3*, and *FATB* were transformed into *E. coli* BL21(DE3)pLysS cells (Promega, Madison WI) by electroporation. These constructs were also transformed into chemically competent K27(DE3), which was created by former Rowland Lab M.Sc .student Tao Song (Lü *et al.*, 2009). The *E. coli* cell line K27 has a knock-out mutation of the acyl-CoA synthetase *FadD* gene. The K27(DE3) lysogen contains a chromosomally integrated T7 RNA Polymerase coding sequence under the control of the *lacUV5* promoter, which allows for inducible expression of genes cloned downstream of the T7 promoter on the pET plasmid. As a negative control, an empty pET28a vector was transformed into each of these cell lines.

2.10 Media analysis

To analyze the media for the synthesis of novel lipid compounds, K27(DE3) cells with empty pET28a or pET28a vectors containing *MEL1*, *MEL2*, *MEL3*, *MEL1(D64A)*, or *FATB* were inoculated into 5 mL of LB containing 50 μg/mL kanamycin. These cultures were grown at 37°C overnight. Larger 50 mL cultures of LB containing 50 μg/mL kanamycin were inoculated with 1 mL of the overnight culture and grown at 30°C with shaking at 200 rpm until the optical density (λ = 600 nm) of the culture was between

0.5 and 0.7. The cells were induced with 1 mM isopropyl β-D-1-thiogalactopyranoside (IPTG) (Bioshop) and grown at 18°C overnight. The culture was pelleted in a chloroform rinsed glass vial by centrifugation at 5000 rpm for 15 minutes in an Eppendorf centrifuge 5804R with an A4-4-4 rotor (Eppendorf, Mississauga ON).

To analyze the LB media for the presence of free fatty acids, 0.5 mL of the media from the pelleted culture was transferred to a fresh glass vial. 1 mL of 1:1 (v/v) chloroform:methanol and 22 μL of glacial acetic acid was added to the media and the solution mixed by inversion. Samples were centrifuged at 5000 rpm for 10 minutes and the lower chloroform phase transferred to a fresh GC vial. The chloroform was evaporated under nitrogen and 1 mL of 2% sulfuric acid in methanol was added and the sample incubated at 90°C for 60 minutes. Once cooled, samples were extracted by the addition of 1 mL of 0.9% NaCl and 2 mL of *n*-hexane (Fisher Scientific). Following centrifugation at 4000 rpm for 5 minutes, the top layer was transferred to a fresh glass vial and dried under a steady stream of nitrogen. The sample was dissolved in 50 μL of *n*-hexane and 2 μL of the sample was analyzed on a Varian 450-GC equipped with a HP-1 capillary column (15m x 250μm i.d., 0.25um film thickness, Varian, Santa Clara, CA) using helium as the carrier gas at a flow rate of 2 mL/min. The injector was held at 225°C and the oven temperature was held at 100°C for 5 minutes and then increased from 100°C to 160°C at a rate of 20°C per minute, followed by an 8 minute hold, and then an increase of 10°C per minute to a final temperature of 240°C. The oven was held at 240°C for 5 minutes (method from Mayer and Shanklin, 2007). Results were compared over three biological replicates.

To analyze the LB media for the presence of β-ketoacids, 1 mL of the media from the pelleted culture was transferred to a fresh solvent-rinsed glass vial. 1 mL of 2 M sulfuric acid was added to the media and the sample incubated at 75°C and subsequently 30°C for 30 minutes each. The 3-ketoacids were then extracted with the addition of 1mL of *n*-hexane. After centrifugation at 4000 rpm for 10 minutes, 2 μL of the hexane were analyzed on a Varian 450-GC fitted with a HP-1 capillary column (15m x 250μm i.d., 0.25um film thickness, Varian) using helium as the carrier gas at a flow rate of 1.5 mL/min. The injector temperature was held at 250°C. The oven temperature was initially 50°C and held for 8 minutes, followed by an increase to 275°C at a rate of 15°C per minute. The oven was held at 275°C for 5 minutes (method from Yu *et al.*, 2010). Results were compared over three biological replicates.

2.11 Western blot analysis

Western blot analysis was carried out to ensure successful induction of the MEL proteins. Each cell pellet was resuspended in 5 mL of PBS and the cell suspensions diluted to an optical density of 0.75 at 600 nm. 100 μL of cell suspension was added to 25 μL of 4X SDS loading dye and the samples boiled for 10 minutes. Following centrifugation at 14000 rpm for 5 minutes, 20 μL aliquots were loaded into a 12% SDS page polyacrylamide resolving gel with a 4% SDS page stacking gel. 5 μL aliquots were also loaded into a second SDS page gel to be transferred to a nitrocellulose membrane for Western blot analysis. The gel was run for 30 minutes at 100 volts and then at 150 volts for approximately another hour using a Bio-Rad Mini-Protean Tetra Cell system (Bio-Rad, Hercules, CA). The gel loaded with more protein was stained with coomassie stain

overnight on a rocker table and destained with 25% methanol. The coomassie gel was imaged with an Alpha Innotech fluorchemQ (Alpha Innotech). The gel loaded with less protein was transferred to a 0.45 μm nitrocellulose membrane (Bio-Rad) in a Bio-Rad Mini Trans-Blot Electrophoretic Transfer Cell system (Bio-Rad) at 100 mA in the cold room overnight.

The Western blot to detect tagged proteins was performed using the Amersham ECL Advance Western Blotting Detection Kit (GE Healthcare, Uppsala SE). The membrane was blocked in 5% fat-free powdered milk in TRIS-buffered saline (TBS-T; 25mM TRIS pH 7.6, 0.8% NaCl, and 0.1% Tween 20), for 1 hour on a rocker table and then incubated for 1 hour with T7 tag monoclonal antibody (Novagen) diluted 1:50,000 in blocking solution. The membrane was rinsed three times with TBS-T and washed for 15 min with TBS-T followed by 3 washes with TBS-T of 5 min each. The membrane was incubated for 1 hour in Amersham ECL anti-mouse IgG, horseradish peroxidase whole antibody (GE Healthcare) diluted 1:50,000 in blocking solution and the washes repeated. The ECL advanced Western blotting detection reagents 1 and 2 were mixed at a 1:1 ratio. The membrane was then incubated in the detection reagent for 3 min in the dark and the excess detection reagent drained off. The membrane was imaged with an Alpha Innotech FluorchemQ.

2.12 Enzyme analysis

His-tagged MEL1 and MEL1(D64A) produced in BL21(DE3) were affinity purified by nickel-agarose chromatography. pET28a-MEL1 and pET28a-MEL1(D64A) in *E. coli* BL21(DE3)pLysS cells were inoculated into 5 mL of LB with 50 μg/mL of

each kanamycin and chloramphenicol and grown overnight at 37°C in a rotating wheel. A 50 mL culture of LB with 50 μg/mL each of kanamycin and chloramphenicol was inoculated with 1 mL of the overnight culture and grown at 30°C, with shaking at 200 rpm, overnight. 20 mL of each 50mL culture was used to inoculate 2 L of LB with 50 μg/mL of each kanamycin and chloramphenicol. These cultures were grown at 30°C until the optical density at 600 nm reached 0.5 to 0.7, at which point the cultures were induced with 0.5 mM IPTG and grown overnight at 18°C with shaking at 180 rpm.

Cells where harvested by centrifugation at 5000 rpm for 15 minutes in a Sorvall RC6+ centrifuge (ThermoScientific, Waltham MA). Cells were then washed with approximately 100 mL of 0.85% NaCl and centrifuged for 15 minutes at 5000 rpm with an Eppendorf centrifuge 5810R and an A4 -6- 2 rotor (Eppendorf, Mississauga ON). The pellets were then resuspended in 80 mL of lysis buffer comprised of 20 mM sodium phosphate buffer (pH 7.4), 0.5 M NaCl, and 15 mM imidazole. Lysozyme (Invitrogen) was added to each tube of resuspended cells to a final concentration of approximately 1 mg/mL and incubated at room temperature for 30 minutes. Cells were then lysed by repeatedly freezing the suspension in liquid nitrogen, allowing it to thaw 3 times, and then sonicated with a sonicator (Sonics and Materials, Newtown CT) for 9 intervals of sonication for 30 seconds with rests in between on ice for 30 seconds. The samples were centrifuged at 15000 rpm for 1 hour at 4°C in a Sorvall RC6+ centrifuge in order to pellet the insoluble fraction. The soluble fraction was then filtered through a 0.45 μM filter into a clean flask and kept at 4°C.

The nickel-agarose (Qiagen, Germantown MD) was resuspended in the storage buffer and poured into a Poly-Prep Chromatography Column (Bio-Rad) so that the final

agarose volume was approximately 0.5 mL. The column was then equilibrated with 30 mL of lysis buffer. The filtered soluble fraction from the cells was applied to the column and then rinsed with 30 mL of lysis buffer. The proteins were eluted with a stepwise imidazole gradient of 50 mM, 100 mM, 150 mM, and 200 mM imidazole. Approximately 10 mL of each elution buffer, comprised of 20 mM sodium phosphate (pH 7.4), 0.5 M NaCl, and varying imidazole concentrations, was added to the column in succession and the elute collected in 1mL fractions. Western blot analysis was carried out as described previously to detect which elute fraction contained the highest levels of MEL1 or MEL1(D64A).

Fractions containing the highest amounts of enzyme were pooled and dialyzed against 50 mM potassium phosphate (pH 7.4) with 1 mM EDTA at 4°C overnight. Following dialysis, 0.5mL of the dialyzed fraction was concentrated using an Amicon Ultra-0.5, Ultracel-3 Membrane, 3kDa (Millipore, Darmstadt Germany) centrifuged at 14000g for 30 min at 4°C. Glycerol was added to the concentrated protein to a final concentration of 15%, and then the protein extract was aliquoted and frozen at -80°C until use.

The acyl-CoA thioesterase activity of MEL1 and MEL1 (D64A) was measured using 5,5'-dithiobis-(2-nitrobenzoic acid) (DTNB) (Sigma Aldrich, Oakville ON). DTNB reacts with the sulfhydryl group in free Coenzyme A to form 5-thio-2-nitrobenzoate (TNB). TNB absorbs light at 412 nm with an extinction coefficient of 13600 $M^{-1}cm^{-1}$ (Ellman, 1958). The enzymatic reactions were carried out in a 96 well plate (Greiner bio-one, Frickenhausen DE) with 50 mM KCl, and 0.3 mM DTNB as outlined by Wei *et al.* (2009). To each 200 µL reaction, palmitoyl-CoA (Sigma Aldrich,

Oakville ON) was added to a final concentration of 50 μM. Reactions were mixed through gentle pipetting and 2 μL of concentrated MEL1 enzyme was added to each reaction. Reactions were carried out at 30°C with absorbance readings taken at 410 nm at 10 minute intervals for 10 hours with a FLUOstar OPTIMA microplate reader (BMG Labtech, Offenburg, DE).

Enzymatic reactions can be influenced by many factors including buffer pH and composition. Reactions were carried out as outlined above with the various buffers: 10 mM sodium citrate pH 5 and pH 6, 10 mM sodium phosphate pH 6, pH 7, pH 7.5, pH 8, 10 mM HEPES pH 7, pH 7.5 and pH 8, and 10 mM TRIS pH 8. Differences in activity were determined by using the Beer's-Lambert law to determine the concentration of hydrolyzed CoA present after 150 minutes, a time point during the linear phase of enzymatic activity for all buffers tested.

Based on the above optimization, the MEL1 thioesterase activity was determined in the final mixture: 10 mM sodium phosphate (pH 8), 50 mM KCl, 0.3 mM DTNB, 50 μM palmitoyl – CoA, and 2 μL of enzyme. All reactions were carried out in triplicate. The blank reactions contained dialysis buffer.

2.13 Co-regulation of extracellular lipid biosynthetic genes

The Expression Angler (http://bar.utoronto.ca/) tool provided by the Bio-Array Resource was used to identify thioesterases that may function in extracellular lipid biosynthesis (Toufighi *et al.*, 2005). The cuticle biosynthetic genes listed in Appendix 3 and the suberin biosynthetic genes listed in Appendix 4 were used to search the NASCArrays 392 dataset with an R-value cutoff of 0.5 for correlated genes. The lists of

correlated genes were then manually mined for genes that correlate with multiple known lipid biosynthetic genes. The microarray data generated by Suh *et al.* (2005) was used to identify candidate genes expressed in the epidermal layer of stems and gene annotations were used to identify putative thioesterases.

2.14 Bioinformatics

Sequences for bioinformatic analysis were aligned with ClustalW (Larkin *et al*, 2007). Sequences for verified and predicted single Hotdog fold proteins from a variety of plant species, based on the alignments in Yu *et al.* (2010) and Ben-Israel *et al.* (2009), were retrieved from NCBI. Catalytic residues were identified by aligning the well characterized 4-HBT protein sequence against the plant sequences (Benning *et al.*, 1998). The tertiary structure of the MEL proteins was predicted using the homology modeling program Swiss-Model, using the *Pseudomonas* sp. Strain CBS-3 4HBT enzyme as a template (pdb:1LO7_A) (Arnold *et al,* 2006, Kiefer *et al.*, 2009, Peitsch *et al.*, 1995). Following sequence alignment, neighbor-joining phylogenetic trees were generated with ClustalW (Larkin *et al.*, 2007) to examine the evolutionary relationship between the MEL enzymes.

Chapter 3: Results

3.1 Identification of a thioesterase gene family associated with extracellular lipid biosynthesis.

In silico co-regulation analysis was used to identify a novel gene encoding a thioesterase associated with cuticle biosynthesis. Genes that consistently co-expressed with 29 known cuticle biosynthetic genes (Appendix 3) were identified by inspection of 392 publically available DNA microarray experiments, using the Expression Angler tool of the Bio-Array Resource for Plant Biology (Toufighi *et al.*, 2005) (http://bar.utoronto.ca/). Thirty-nine candidate genes annotated as encoding lipid biosynthetic enzymes were identified as significantly co-regulated with 2 or more cuticle-associated genes (Table 2). Of these, 26 were expressed in the epidermal cell layer at levels high enough to be detected above the background noise in the DNA microarray study of Suh *et al.*, 2005, which identified epidermally enriched transcripts in *Arabidopsis*. Twenty-one of these 26 genes were found to be preferentially expressed at least 2-fold in the epidermal layer compared to underlying tissues either at the top or bottom of the stem (Suh *et al.*, 2005) (Table 2). Members of several families of lipid biosynthetic genes were identified as being co-regulated, such as lipid transfer proteins, β-ketoacyl-CoA synthases, and fatty acid ω-hydroxylases. Of these co-regulated and epidermally expressed genes, one was annotated as a thioesterase, At1g35290, which co-regulates with 6 cuticle biosynthetic genes (Table 2). We have tentatively named At1g35290 as *MODIFIER OF EXTRACELLULAR LIPIDS 1* (*MEL1*). By using *MEL1* as bait in the Expression Angler tool, the reverse analysis was carried out and co-regulated

genes identified. As expected, the same 6 known cuticle-associated genes were co-regulated with a Pearson correlation coefficient greater then 0.5 (Table 3). Based on a DNA microarray experiment, *MEL1* transcript levels are increased by 3-fold at the stop of the stem, relative to underlying tissues, and 2-fold at the base of the stem (Suh *et al.*, 2005) (Table2).

Three genes related to *MEL1* were identified in the *Arabidopsis* genome: At1g35250 (*MEL2*), At1g68260 (*MEL3*), and At1g68280 (*MEL4*). The Expression Angler tool was also used to identify co-regulated genes with known suberin-associated genes (Appendix 4). 28 genes were identified that co-regulate with known suberin biosynthetic genes with a Pearson correlation coefficient greater then 0.5, including *MEL2* (Table 4). Using *MEL2* as bait in the Expression Angler tool, 7 known suberin associated co-regulated genes were identified (Table 5). While both *MEL1* and *MEL2* co-regulate with extra-cellular lipid biosynthetic genes, *MEL3* gene expression did not obviously correlate with any extracellular lipid biosynthetic genes by inspection of previously published DNA microarray experiments. *MEL4* is not present on any current DNA microarrays and therefore co-regulation analysis is not possible.

Table 2: Genes that are co-expressed with known cuticle biosynthetic genes in DNA microarray experiments.

Candidate cuticle associated genes were identified using the known cuticle genes listed in Appendix 3 as baits in the BAR Expression Angler tool (Toufighi *et al.*, 2005). Candidate genes were further narrowed based on whether or not they showed epidermal expression in microarray experiment carried out by Suh *et al.* (2005). [a] The mean fold change in transcript levels found in the epidermis compared to underlying cell layers (Suh *et al.*, 2005).

Annotation	AGI number	Number of co-regulated known cuticle-associated genes	Epidermal expression	Top epidermal ratio [a]	Base epidermal ratio [a]
Lipid transfer protein	At1g62500	8	Y	1.5	1.2
Lipid transfer protein (LTP6)	At3g08770	6	Y	1.2	3.9
Lipid transfer protein (LTP5)	At3g51600	5	Y	2.8	3.6
Lipid transfer protein	At3g43720	4	Y	3.2	4.7
Lipid transfer protein	At5g62080	4	Y	1.6	1.2
Lipid transfer protein (LTP4)	At5g59310	4	Y	1.5	1.4
Lipid binding	At1g55260	3	Y	2.6	10.6
Lipid transfer protein (LTP7)	At2g15050	2	Y	4.3	3.4
Lipid transfer protein	At2g10940	2	Y	0.5	10.3
Lipid transfer protein (LTP3)	At5g59320	2	Y	1.6	1.5
β-ketoacyl-CoA synthase (CER60/KCS5)	At1g25450	4	Y	5.8	10.9
β-ketoacyl-CoA synthase (KCS10/FDH)	At2g26250	4	Y	4	3.9
β-ketoacyl-CoA synthase (KCS3)	At1g07720	4	Y	9.9	2.7
β-ketoacyl-CoA synthase (KCS19)	At5g04530	2	Y	8.7	41.3
Transferase	At1g65450	8	Y	3.8	6.5
Acyltransferase (LPAT5)	At3g18850	7	Y	2.3	2.2

Transferase	At3g48720	4	Y	4	4.8
Oxidoreductase (HOTHEAD)	At1g72970	6	Y	4.1	4.3
Oxidoreductase (CER1 LIKE)	At1g02190	7	Y	9.8	2.6
ABC transporter (WBC18)	At3g55110	9	Y	3	2.3
ABC transporter	At1g51460	6	Y	1	0.6
Fatty acid ω-hydroxylase (CYP86A7)	At1g63710	7	Y	2.7	6.5
Fatty acid ω-hydroxylase (CYP86A4)	At1g01600	4	Y	2.5	18.1
Thioesterase	At1g35290	6	Y	3	2.2
Fatty acid desaturase	At1g06350	4	Y	3.1	41.3
Aldehyde dehydrogenase (ALDH3F1)	At4g36250	4	Y	4.6	6.3
Lipid transfer protein	At1g66850	7	N	N/A	N/A
Lipid transfer protein	At5g07230	6	N	N/A	N/A
Lipid transfer protein	At3g07450	2	N	N/A	N/A
Lipid transfer protein (LTP12)	At3g51590	2	N	N/A	N/A
Glycine rich protein 19	At5g07550	5	N	N/A	N/A
Glycine rich protein 20	At5g07560	2	N	N/A	N/A
Glycerol 3-phosphate acytransferase (GPAT6)	At2g38110	6	N	N/A	N/A
Transferase	At5g23970	2	N	N/A	N/A
Short-chain dehydrogenase/reductase (SDR)	At3g55290	6	N	N/A	N/A
Fatty Acid Reductase (MS2)	At3g11980	2	N	N/A	N/A
ABC transporter	At3g13220	2	N	N/A	N/A
3-ketoacyl-CoA synthase (KCS13)	At2g46720	4	N	N/A	N/A
Acyl-CoA synthetase (ACOS5)	At1g62940	2	N	N/A	N/A

Table 3: *MEL1* co-expresses with known cuticle biosynthetic genes.

R^2 is the Pearson correlation coefficient that represents the similarity of the gene expression patterns over 392 DNA microarray experiments. The closer the value is to 1, the more similar the gene expression pattern in the analyzed DNA microarray experiments (Toufighi *et al.*, 2005).

AGI number	Gene Name	R^2
At1g35290	*MEL1*	1.00
At1g57750	*MAH1*	0.712
At4g33790	*CER4*	0.643
At5g25390	*SHN2*	0.595
At5g37300	*WSD1*	0.587
At1g02205	*CER1*	0.545
At5g57800	*CER3*	0.517
At2g47240	*CER8*	0.512

Table 4: Genes that are co-expressed with known suberin biosynthetic genes in DNA microarray experiments.

Candidate suberin associated genes were identified using the known suberin associated genes listed in Appendix 4 as baits in the BAR Expression Angler tool (Toufighi *et al.*, 2005).

Annotation	AGI number	Number of co-regulated known suberin-associated genes
Lipid transfer protein	At5g13900	6
Lipid transfer protein	At2g18370	6
Lipid transfer protein	At3g58550	5
Lipid transfer protein	At2g48130	5
Lipid transfer protein	At3g22620	5
Lipid transfer protein	At3g53980	5
Lipid transfer protein	At4g22610	5
Lipid transfer protein	At5g05960	4
Lipid transfer protein	At5g46890	4
Lipid transfer protein related	At2g44300	4
Lipid transfer protein	At2g37870	3
Transferase	At1g78990	6
Transferase	At5g07870	5
Transferase	At5g63560	5
Transferase	At4g31910	4
ABC transporter	At5g13580	7
ABC transporter	At3g53510	6
ABC transporter	At1g53270	5
ABC transporter	At2g37360	4
ABC transporter	At5g19410	2
Thioesterase	At1g35250	6
FATA	At3g25110	2
Fatty acid desaturase	At1g06090	3
Short-chain dehydrogenase/reductase (SDR)	At1g64590	6
Alcohol dehydrogenase	At1g22440	4
Short-chain dehydrogenase/reductase (SDR)	At4g13180	4
Short-chain dehydrogenase/reductase (SDR)	At3g26760	2
Lipid binding	At4g33550	6

Table 5: *MEL2* co-expresses with known suberin biosynthesis genes.

R^2 is the Pearson correlation coefficient that represents the similarity of the gene expression patterns over 392 DNA microarray experiments. The closer the value is to 1, the more similar the gene expression pattern in the analyzed DNA microarray experiments (Toufighi *et al.*, 2005).

AGI number	Gene Name	R^2
At1g35250	*MEL2*	1.00
At3g44540	*FAR4*	0.74
At5g58860	*CYP86A1*	0.715
At5g23190	*CYP86B1*	0.709
At5g41040	*AFST*	0.657
At2g11430	*GPAT5*	0.607
At3g44550	*FAR5*	0.502

3.2 The predicted MEL proteins are Hotdog fold thioesterases

The predicted MEL proteins are relatively small, about 180 amino acids in length with a molecular weight of about 20 kDa. The MEL proteins share greater then 80% similarity with one another at the amino acid level (Figure 10A and B). The conserved domain database from NCBI identifies a single Hotdog fold domain within each of the MEL proteins, related to the 4HBT Hotdog fold subfamily (Figure 10C) (Marchler-Bauer *et al.*, 2009). All MEL proteins contain the conserved catalytic aspartate, position 64 in MEL1, identified in the bacterial 4HBT thioesterase, and two other conserved residues, a glycine at position 67 and a valine at position 69 in MEL1, which contribute to the binding pocket of the 4HBT thioesterase (Figure 10A). Many bacterial members of the 4HBT subfamily contain a conserved tyrosine residue at position 24 in 4HBT, which is predicted to function in nucleophilic attack (Thoden *et al.*, 2003), but this residue not conserved in the MELs. However a conserved tyrosine at position 27 in 4HBT may fulfill this role (Figure 10A; Appendix 5). These proteins are not only similar to the well-characterized 4HBT bacterial thioesterase (Benning *et al.*, 1998), but to several thioesterases from other plant species, including the recently characterized METHYLKETONE SYNTHASE 2 (MKS2) protein from *Solanum Habrochaites glabratum,* a species of tomato (Yu *et al.*, 2010) (Appendix 5).

Figure 10: The MEL protein family shares a high level of similarity and contains a single characteristic Hotdog fold domain.

The structure of the Hotdog fold is annotated on the alignment (α-helix (α) and β-sheet (β)). The catalytic aspartic acid mutated in the MEL1(D64A) mutant is indicated with an asterisk (A). The phylogenetic tree indicates the similarity between MEL1 and MEL2 and MEL3 and MEL4, suggesting a possible gene duplication event. Distances are indicated on the tree (B). A three dimensional representation of the MEL1 protein sequence modeled on the *Pseudomonas* 4-HBT backbone shows the characteristic Hotdog fold architecture using SWISS-MODEL (http://swissmodel.expasy.org/) (C). Accession numbers: At1g35290, NP_564457; At1g35250, NP_174759; At1g68260, NP_564926; At1g68280, NP_176995; 4HBT, 1LO7_A.

A)

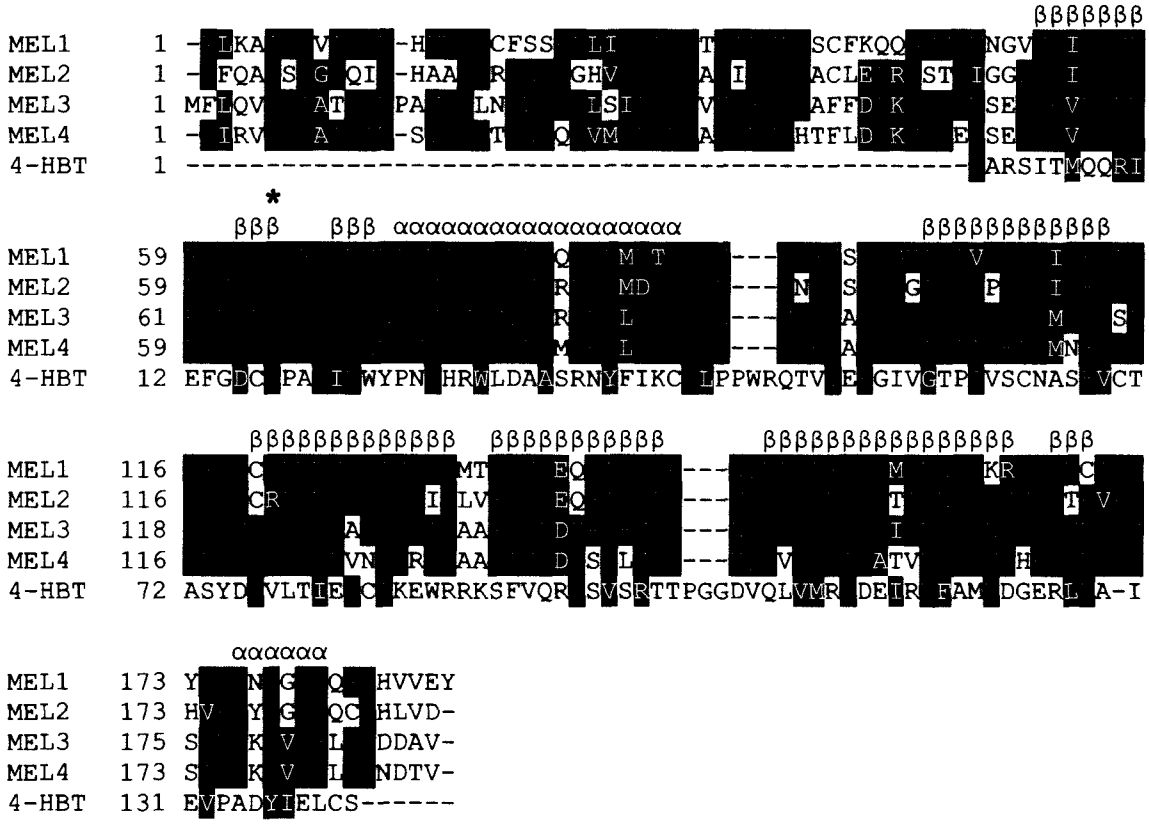
MEL1
MEL2
MEL3
MEL4
4-HBT

B)

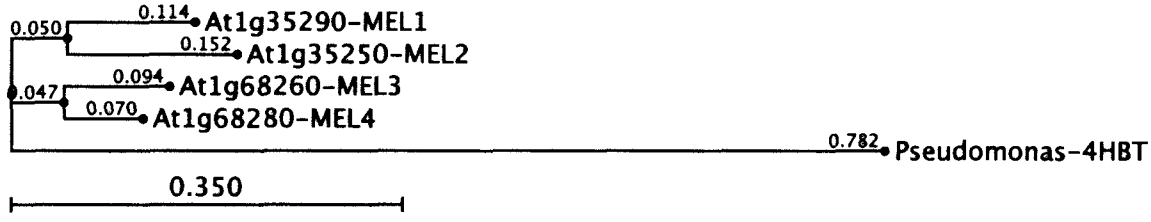
0.050
0.114
At1g35290-MEL1
0.152
At1g35250-MEL2
0.047
0.094
At1g68260-MEL3
0.070
At1g68280-MEL4
0.782
Pseudomonas-4HBT
0.350

C)

3.3 The *MEL* family members have distinct gene expression patterns

The tissue-specific gene expression patterns of the *MEL* genes were first determined by RT-PCR with RNA derived from the roots of 15 day-old seedlings, as well as stems, rosette leaves, and flowers of 6-week-old wild-type plants (Figure 11). *MEL1* expression was highest in stems and flowers, while *MEL2* was strongly expressed in roots. *MEL3* was expressed constitutively in all tissues tested. The gene expression patterns observed for *MEL1, MEL2,* and *MEL3* are in agreement with previously published DNA microarray data (Schmid *et al.*, 2005; Winter *et al.*, 2007). RT-PCR was also carried out for *MEL4*, which showed low levels of flower specific expression. However, upon sequencing of the cloned amplified products it was revealed to be *MEL3* transcript, indicating non-specific binding of the MEL4 RT primers.

The gene expression patterns of the *MEL* family were further investigated by fusing approximately 1800 bp of the genomic sequence upstream of the start codon of each gene in frame with the GUS reporter gene. Following transformation of wild-type *Arabidopsis*, GUS staining was carried out on at least 10 individual transformants in the first generation and repeated with several lines in the second generation. The promoter of *MEL1* drove the expression of GUS in the stem, flower, and siliques of *Arabidopsis,* which is consistent with the RT-PCR results (Figure 12A). Within the stem, GUS expression was specifically localized to the epidermal cell layer. Weak, but consistent, GUS expression driven by the *MEL1* promoter was also seen in the leaf (Figure 12A). This expression however was not detected by RT-PCR. *MEL1* is primarily expressed in the epidermis and therefore the transcript may be diluted by sub-surface cells in the whole leaf RNA extraction (Figure 12A) (Rowland *et al.*, 2006). GUS expression driven

by the *MEL2* promoter was found in the endodermal cell layer of the root (Figure 12B). The *MEL4* promoter drove GUS expression within the tapetal cells in flower anthers (Figure 12C). Expression of *MEL3* was also monitored with GUS expression. However, the expression pattern observed did not match the RT-PCR results and no consistent staining pattern was observed between individual lines. This indicates that the expression observed by GUS analysis was not representative of the native transcript.

To confirm *MEL1* epidermal-specific gene expression, an *in situ* hybridization experiment was carried out. This helped to ensure the expression patterns observed with the *MEL1* promoter GUS were representative of the endogenous transcript. A digoxygenin labeled antisense RNA probe was synthesized from the cDNA coding sequence in order to detect which cells in a stem cross section express *MEL1*. *MEL1* transcript was found exclusively in the epidermal cell layer of the stem (Figure 13). This supports the GUS expression, and is also consistent with previously published DNA microarray data (Table 2) (Suh *et al*, 2005).

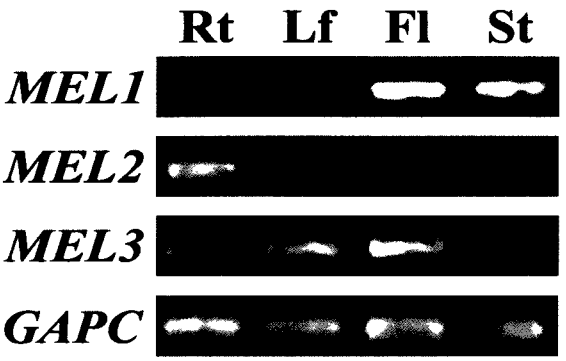

Figure 11: RT-PCR for the tissue specific expression patterns of the *MEL* gene family. RT-PCR to test for transcript was carried out in roots (Rt), leaf (Lf), flower (Fl), and stem (St). *GAPC* was used as a constitutively expressed loading control.

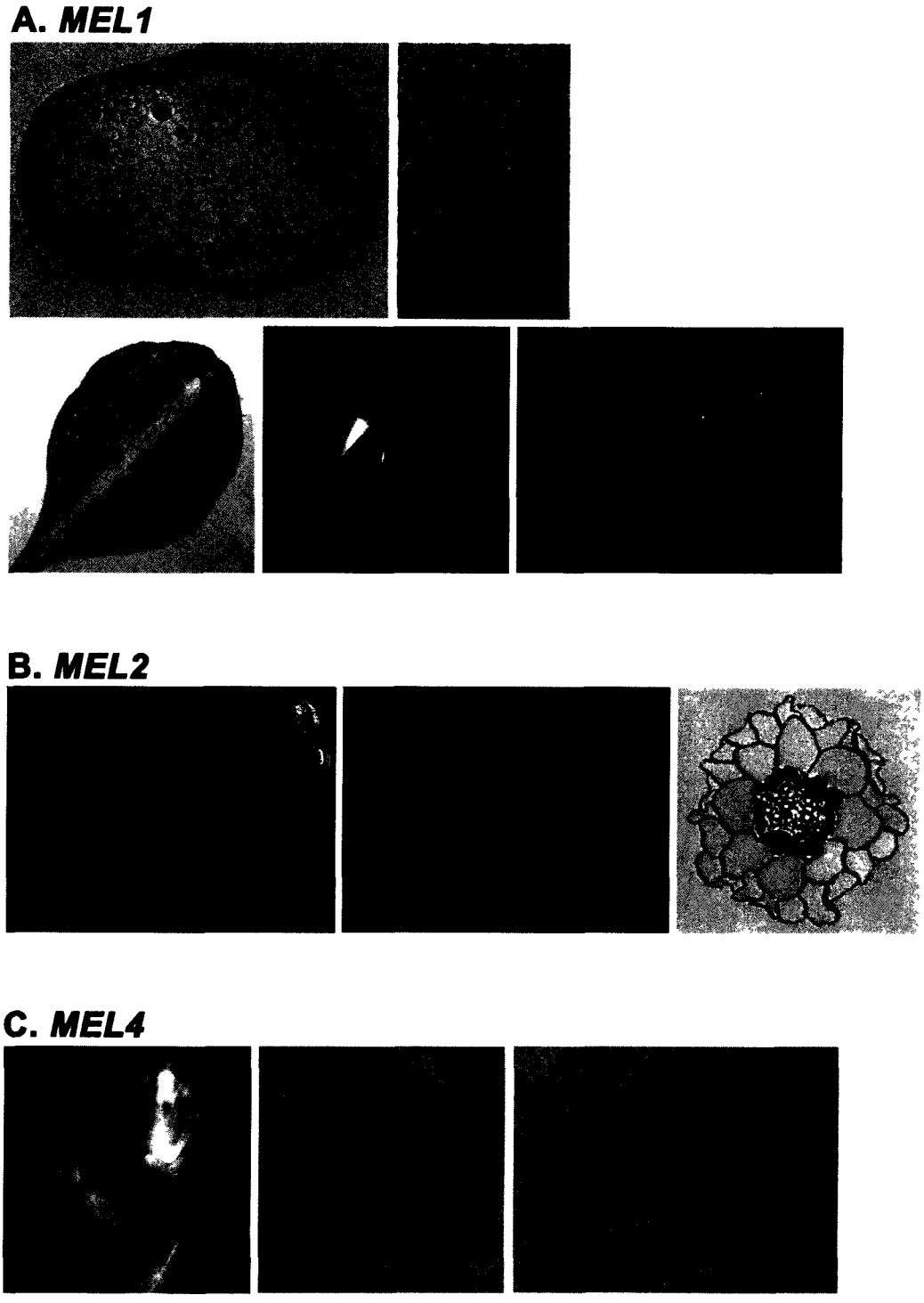

Figure 12: Expression of the GUS reporter gene driven by the *MEL* promoters. *MEL1* expression was found in stem, leaf, flower, and silique (**A**), *MEL2* expression was found in the root, specifically in the endodermal layer (**B**), and *MEL4* expression was found in tapetal cells of the anther (**C**).

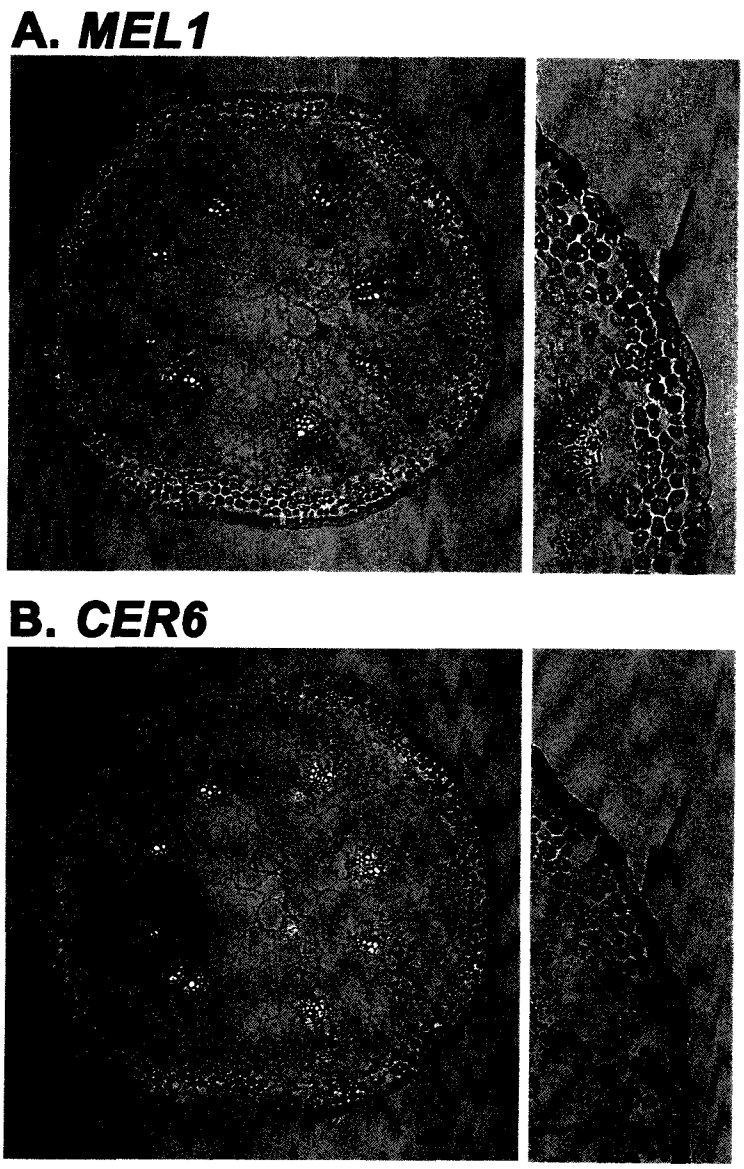

Figure 13: *MEL1* epidermal-specific expression as determined by *in situ* hybridization. Hybridization was carried out with a digoxygen labeled *MEL1* RNA antisense probe (**A**). *CER6* expression, which is epidermal specific, was used as a positive control (Hooker *et al.*, 2002) (**B**).

3.4 Silencing and over-expression of *MEL1* in *Arabidopsis*

There were no T-DNA or transposon insertion lines available for any of the *MEL* family members and therefore we were unable to obtain knock-out mutants for these genes commercially. To overcome this, artificial microRNAs (amiRNAs) were employed to decrease the *MEL1* transcript levels. Two separate amiRNA sequences (A and B) specifically targeting the *MEL1* transcript were cloned into binary vectors, downstream of the cauliflower mosaic virus 35S promoter, and transformed into *Arabidopsis* (Figure 14). The amiRNA sequences were cloned into both pBAR::35S and pVKH18::35S to maximize the odds that a successful knockdown line could be achieved. The pBAR::35S contains the core 35S promoter with one enhancer sequence and pVKH18::35S contains the core 35S promoter with six enhancer sequences. Within the first generation of transgenic plants, 5 of the 12 lines examined were identified by RT-PCR with decreased *MEL1* transcript in the flowers (Figure 15A and B). The numbering system for these five lines is found in Figure 15A. The progeny from the *MEL1 amiRNA-2* and *MEL1 amiRNA-5* lines, expressing amiRNA sequence A and B, respectively, were first analyzed in the second generation for alterations in the cuticular wax composition. In spite of decreased transcript in the flowers of the first generation, progeny from *MEL1 amiRNA-2* and *MEL1 amiRNA-5* showed varying transcript levels in the stem between individual plants in the T2 generation (Figure 16A). This is an indication that the *MEL1 amiRNA-2* and *MEL1 amiRNA-5* lines, which were generated using amiRNA sequences cloned into the pBAR::35S vector backbone, likely have unstable expression of the transgene. Nonetheless, the cuticular wax composition of *MEL1 amiRNA-2* and *MEL1 amiRNA-5* stems was analyzed by GC-FID. In comparison

to wild-type plants, the cuticular wax composition of *MEL1 amiRNA-2* and *MEL1 amiRNA-5* was not significantly changed (Figure 16C). This is in agreement with observations in the first generation, as no dramatic changes in cuticular wax composition were observed in that generation either (Appendix 6). However, the inconsistent silencing of the lines makes it difficult to make conclusions about the effects on wax load. Following the analysis of the cuticular wax composition of these plant lines, all subsequent analysis was carried out with *MEL1 amiRNA-1* and *MEL1 amiRNA-4* lines, which were generated using amiRNA sequences cloned into the pVKH18::35S vector in order to perhaps obtain consistently silenced lines.

MEL1 over-expression lines were also developed to determine if *MEL1* functions in cuticle biogenesis. Over-expression constructs were generated by cloning the *MEL1* cDNA sequence downstream of the 35S promoter in both the pBAR::35S and pVKH18::35S vectors. Following *Agrobacterium*-mediated transformation of *Arabidopsis,* transformants were screened by RT-PCR to identify transformants with increased *MEL1* transcript. Of 10 lines examined in the first generation, only 1 was identified with dramatically increased *MEL1* transcript levels: pBAR::35S-MEL1(5-4).11, which from herein is termed *MEL1-35S.* In the second generation, all plants examined by RT-PCR showed increased *MEL1* transcript levels in the stem (Figure 16B). Stems from individuals in the second generation were examined by GC-FID to determine if over-expression of *MEL1* influenced cuticular waxes. Similar to the results seen with *MEL1 amiRNA* lines, there was no obvious cuticular wax composition changes in the over-expression line when compared to wild-type (Figure 16C).

The cutin composition of *MEL1 amiRNA* lines was examined by GC-MS to observe if decreasing *MEL1* expression would influence the cutin composition of the leaves or stems. Due to the inconsistent silencing observed in *MEL1 amiRNA-2* and *MEL1 amiRNA-5* lines, *MEL1 amiRNA-1* and *MEL1 amiRNA-4* lines were used for cutin analysis. The transcript levels of *MEL1* in the progeny of *MEL1 amiRNA-1* and *MEL1 amiRNA-4* in the flowers were verified by RT-PCR and found to be nearly undetectable in 3 of 6 *MEL1 amiRNA-1* and 3 of 3 *MEL1 amiRNA-4* T2 plants (Figure 17). The cutin monomer composition in the stem or leaf was not significantly affected in the silenced lines in comparison to wild-type (Figure 18).

Figure 14: The MEL1_amiRNA-A and MEL1_amiRNA-B sequences aligned with the coding sequence from the various *MEL* genes.

Ideal amiRNA sequences have no mismatches in positions 1-9 and 12, and only have 1 or 2 mismatches in positions 13 – 21. The less mismatches that are present means the higher the specificity the amiRNA will have for the target (Ossowski *et al.*, 2008). Cross-specificity of MEL1_amiRNA-A with *MEL3* is unlikely due to the 2 mismatches in the 5' end of the amiRNA. Similarly, 3 mismatches are present in the 5' region between MEL1_amiRNA-A and *MEL2* as well as *MEL3*. There is a possibility for cross hybridization of MEL1_amiRNA-B with *MEL4* as there are no mismatches between MEL1_amiRNA-B and *MEL4* in the 5' end and only 2 mismatches in the 3' end. The tissue specificity, however, makes pleiotrophic effects unlikely. Between MEL1_amiRNA-B and *MEL3* and *MEL2,* cross hybridization is unlikely as *MEL3* contains a mismatch in the 5' region and *MEL2* contains 2 mismatches in the 5' region.

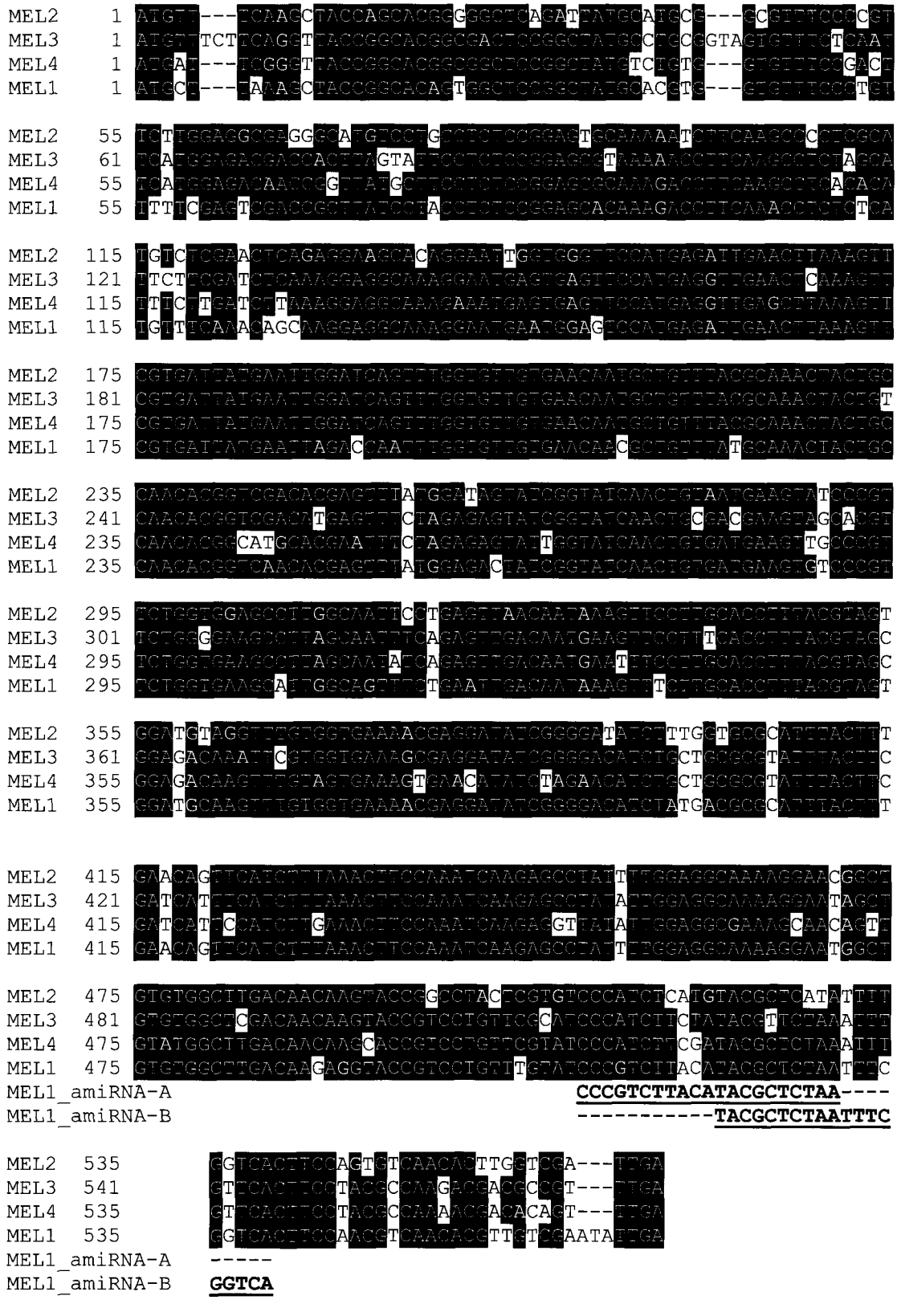
MEL2 1
MEL3 1
MEL4 1
MEL1 1
MEL2 55
MEL3 61
MEL4 55
MEL1 55
MEL2 115
MEL3 121
MEL4 115
MEL1 115
MEL2 175
MEL3 181
MEL4 175
MEL1 175
MEL2 235
MEL3 241
MEL4 235
MEL1 235
MEL2 295
MEL3 301
MEL4 295
MEL1 295
MEL2 355
MEL3 361
MEL4 355
MEL1 355
MEL2 415
MEL3 421
MEL4 415
MEL1 415
MEL2 475
MEL3 481
MEL4 475
MEL1 475
MEL1_amiRNA-A CCCGTCTTACATACGCTCTAA----
MEL1_amiRNA-B ----------TACGCTCTAATTTC
MEL2 535
MEL3 541
MEL4 535
MEL1 535
MEL1_amiRNA-A -----
MEL1_amiRNA-B GGTCA

A)

Revised plant line nomenclature	Vector backbone and amiRNA sequence
MEL1 amiRNA-1	pVKH18::35S-MEL1_amiRNA-B
MEL1 amiRNA-2	pBAR::35S-MEL1_amiRNA-A
MEL1 amiRNA-3	pBAR::35S-MEL1_amiRNA-B
MEL1 amiRNA-4	pVKH18::35S-MEL1_amiRNA-A
MEL1 amiRNA-5	pBAR::35S-MEL1_amiRNA-B

B)

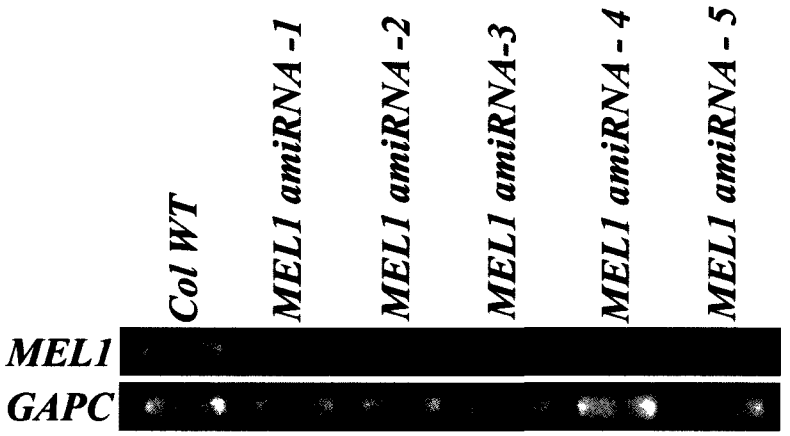

Figure 15: AmiRNA lines were developed to decrease *MEL1* transcript levels. Artificial microRNAs are synthesized by overlapping PCR to replace the naturally occurring *Arabidopsis miR319a* microRNA with artificial microRNAs directed against *MEL1* in the pre-*miR*319*a* backbone. Residues were selectively mutated to generate microRNAs specific to the *MEL1* sequence. (**A**) The nomenclature used to describe the individual plant lines in the text is outlined. (**B**) Several lines in the first generation were identified by RT-PCR with decreased *MEL1* transcript in flowers. *GAPC* was used as a constitutively expressed loading control in panel B.

Figure 16: Altering the transcript level of *MEL1* does not appear to affect the cuticular wax composition.

The lines *MEL1 amiRNA-5* and *MEL1 amiRNA-2* did not show consistent silencing in stem tissue (**A**). The *MEL1-35S* over-expression line identified in the first generation with increased *MEL1* transcript levels in stem tissue has consistently increased transcript in the second generation (**B**). *GAPC* was used as a constitutively expressed loading control for panels A and B. The levels of cuticular wax was quantified by GC-FID using methyl heptadecanoate as an internal standard and reported as $\mu g/dm^2$ (n=4) (**C**). Progeny from the *MEL1 amiRNA-5, MEL1 amiRNA-2*, and *MEL1-35S* lines were used either for RT-PCR or for cuticular wax analysis. ALK, alkane; ALD, aldehyde; FFA, free fatty acid; 1-OH, primary alcohol; KET, ketone; 2-OH, secondary alcohol.

A)

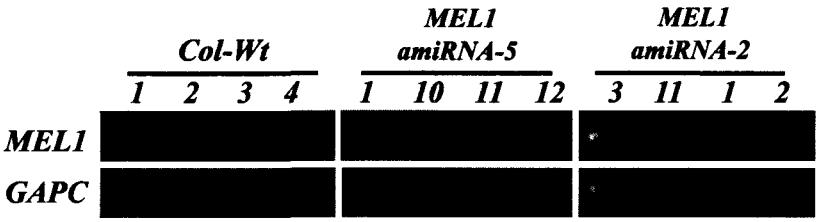
Col-Wt
MEL1 amiRNA-5
MEL1 amiRNA-2
1 2 3 4
1 10 11 12
3 11 1 2
MEL1
GAPC

B)

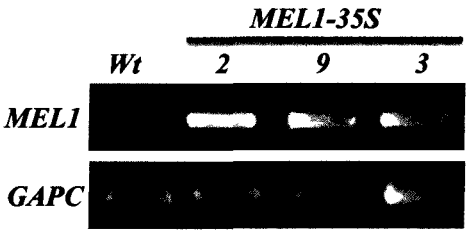
MEL1-35S
Wt
2
9
3
MEL1
GAPC

C)

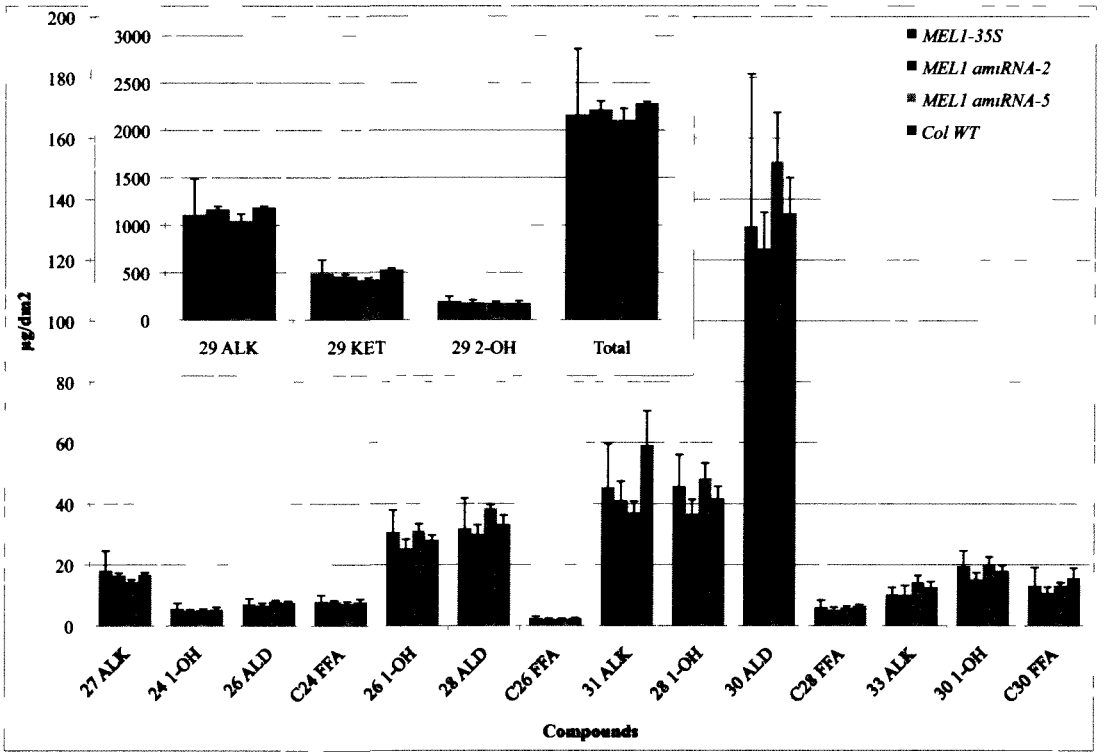
MEL1-35S
MEL1 amiRNA-2
MEL1 amiRNA-5
Col WT
pg/dm2
29 ALK
29 KET
29 2-OH
Total
27 ALK
24 1-OH
26 ALD
C24 FFA
26 1-OH
28 ALD
C26 FFA
31 ALK
28 1-OH
30 ALD
C28 FFA
33 ALK
30 1-OH
C30 FFA
Compounds

Figure 17: *MEL1 amiRNA* lines used for cutin composition analysis.

In the second generation, several plants were identified with having decreased *MEL1* transcript in flowers. *GAPC* was used as a constitutively expressed loading control. Cutin analysis was carried out on leaf and stem samples from the same T2 plants: *MEL1 amiRNA1-3*, *MEL1 amiRNA1-7*, *MEL1 amiRNA1-8* and all three of the *MEL1 amiRNA4 progeny* (Figure 18).

Figure 18: The cutin composition of leaf (**A**) and stem (**B**) samples from *MEL1 amiRNA-1* and *MEL1 amiRNA-4* lines.

Following delipidation, samples were sent to Dr. Frédéric Domergue, CNRS, Laboratory of Membrane Biogenesis, Bordeaux, France. The levels of various cutin-associated compounds were quantified by GC-MS and reported as μg/mg dry weight (DW) (n=3). OH, Alcohol; FFA, Free fatty acids; DCA, Dicarboxylic acid; wOH, ω-hydroxy fatty acid; diOH, 9,10 dihydroxy fatty acid; 2OH, 2-hydroxy fatty acid.

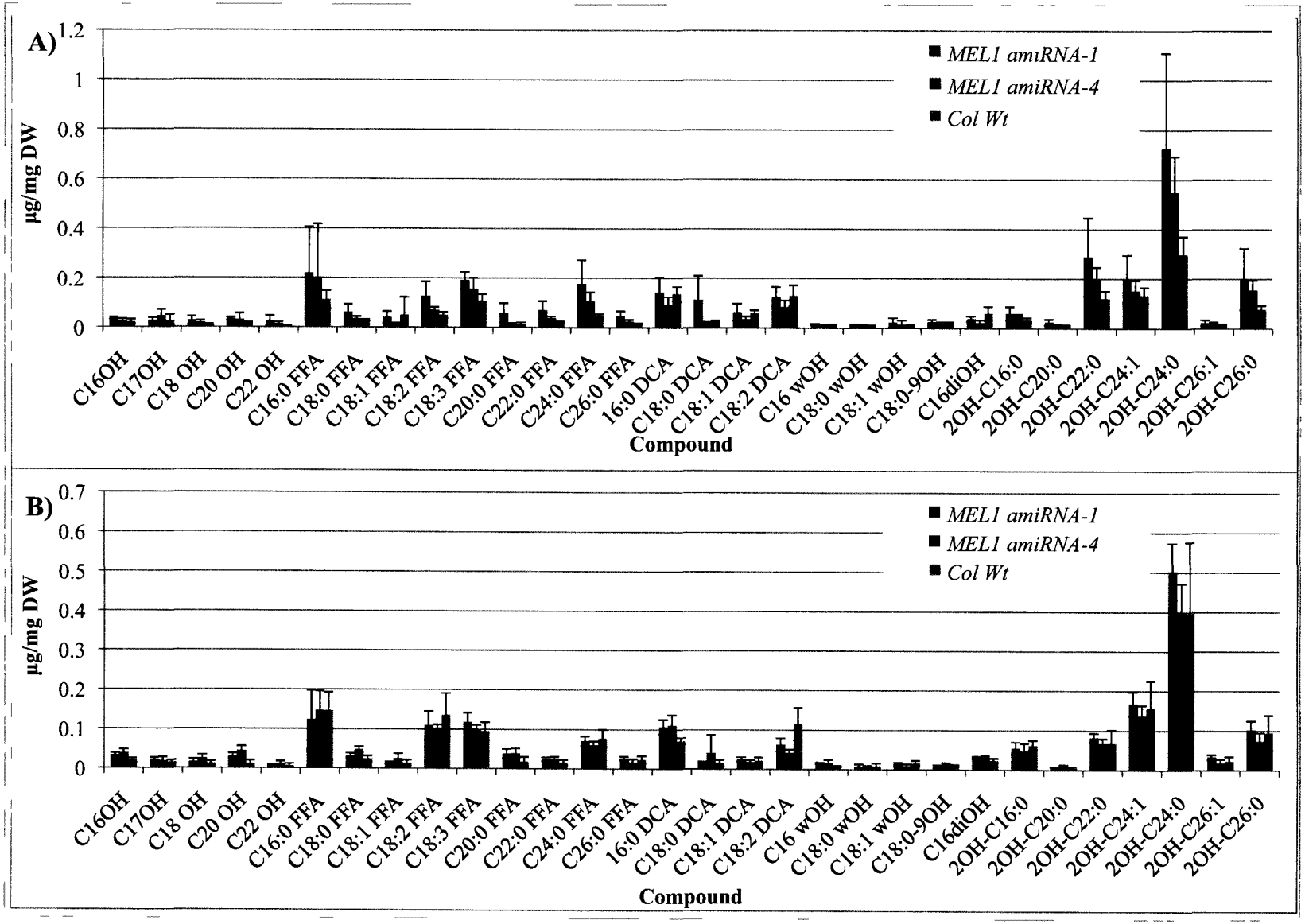
A)
µg/mg DW
1.2
1
0.8
0.6
0.4
0.2
0
MEL1 amiRNA-1
MEL1 amiRNA-4
Col Wt
C16OH
C17OH
C18 OH
C20 OH
C22 OH
C16:0 FFA
C18:0 FFA
C18:1 FFA
C18:2 FFA
C18:3 FFA
C20:0 FFA
C22:0 FFA
C24:0 FFA
C26:0 FFA
16:0 DCA
C18:0 DCA
C18:1 DCA
C18:2 DCA
C16 wOH
C18:0 wOH
C18:1 wOH
C18:0-9OH
C16diOH
2OH-C16:0
2OH-C20:0
2OH-C22:0
2OH-C24:1
2OH-C24:0
2OH-C26:1
2OH-C26:0
Compound
B)
µg/mg DW
0.7
0.6
0.5
0.4
0.3
0.2
0.1
0
MEL1 amiRNA-1
MEL1 amiRNA-4
Col Wt
C16OH
C17OH
C18 OH
C20 OH
C22 OH
C16:0 FFA
C18:0 FFA
C18:1 FFA
C18:2 FFA
C18:3 FFA
C20:0 FFA
C22:0 FFA
C24:0 FFA
C26:0 FFA
16:0 DCA
C18:0 DCA
C18:1 DCA
C18:2 DCA
C16 wOH
C18:0 wOH
C18:1 wOH
C18:0-9OH
C16diOH
2OH-C16:0
2OH-C20:0
2OH-C22:0
2OH-C24:1
2OH-C24:0
2OH-C26:1
2OH-C26:0
Compound

3.5 MEL1 has thioesterase activity *in vitro*

To examine the possibility that MEL1 has thioesterase activity *in vitro*, MEL1 was heterologously expressed as a fusion with a T7 epitope and Hisx6 tag. A key catalytic residue required for thioester bond cleavage has been identified in the related proteins 4HBT from *Pseudomonas* and MKS2 from *S. habrochaites* (Benning *et al.*, 1998; Yu *et al.*, 2010). This aspartate residue is not only 100% conserved in the MEL proteins, but also among 15 other uncharacterized single domain Hotdog fold proteins found in plant (Appendix 5). As a control to confirm that MEL1 is carrying out any measured hydrolytic activity, the catalytic aspartate codon at position 64 in *MEL1* was mutated to an alanine and the *MEL1(D64A)* coding region cloned into the *E. coli* expression vector as was done with wild-type *MEL1*. The MEL proteins were induced in BL21(DE3)pLysS *E. coli* cells. For comparison, the *MEL2* and *MEL3* coding sequences were also expressed in *E. coli*. A cDNA for *MEL4* was not successfully isolated. None of the MEL proteins expressed to high levels in BL21 cells, but the expression of the tagged proteins was detectable by Western blot analysis (Figure 19).

The MEL1 and MEL(D64A) proteins produced in BL21(DE3)pLysS were purified using a nickel agarose column. Neither of the proteins was able to be purified to high concentrations, even after centrifugal membrane filtration. It appears that MEL1 purified to near homogeneity, but the MEL1(D64A) extract had a contaminant band at approximately 46 kDa (Figure 20). Following purification, the MEL1 and MEL1(D64A) enzymes were used to test for thioesterase activity with palmitoyl-CoA (C16:0-CoA) substrate.

Using the general reaction conditions outlined in Wei *et al* (2009), an optimal buffer composition and pH was found. The optimal buffer was found to be phosphate buffer (pH 8) (Figure 21). In phosphate buffer (pH 8) MEL1 hydrolyzed palmitoyl-CoA at a rate of approximately 0.09 μmol/min, which is approximately 0.01 μmol/min higher then in HEPES (pH 7.5), the second most active buffer. Based on this, the final enzyme reaction contained 10 mM sodium phosphate pH 8, 50 mM KCl, 0.3 mM DTNB, 50 μM palmitoyl-CoA, and 2 μL of each enzyme. Purified MEL1 was able to hydrolyze approximately 75% of the palmitoyl-CoA available as the concentration of hydrolyzed palmitoyl-CoA reached a maximum of 38 μM. MEL1(D64A) enzyme only hydrolyzed 12% of available substrate indicating that the MEL1 enzyme has significant acyl-CoA thioesterase activity (Figure 22A). The activity of MEL1 toward palmitoyl-CoA was 0.082 ± 0.028 μmol/min while the activity of MEL1(D64A) was 0.021 ± 0.014 μmol/min after 150 minutes, which is statistically significant based on a students T-test ($p = 0.007$, $\alpha = 0.05$) (Figure 22B).

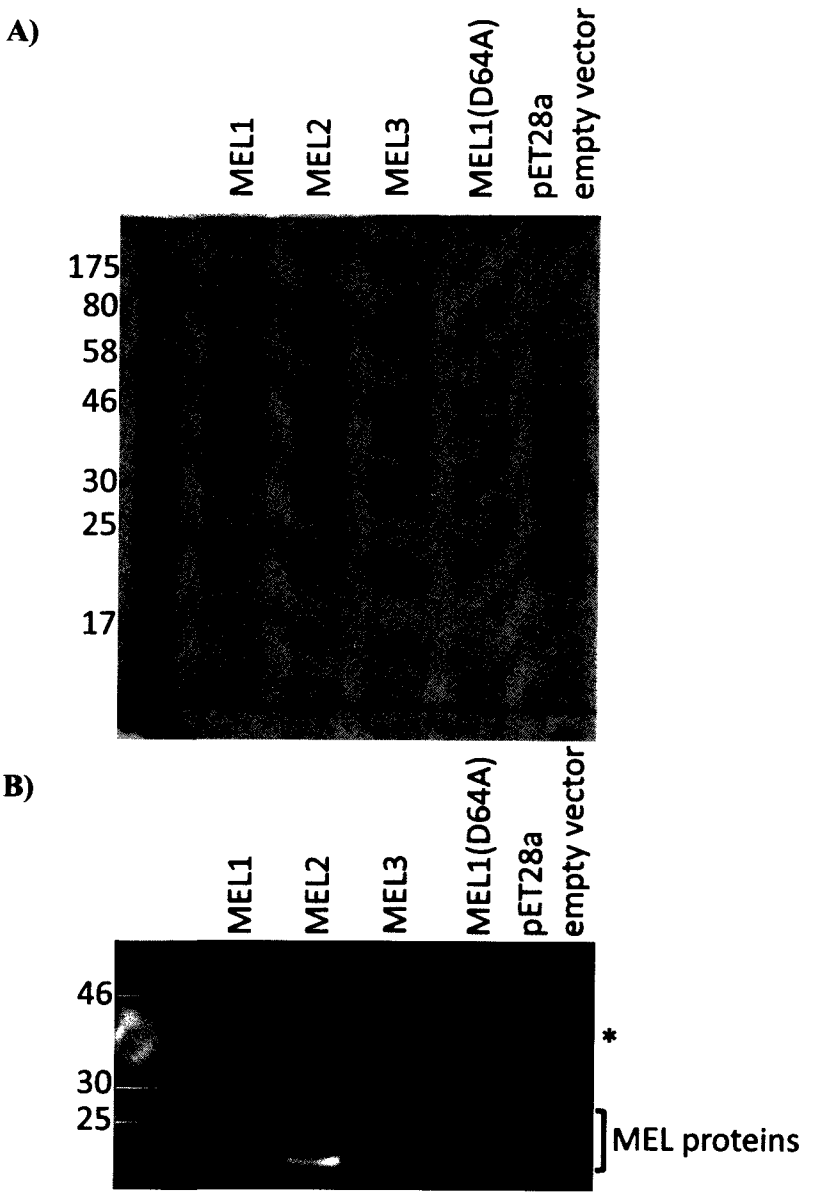

Figure 19: The MEL proteins expressed in BL21(DE3)pLysS *E. coli* cells. Crude protein fractions MEL1, MEL2, MEL3, MEL1 (D64A) and empty pET28a vector control run on a 12% SDS-PAGE gel stained with Coomassie Blue (**A**). Western blot analysis was performed on the same crude protein fractions using an antibody for the T7 epitope tag at the amino terminus (**B**). * indicates a non-specific band found in all samples, including empty vector controls.

A)

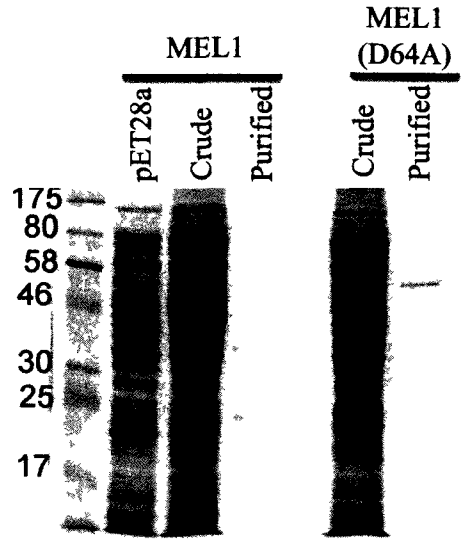

B)

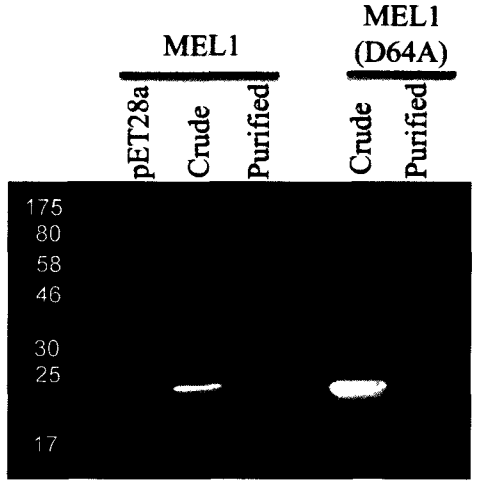

Figure 20: Purification of MEL1 and MEL1(D64A)

The proteins were purified by nickel agarose chromatography and concentrated with an Amicon Ultra-15 centrifuge filter. Protein from concentrated MEL1 and MEL1(D64A) fractions were run on a 12% SDS-PAGE gel with crude fractions from induced MEL1, MEL1(D64A) and pET28a empty vector and stained with Coomassie blue . The expected size of MEL1 and MEL1(D64A) was approximately 23 kDa (**A**). Western blot analysis was performed on the protein fractions used for Coomassie stain with an antibody for the T7 tag (**B**).

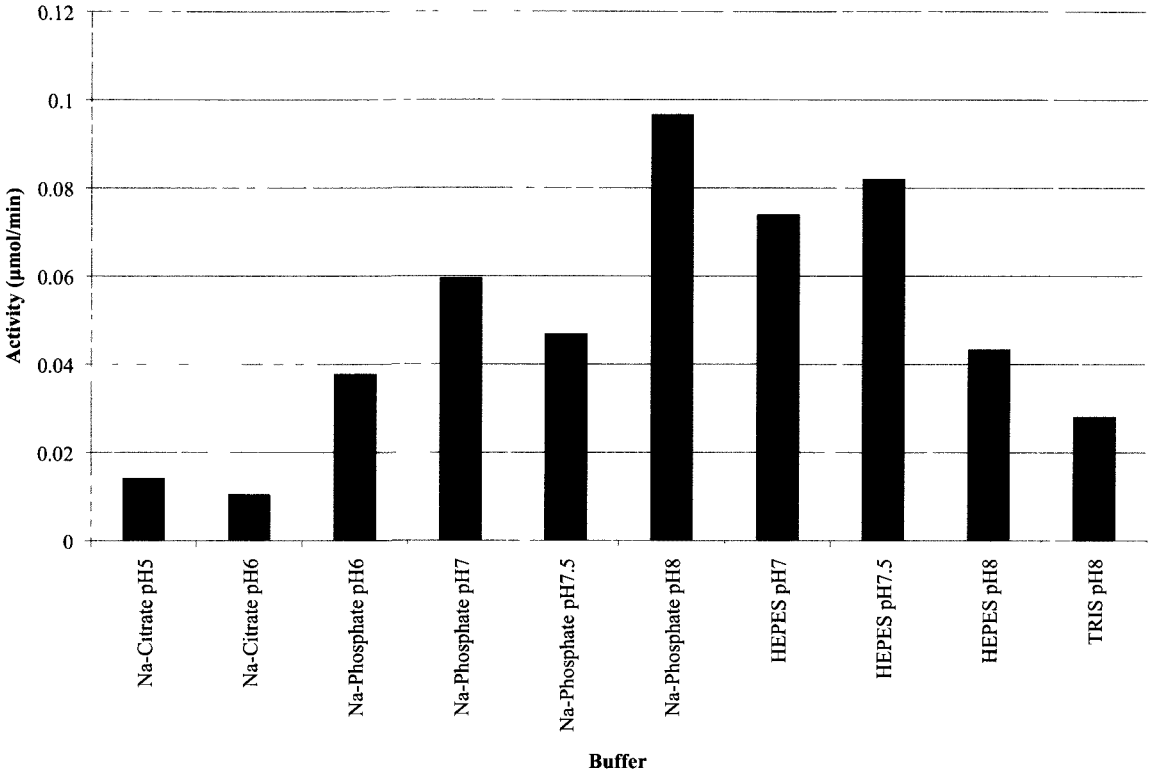

Figure 21: MEL1 is most active in sodium phosphate buffer (pH 8) (n=1).

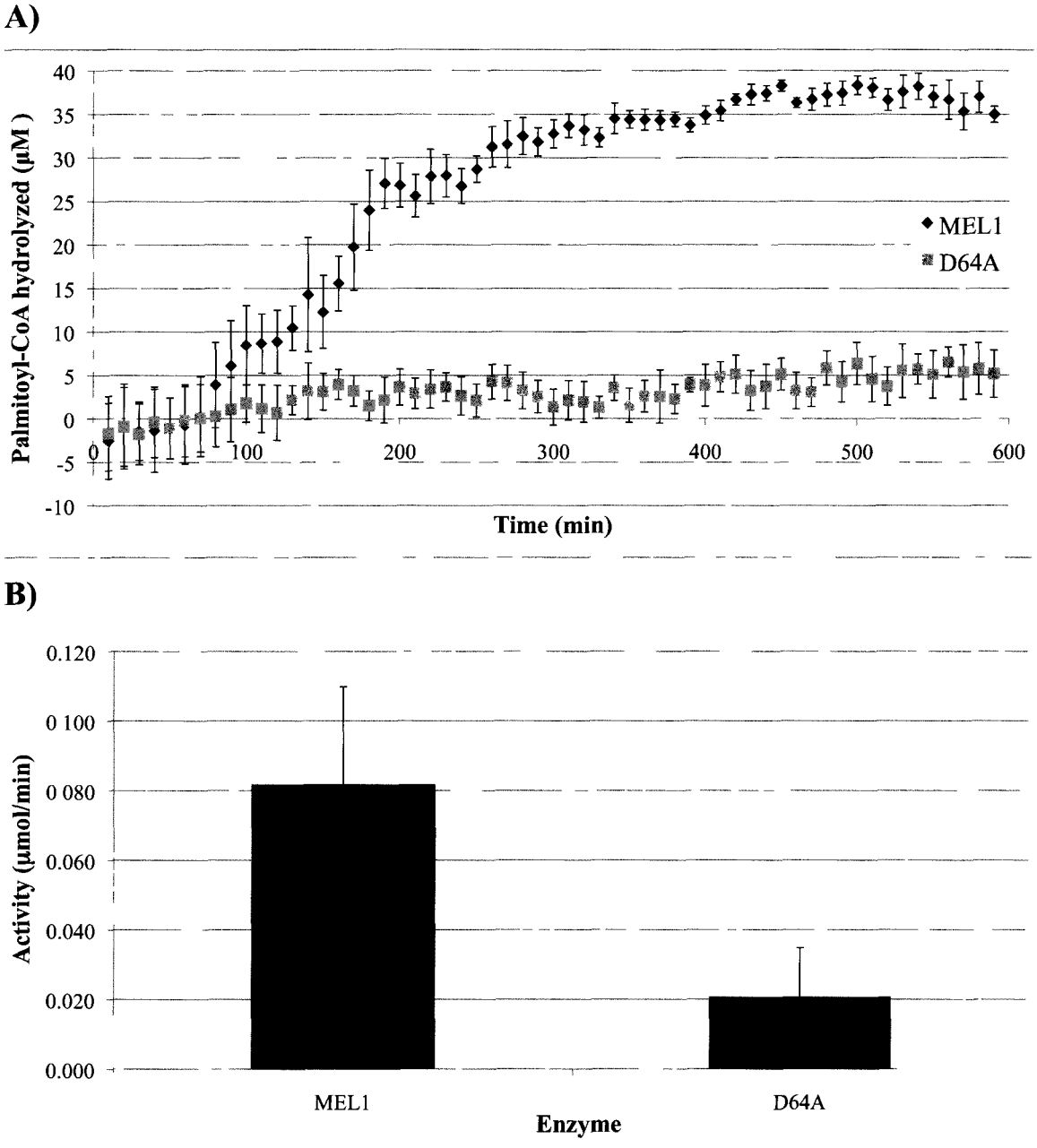

Figure 22: MEL1 is an active thioesterase using palmitoyl-CoA as a substrate.

The overall amount of palmitoyl – CoA hydrolyzed by the MEL1 enzyme is significantly higher then the mutant (**A**). After 150 min, the activity of MEL1 is much higher then the MEL1(D64A) mutant (**B**) (n=3).

3.6 The expression of MEL proteins in K27 *E. coli* cells leads to the detection of novel compounds in the media.

The MEL proteins were also expressed in K27(DE3) *E. coli* cells to test for the accumulation of fatty acids in the media. The K27 strain contains a mutation in the *FadD* gene, which prevents cells from importing fatty acids from the media and thus allows for the accumulation of lipids in the media for analysis by GC-FID (Overath *et al.*, 1969). The K27 cells were made lysogenic for T7 polymerase to allow inducible expression of proteins by IPTG (Lü *et al.*, 2009). A truncated version of FATB, a known thioesterase, lacking the plastid transit sequence was also expressed in these cells as a positive control for the accumulation of fatty acids (Mayer and Shanklin, 2007). The expression of MEL1, MEL2, MEL3, and MEL1(D64A) in K27(DE3) cells led to significantly higher levels of protein accumulation than observed in BL21(DE3)pLysS cells, such that induced proteins were now easily seen on a coomassie-stained gel (Figure 19A; Figure 23A). Following the expression of the MEL enzymes, the spent media was analyzed by GC-FID for the presence of fatty acids using palmitic acid (C16:0) and stearic acid (C18:0) as retention time standards. Expression of MEL1, MEL2, and MEL3 caused increased amounts of C18:1 fatty acid in the media. MEL1 expression also led to the production of C16:1 fatty acid in the media (Figure 24). C16:1 and C18:1 are the primary compounds that accumulate when FATB is expressed in K27(DE3) cells, providing a reference for the retention times of these compounds (Mayer and Shanklin, 2007). In addition to the accumulation of C16:1 and C18:1, the expression of MEL1, MEL2, and MEL3 lead to the accumulation of several other unidentified compounds not observed in either the empty vector or MEL1(D64A) mutant (Figure 24). The activity of

MEL1 to similar substrates as FATB confirms that the MEL protein family has acyl-ACP thioesterase activity.

The MKS2 protein from *S. habrochaites*, which is 73% similar to MEL1 at the amino acid level, has recently been characterized and found to have thioesterase activity towards β-ketomyristoyl-ACP in the tomato methylketone biosynthesis pathway in glandular trichomes (Ben-Israel *et al.,* 2009; Yu *et al.*, 2010). Following expression of MKS2 in BL21(DE3) *E. coli* cells, several methylketones, including 2-tridecanone (C13:0), were detected in the media following heat and acid treatment (Yu *et al.*, 2010). Due to the similarity between MKS2 and the MEL family of enzymes (Appendix 5), the MEL proteins were initially expressed in BL21(DE3) cells to test for the accumulation of methylketones via a β-ketoacid intermediate. However, upon discovering that the MEL proteins accumulated to much higher levels in K27(DE3) cells than in BL21(DE3) cells, the K27(DE3) cell line was used for this analysis (Figure 19A; Figure 23A). The expression of MEL proteins in K27(DE3) *E. coli* cells led to the accumulation of novel compounds in the media. MEL3 expression led to the accumulation of 2-tridecanone (C13:0) and 2-tridecenone (C13:1), with low levels of 2-undecanone (C11:0) and 2-petadecenone (C15:1) (Figure 25). The retention time of 2-tridecanone was verified with a commercial standard. However, the retention times associated with 2-tridecenone, 2-undecanone, and 2-pentadecenone were estimated based on the data presented by Yu *et al.* (2010). MEL2 expression led to the accumulation of low levels of the above-mentioned compounds and a large amount of an unknown compound with a retention time of 1.82 minutes (Figure 25). While the expression of MEL1 led to the accumulation of 2-undecanone, it did not appear to cause the accumulation of any of the other

identified methylketones (Figure 25). None of the methylketone compounds analyzed were present in either the vector alone control, MEL(D64A), or FATB-expressing cells, indicating that the accumulation is due to the activities of the MEL proteins (Figure 25). In addition to the presence of known methylketones, the expression of MEL1 and MEL2 lead to the accumulation of several other unidentified compounds in the spent media that were not found in the controls (Figure 25). The presence of methylketones in the media of K27(DE3) cells expressing the MEL proteins indicates that the MELs are able to hydrolyze the thioester bond in β-ketoacyl-ACP compounds to form β-ketoacids, which are then chemically converted to methylketones.

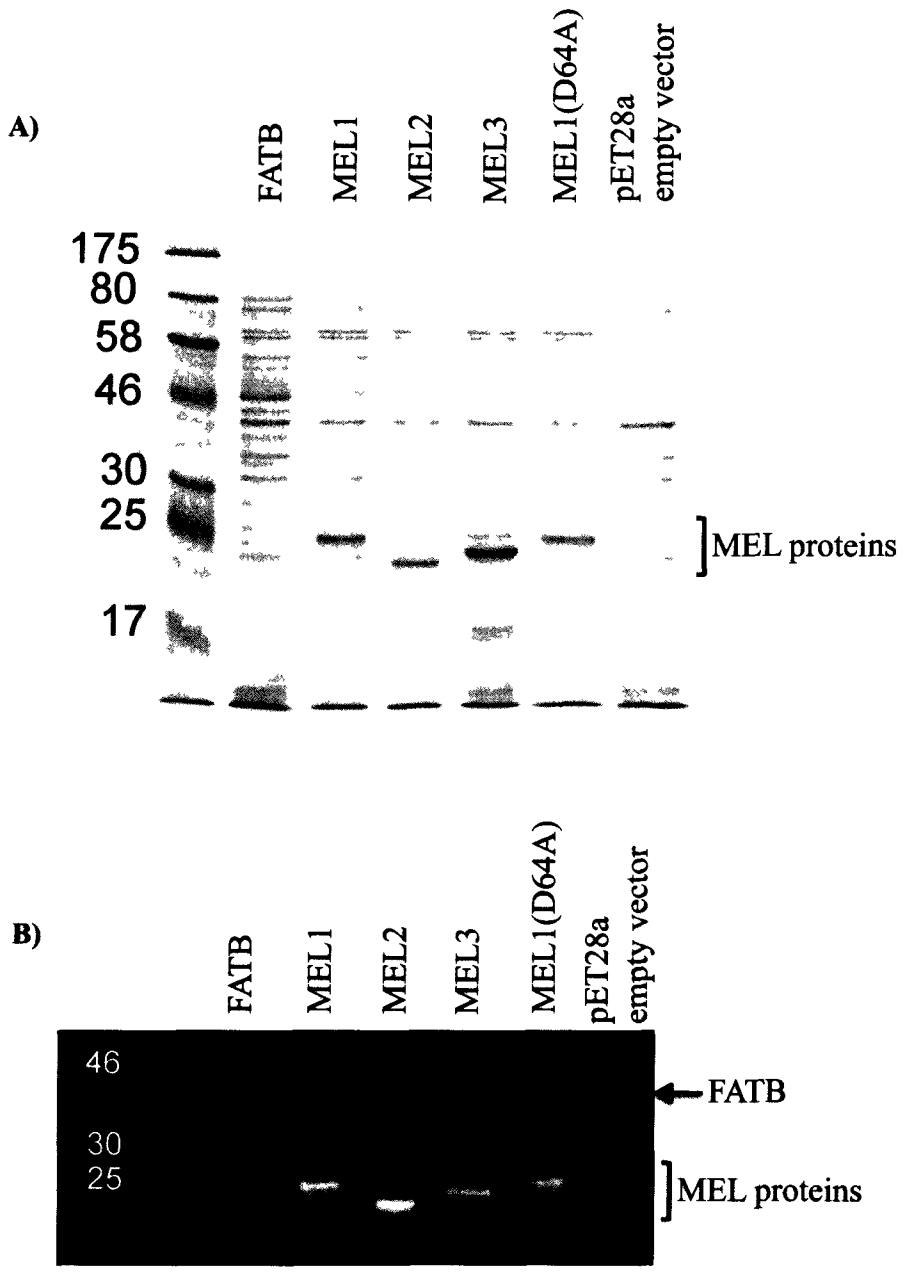

Figure 23: Expression of MEL1, MEL2, MEL3, MEL1(D64A), and FATB in the K27(DE3) *E. coli* cell line.

Crude protein fractions from MEL1, MEL2, MEL3, MEL1 (D64A) and the empty pET28a vector were run on a 12% SDS-PAGE gel and stained with Coomassie Blue (**A**). Western blot analysis was carried out on the protein fractions using an antibody against the T7 epitope (**B**).

Figure 24: Expression of MEL proteins in the K27 strain of *E. coli* leads to the accumulation of free fatty acids in the media.

The indicated C16:0 and C18:0 fatty acid retention times of 10.09 and 14.68 minutes, respectively, were confirmed by the retention time of commercial standards. The indicated C16:1 and C18:1 fatty acid peaks were predicted based on data presented by Mayer and Shanklin (2007). Peaks notated with an asterisk are novel peaks not seen in either the empty vector or mutant enzyme, which have yet to be identified. The traces presented are representative of 3 biological replicates.

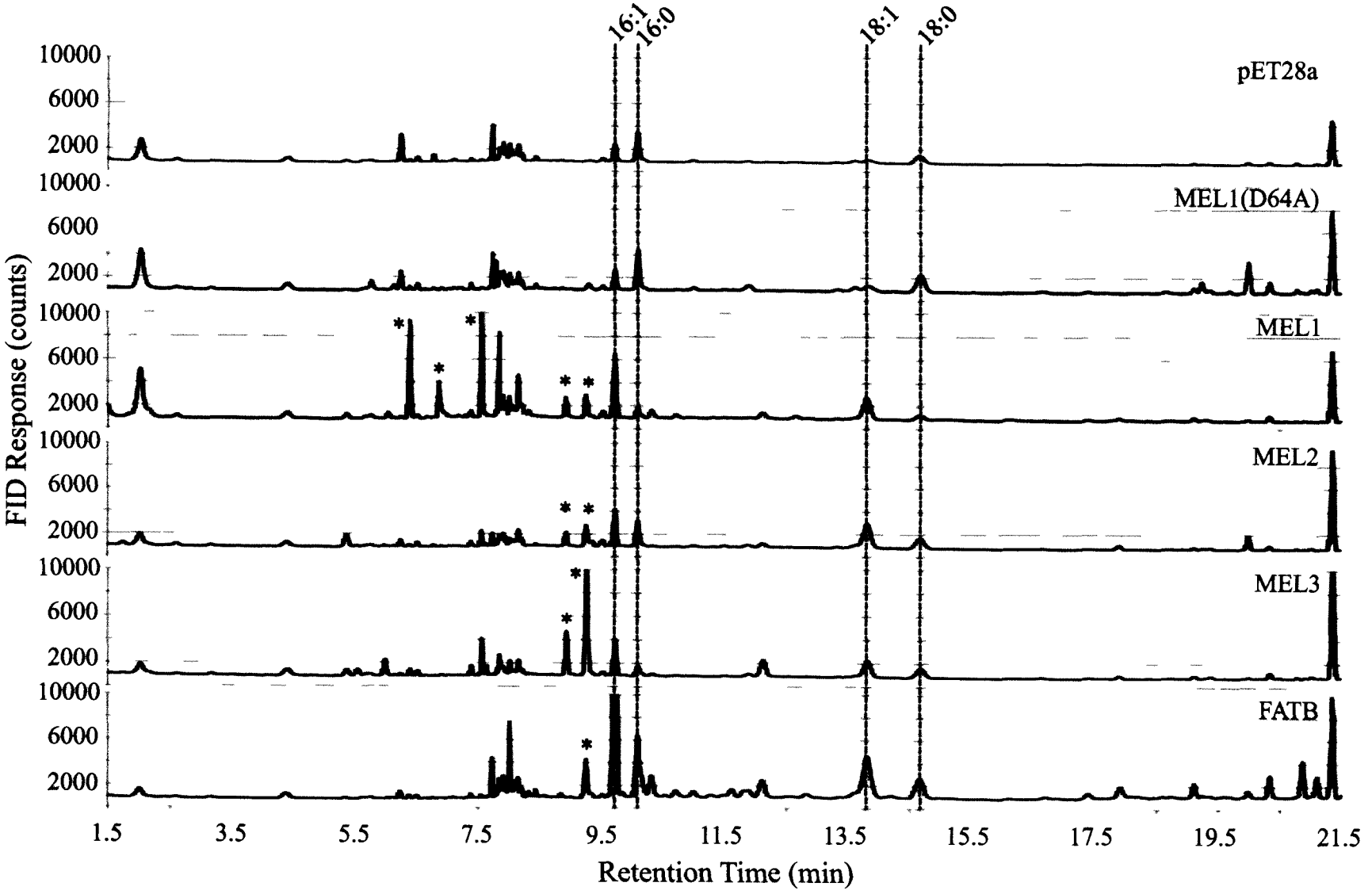
16:1
16:0
18:1
18:0
pET28a
MEL1(D64A)
MEL1
MEL2
MEL3
FATB
10000
6000
2000
FID Response (counts)
1.5
3.5
5.5
7.5
9.5
11.5
13.5
15.5
17.5
19.5
21.5
Retention Time (min)

Figure 25: The expression of MEL proteins in the K27 strain of *E. coli* leads to the accumulation of novel β-ketoacids in the media.

β-ketoacids are converted to methylketones chemically using 2M sulfuric acid for quantification as β-ketoacids are naturally unstable compounds. 2-tridecanone (C13:0) with a retention time of 13.72 minutes was confirmed by the retention time of the commercial standard. The compounds 2-undecanone (C11:0), 2-tridecenone (C13:1), and 2-pentadecenone (C15:1) were predicted based on the data presented in Yu *et al.* (2010). Peaks notated with an asterisk are novel peaks not seen in either the empty vector or mutant enzyme that have yet to be identified. The traces presented are representative of 3 biological replicates.

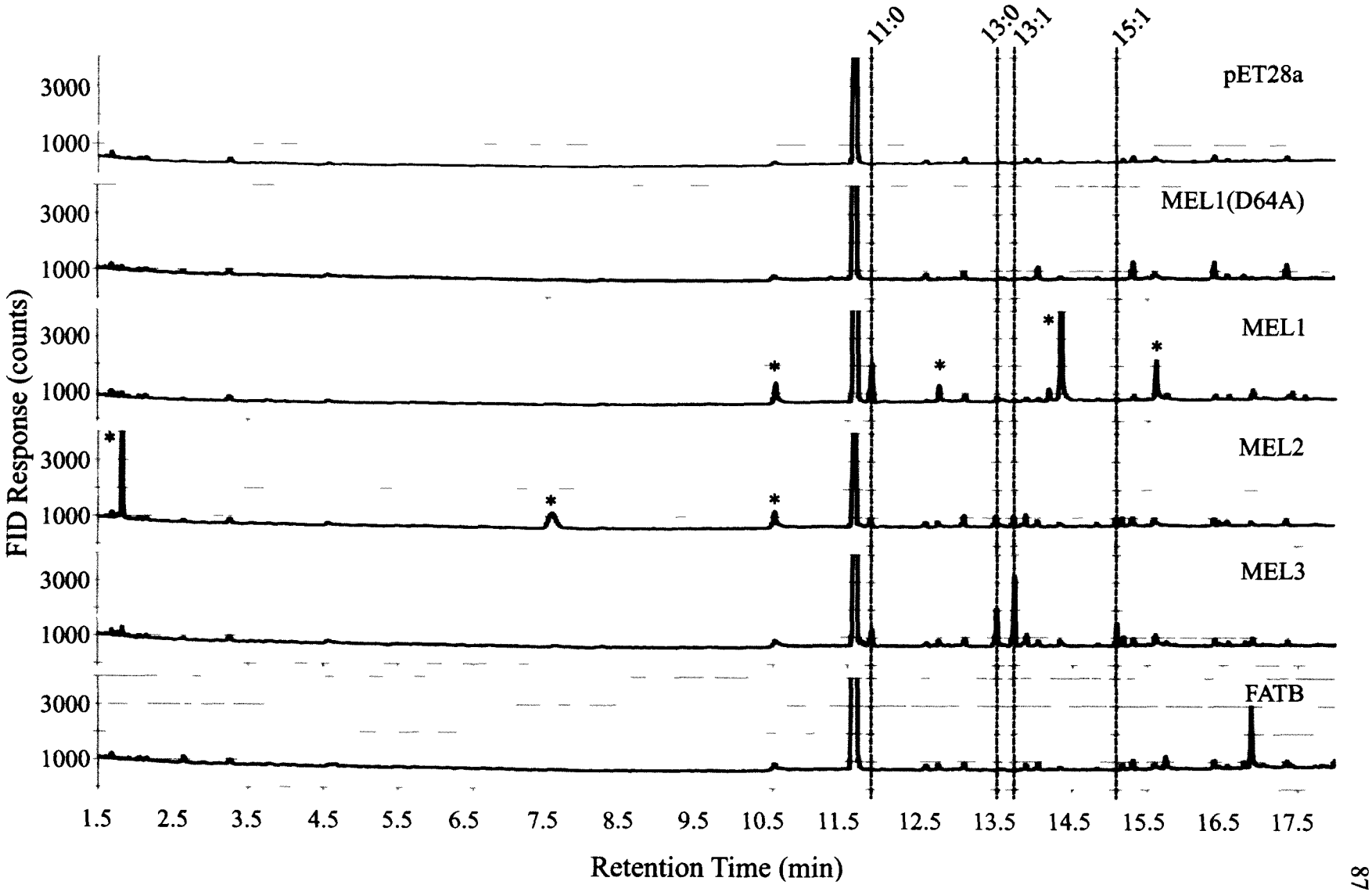
11:0
13:0
13:1
15:1
pET28a
MEL1(D64A)
MEL1
MEL2
MEL3
FATB
3000
1000
FID Response (counts)
1.5
2.5
3.5
4.5
5.5
6.5
7.5
8.5
9.5
10.5
11.5
12.5
13.5
14.5
15.5
16.5
17.5
Retention Time (min)

Chapter 4: Discussion

In this study, I have identified a four member gene family encoding thioesterases whose gene expression patterns are consistent with roles in extracellular lipid biosynthesis. The gene expression patterns of *MEL1*, *MEL2,* and *MEL4* were found to be associated with cells that produce cuticle, suberin, and sporopollenin, respectively. This division of roles is also found amongst gene family members encoding other enzyme types involved in generating these surface lipid barriers. The alcohol-forming fatty acyl-CoA reductase (FAR) family that produces various chain-length primary alcohols in each of the three barriers also shows this division of function (Aarts *et al.*, 1997; Rowland *et al.*, 2007; Domergue *et al.*, 2010). The strong expression of *MEL1* in the stem epidermis and flowers is reminiscent of *FAR3/CER4*, which is involved in synthesizing C24:0 to C30:0 primary alcohols found in cuticular wax (Rowland *et al.*, 2006). *MEL2*, with root endodermal expression, has an expression pattern that is more comparable to *FAR1, FAR4,* and *FAR5* that generate C18:0 to C22:0 primary alcohols associated with suberin (Domergue e*t al.*, 2010). Lastly, the expression of *MEL4* exclusively in the tapetal cells of the anther is similar to that of *FAR2/MS2*, which is thought to produce primary fatty alcohols specific for sporopollenin (Aarts *et al.*, 1997). *MEL3* was more widely expressed and therefore may have a more general role in lipid metabolism, rather than specific to extracellular lipids.

In cuticle biosynthesis, there are several roles for which thioesterases may be needed. These are: (1) production of free fatty acids (FFA) from C16 and C18 acyl-ACPs in the plastid to allow for export to cytosol, (2) production of free very-long-chain fatty acids following elongation at the ER, (3) production of FFA intermediates leading to

the synthesis of methylketones and then perhaps to alkanes, (4) production of FFA as a substrate for cytochrome P450 enzymes in the cutin biosynthetic pathway, and (5) production of balanced levels of FFA with the acyl-CoA pool for the control of gene expression of lipid biosynthetic genes as FFAs and acyl-CoAs have been shown to directly influence transcription factor activity in animals and bacteria. Apart from role (1), no thioesterase has yet been identified in *Arabidopsis* fulfilling any of the other postulated roles. The family of *Arabidopsis* thioesterases described here may fulfill one or more of these roles as discussed below.

4.1 Thioesterases in the plastid

The acyl-ACP thioesterases FATA and FATB in the plastid produce free fatty acids so that the acids can be exported through the plastid envelope and to the cytosol (Salas and Ohlrogge, 2002). Unlike thioesterases found in the ER, plastid localized thioesterases utilize substrates activated with ACP. FATB preferentially hydrolyzes C16:0 fatty acyl-ACP and FATA preferentially hydrolyzes C18:1 fatty acyl-ACP. Loss of the FATB gene in *Arabidopsis* leads to a 50% reduction in the overall wax load (Bonaventure *et al.*, 2003). While approximately 50% of the cuticular wax comes from C16:0 precursors derived from FATB activity, the other 50% must derive from the activity of some other thioesterase (Bonaventure *et al.*, 2003). Presumably, a portion of the other 50% comes from C16:0 and C18:0 fatty acids released via FATA activity, but given that FATA has a preference for C18:1 substrates it is possible that other plastid localized thioesterases are contributing to this 50% of saturated fatty acids emerging from the plastid (Liu and Post-Beittenmiller, 1995; Salas and Ohlrogge, 2002). Strong

candidates for these thioesterases may be the MEL proteins. The slow rate of hydrolysis observed with MEL1 toward palmitoyl-CoA may be because MEL1 prefers acyl-ACP substrates. Our evidence in *E. coli* shows that the MEL enzymes are able to utilize long-chain acyl-ACP substrates, which supports the hypothesis that MEL enzymes utilize activated substrates in the plastid. Salas and Ohrogge (2002) have shown that the activity of FATB toward acyl-ACP substrates prepared from *E. coli* is significantly less than its activity toward acyl-ACP substrates prepared from spinach. Therefore, to verify the activity of MEL1 for long-chain acyl-ACPs, long-chain acyl-ACPs should be synthesized from spinach extracts to observe if MEL1 has preferred activity for ACP activated substrates over CoA as presented here.

The MEL family shows high sequence similarity to a tomato enzyme MKS2, which has been shown to catalyze the thioesterase reaction forming free β-ketoacids (Yu *et al.*, 2010). MKS2 localizes to the plastid and therefore methylketones found in the trichomes of *S. habrochaites* are generated from β-ketoacyl-ACPs, which are intermediates in the fatty acid synthesis pathway (Yu *et al.*, 2010). Following the expression of the MEL enzymes in *E. coli,* both methylketones and free fatty acids accumulated in the media (Figure 24; Figure 25). The expression of FATB in these cells, however, only led to the accumulation of fatty acids and not methylketones. This indicates that MEL enzymes may have some dual functionality, cleaving ACP from both fully reduced fatty acyl-ACP and β-ketoacyl-ACP moieties. The ability of single Hotdog fold thioesterases to accommodate multiple substrates *in vitro* has previously been seen with hTHEM2, a thioesterase found in human mitochondria (Cheng, *et al.*, 2006). The first reported activity of this enzyme identified a preference for aromatic substrates, such

as 3,4-dihydroxyphenylacetyl-CoA (Cheng, *et al.*, 2006). Subsequent studies however identified an affinity for medium and long-chain fatty acyl-CoA substrates (Wei *et al.*, 2009). MEL enzymes may function primarily in the release of free fatty acids from the plastid, but when presented with β-ketoacyl-ACPs, free β-ketoacids can be produced that subsequently form methylketones. However, medium or long-chain methylketones have not been reported amongst the surface lipids of *Arabidopsis*. In tomato glandular trichomes, MKS2 may be specific for β-ketoacyl-ACPs and natural selection has lead to the high expression of this gene in trichomes for the accumulation of these methylketones. To test this hypothesis, the kinetics of paltmitoyl-ACP and various β-ketoacyl-ACP substrates can be compared using MKS2 and the various MEL enzymes. Testing the MKS2 spent media for the presence of free fatty acids would ascertain whether the duel substrate specificity seen with MELs is also present in MKS2. The preparation of the media and GC conditions to detect β-ketoacids and fatty acids are quite different and therefore fatty acids cannot be detected in samples prepared for methylketone analysis and vice versa.

4.2 Thioesterases in the production of very-long-chain free fatty acids

Very-long-chain free fatty acids are components of the cuticular waxes and account for 3.2% of total amounts in Arabidopsis stems (Jenks *et al.*, 1995; Pollard *et al.*, 2008). The FAE complex utilizes acyl-chains activated with CoA and therefore a very-long-chain thioesterase would likely be needed to release the free fatty acid for subsequent secretion to the cuticle. *In vitro*, MEL1 is able to hydrolyze palmitoyl-CoA, but the rate of hydrolysis observed was quite slow (Figure 22). However, MEL1 may be

more active toward very-long-chain fatty acyl-CoAs instead of long-chain acyl-CoAs. The expression of MEL1, MEL2, and MEL3 in *E. coli* cells led to the accumulation of a variety of fatty acids in the media including C18:1 and C16:1 (Figure 24). This activity observed in *E. coli* would suggest that the MELs can utilize monounsaturated long-chain fatty acyl substrates, but these may not be biologically relevant. *E. coli* do not produce very-long-chain substrates and therefore the activity observed by MEL1, MEL2, and MEL3 could be limited by substrate availability. This has previously been seen with FAR enzymes when expressed in *E. coli* (Doan *et al*, 2009). By examining the cuticular waxes of the *cer4/far3* mutant, it has been determined that the *in planta* substrate specificity of CER4/FAR3 is C24:0 to C30:0 acyl-CoAs (Rowland *et al.*, 2006). However, CER4 expression in *E. coli* caused the accumulation of C18:1 and C16:0 primary alcohols (Doan *et al.*, 2009). Conversely, expression of CER4/FAR3 in yeast yielded C24:0 and C26:0 primary alcohols, which is consistent with the mutant phenotype (Rowland *et al.*, 2006). To further assess the substrate specificities of the MEL proteins, they could be expressed in yeast and the spent media examined for the presence of very-long-chain fatty acids as yeast possess up to C26:0 very-long-chain fatty acyl-CoAs. *In vitro* assays with very-long-chain acyl-CoAs are difficult, if not impossible, due to the hydrophobicity of very-long-chain fatty acids and therefore yeast heterologous expression may be the best technique with which to test the substrate specificities of the various MELs.

4.3 Thioesterases in the biosynthesis of β-ketoacids and alkanes

The current proposed model of alkane synthesis involves a two-enzyme system in which the first is an aldehyde-forming FAR and the second is an aldehyde decarbonylase (Figure 26A) (Cheesborough and Kolattukudy, 1984). Evidence for this came from studies in *Pisum sativum* where partial enzyme purification indicated an aldehyde decarbonylase activity releasing carbon monoxide from the aldehyde intermediate (Cheesborough and Kolattukudy, 1984; Schneider-Belhaddad and Kolattukudy, 2000). There are reports of an aldehyde-forming FAR protein in both *P. sativum* and *Botryococcus braunii*, but neither corresponding gene has been identified (Wang and Kolattukudy, 1995; Vioque and Kolattukudy, 1997). Compelling evidence of a two-enzyme system utilizing an aldehyde intermediate has been reported in cyanobacteria (Schirmer *et al.*, 2010). However, this mechanism of alkane and aldehyde synthesis remains to be demonstrated *in planta* (Samuels *et al.*, 2008).

An alternative pathway for alkane synthesis may involve a thioesterase activity. The β-ketoacyl synthase enzyme in the FAE complex generates β-ketoacyl-CoAs from fatty acyl-CoAs. In addition to being an intermediate in fatty acid elongation, the β-ketoacyl-CoAs can also possibly serve as precursors to methylketones in other plant species. In tomato, medium-chain β-ketoacyl-ACPs are converted to a β-ketoacid by a thioesterase and the β-ketoacid is decarboxylated to a methylketone (Fridman *et al.*, 2005; Ben-Israel *et al.*, 2009; Yu *et al.*, 2010). As stated previously, the MEL family shows high similarity to MKS2, which has been shown to catalyze the thioesterase reaction forming free β-ketoacids (Yu *et al.*, 2010). Using β-ketoacyl-CoAs as a substrate, MEL1 could catalyze the conversion of β-ketoacyl-CoAs to β-ketoacids. It is

then possible that either an unknown decarboxylase reduces the β-ketoacid to a methylketone or that this decarboxylation occurs spontaneously (Fridman *et al.*, 2005). An oxidoreductase, such as CER3 and CER1, may then be able to successively reduce the methylketone to form alkanes (Figure 26B). In *cer1* mutants, alkanes, secondary alcohols, and ketones are all decreased while aldehydes are increased (Jenks *et al.*, 1995). This could support the proposed alternative pathway, if the loss of the oxidoreductase causes an accumulation of methylketones, which could then inhibit the thioesterase activity. The decreased flux through this branch of the wax biosynthetic pathway could allow for more β-ketoacyl-CoAs to continue in FAE to form more fatty acyl-CoAs, where they could then be available to a putative aldehyde-forming FAR. In *cer3* mutants however, it appears aldehydes, alkanes, secondary alcohols, and ketones are all decreased which doesn't fit perfectly with either model for alkane biosynthesis, unless CER3 itself is involved in aldehyde synthesis (Jenks *et al.*, 1995). Expression of MEL1, MEL2, and MEL3 in *E. coli* leads to the accumulation of C11 to C15 methylketones in the spent media, in spite of the fact that *Arabidopsis* does not have detectable levels of medium chain methylketones (Yu *et al.*, 2010). *E. coli* do not synthesize alkanes and therefore the lack of an oxidoreductase that could convert methylketones into alkanes, would allow for the accumulation of β-ketoacids that are then chemically converted to methylketones. If methylketones are an intermediate in alkane synthesis, then some plants may have evolved to have increased expression of this methylketone-forming thioesterase in specialized cells (Yu *et al.*, 2010; Perera *et al.*, 2010). The accumulation of methylketones may overwhelm the oxidoreductase, if the oxidoreductase is expressed at all, and therefore an accumulation of methylketones is found in these cells, such as in the

trichomes of *S. habrochaites* or in the silk cuticular wax of maize (Fridman *et al.*, 2005; Perera *et al.*, 2010).

A thioesterase in alkane synthesis would need to have activity for very-long-chain acyl-CoAs, but expression in *E. coli* indicates that MEL1, MEL2, and MEL3 utilize medium to long-chain substrates (Figure 25). However, as described above, expression in *E. coli* gives an indication of the activity that the MEL proteins can carry out, but the substrate specificity may not be relevant as very-long-chain acyl substrates are not produced in *E. coli.* Expressing the MEL proteins in yeast may determine if MEL enzymes can utilize both long-chain and very-long-chain acyl substrates. It has been reported that suberin has associated waxes, including alkanes, and therefore MEL2 could be functioning in the production of suberin waxes while MEL4 is potentially generating alkanes for the pollen exine (Li *et al.*, 2007b). Alkanes specifically within the pollen exine have not been reported, but this is difficult to measure experimentally due to low tissue availability. Alkanes, however, have been reported associated with tapetal cells and are thought to coat the pollen surface in the final stages of pollen grain formation (Hsieh and Huang, 2007). The mutants that affect alkane levels, *cer3* and *cer1*, show male sterility, indicating a critical role for alkanes in pollen viability.

It is possible that the MEL enzymes carry out the same function as MKS2 in tomato and are indeed primarily responsible for the synthesis of methylketones. Methylketones in tomato can be detected due in part to the high levels at which they accumulate in these glandular trichomes (Yu *et al.*, 2010; Ben-Israel *et al.*, 2009; Fridman *et al.*, 2005). It is possible that long-chain and very-long-chain methylketones are present in *Arabidopsis* but at levels that are not yet detectable.

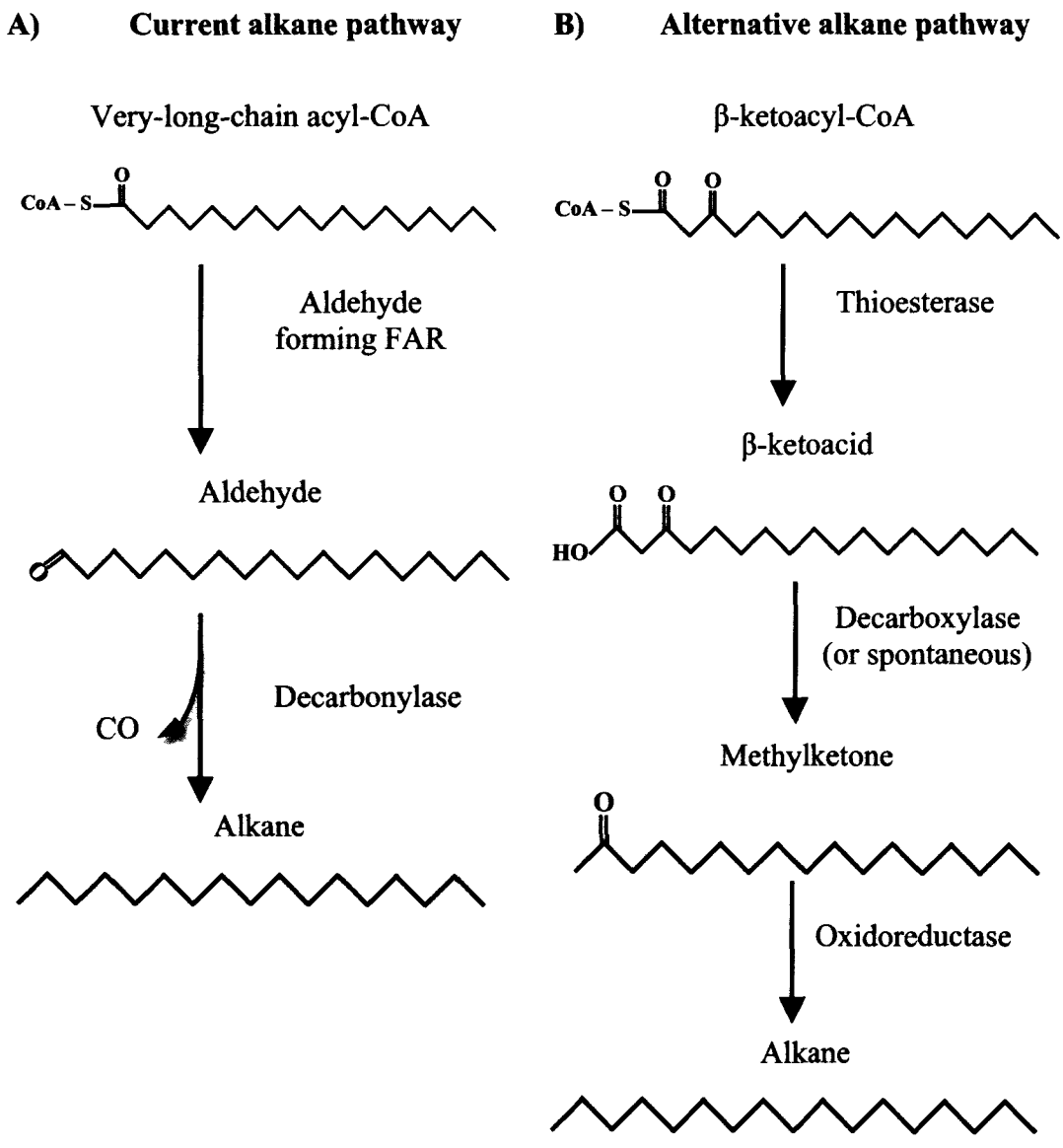

Figure 26: Two models for alkane biosynthesis in plants.

The current hypothesis for alkane formation involves an aldehyde-forming fatty acyl-CoA reductase and a decarbonylase (**A**). The alternative alkane biosynthetic pathway involves an acyl-CoA thioesterase and a methylketone intermediate (**B**).

4.4 Thioesterases in cutin biosynthesis

Many of the enzymes associated with cutin biosynthesis have been identified, but the sequence of reactions in cutin monomer synthesis is currently unknown (see section 1.2.1). In one model, a long-chain thioesterase is needed to generate a free fatty acid from the acyl-CoA pool, which is then subsequently oxidized by a cytochrome P450 to a hydroxy-fatty acid and reactivated to a hydroxy fatty acyl-CoA before being transferred to glycerol (Figure 4A). The known P450 hydroxylases ATT1 and LCR in *Arabidopsis* that are associated with cuticle biosynthesis have demonstrated activity toward free fatty acids *in vitro* and ATT1 does not appear to have any activity toward acyl-CoAs (Benveniste *et al.*, 2006; Wellesen *et al.*, 2001). This indicates that the activated acyl-CoA substrates in the ER are likely converted to a free fatty acid prior to hydroxylation. These free hydroxy-fatty acids would need to be reactivated by a LACS, such as LACS1 or LACS2, for the GPAT to form the mono and diacylglycerolipids (Lü *et al.*, 2009). This sequence of reactions is supported by data indicating that LACS2 has some activity for C16:0 fatty acids, but higher activity for hydroxylated C16 fatty acids (Schnurr *et al.*, 2004). While this sequence of reactions is supported in *Arabidopsis*, recent work in *Petunia hybrida* presents an alternative. The fatty acyl-CoA ω-hydroxylase, *CYP86A22*, identified as important for the synthesis of ω-hydroxy fatty acids in the *P. hybrida* stigma preferentially hydroxylates long-chain fatty acyl-CoAs over free fatty acids in the synthesis of flower cutin. This is unlike the known hydroxylases from *Arabidospsis* that seem to use free fatty acids as their substrate (Han *et al.*, 2010). However, the authors note that the use of activated CoA substrates is unusual for a cytochrome P450 hydroxylase. If the hydroxylation of fatty-acyl-CoAs is occurring in *Arabidopsis,* there

would be no need for a thioesterase as free fatty acids would be activated to a fatty acyl-CoA, which could then be hydroxylated and transferred to glycerol. Support for this alternative pathway, however, is weak. *In vitro,* MEL1 has activity for palmitoyl-CoA, and long-chain fatty acids are produced when MEL proteins are expressed in *E. coli.* This illustrates that the MEL enzymes can use long-chain acyl chains as substrates. Hydroxylated fatty acids are also found in suberin and most likely sporopollenin (Dominguez *et al.*, 1999; Franke *et al.*, 2005). Similar to the cutin biosynthetic pathway, two fatty acid hydroxylases, CYP86A1 and CYP86B1, contribute to the biosynthesis of hydroxy fatty acids in suberin, one of which has been shown to be active toward mid- and long-chain fatty acids (Benveniste *et al.*, 1998; Compagnon *et al.*, 2009). This indicates that the hydroxylated fatty acids found in suberin are likely synthesized through a mechanism analogous to that seen in *Arabidopsis* cutin biosynthesis and MEL2 is a candidate thioesterase in this pathway. Due to the similarities between cutin and suberin biosynthetic pathways, it is likely that the biosynthesis of sporopollenin is similar and therefore MEL4 may generate free fatty acids needed for generating hydroxylated fatty acids in sporopollenin. Based on this model there could be a role for MEL enzymes in the production of hydroxylated fatty acids found in the three extracellular lipid barriers.

4.5 Thioesterases in gene regulation

Fatty acyl-CoAs and free fatty acids have also been implicated in gene regulatory roles in both bacteria and humans. In humans, the human nuclear factor (HNF)-4α and peroxisome proliferator-activated receptor (PPAR)α are transcription factors regulating lipid metabolism (Desvergne and Wahli, 1999). The HNF-4α transcription factor is

activated by mid- to long-chain saturated and mono-unsaturated fatty acyl-CoA ligands, but is suppressed by long-chain polyunsaturated fatty acids (Hertz *et al.*, 2005). The thioesterase activity possessed by HNF-4α may serve as a mechanism for the cell to monitor the state of cellular acyl-CoA pools and prevent over-stimulation of the downstream targets (Hertz *et al.*, 2005). The PARRα enzyme from animal cells also functions in the lipid metabolism pathway and responds to the pools of free fatty acids and fatty-acyl-CoAs in the cell. In contrast to HNF-4α, it appears that PPARα has decreased activity in the presence of all long-chain acyl-CoA substrates and is thought to be activated by free-fatty acids (Keller *et al.*, 1992; Elholm *et al.*, 2001; Murakami *et al.*, 2001). A similar regulatory mechanism controls fatty acid metabolism in bacteria (Fujita *et al.*, 2007). The FapR protein functions as a repressor for many lipid biosynthetic genes and binds both malonyl-CoA and malonyl-ACP used in fatty acid synthesis (Schujman *et al.*, 2006; Martinez *et al.*, 2010). Malonyl-CoA is used to initiate fatty acid biosynthesis, but for further fatty acid synthesis malonyl-CoA must be converted to malonyl-ACP (Fujita *et al.*, 2007). The binding of the malonyl-CoA or malonyl-ACP ligands to FapR causes a conformational change that relieves the repression of many lipid metabolism genes. The accommodation of ligands needed for two different steps of the lipid biosynthetic pathway may be a mechanism for monitoring the progression of lipid biosynthesis (Schujman, *et al.*, 2006; Martinez *et al.*, 2010). These are two known examples of fatty acyl-CoAs/FFAs functioning as allosteric transcriptional modulators of lipid metabolic genes. It is possible that the MEL enzymes, or another thioesterase, are functioning in conjunction with a LACS to regulate lipid metabolism by maintaining balanced levels of acyl-CoA pools.

4.6 Analysis of the *MEL* gene family

If MELs were involved in extracellular lipid biosynthesis, it was expected that the cutin or cuticular wax content of *MEL1 amiRNA* or *MEL1-35S* lines would be altered. However, this was not the case, as the cutin and wax composition of *MEL1 amiRNA* and *MEL1-35s* lines were indistinguishable from wild-type (Figure 16; Figure 18). In the case of the over-expression line, it is possible that while *MEL1* transcript is increased, the protein level is not increased significantly enough to cause observable phenotypic change. The lack of phenotype in *MEL1 amiRNA* lines may be due to incomplete silencing of *MEL1*. In maize, RNAi was used to decrease the expression of an epidermal specific transcription factor and in spite of significant decreases in transcript, no phenotype was observed (Javelle *et al.*, 2010). This could also be the case in the *MEL1 amiRNA* lines, where even a small amount of protein may be able to function well enough to prevent any obvious phenotype. MEL3 and MEL1 may also function redundantly and therefore the constitutive expression of *MEL3* may mask phenotypes that could otherwise be observed by knocking down *MEL1*. Examining a plant in which both of these genes are knocked down would test this hypothesis. If these two enzymes are truly redundant, then it would be expected that the compounds produced by their expression in *E. coli* would be very similar if not identical. However, when MEL1 and MEL3 were expressed in *E. coli* only a few shared compounds, such as undecanone and C18:1 fatty acid, accumulated (Figure 24; Figure 25). The overall profile of compounds produced by these enzymes is quite different and therefore it is unlikely that the two have enough redundancy to mask a phenotype.

It is possible that other thioesterases functioning in the same pathway are partially redundant, which would also mask any phenotype seen in the *MEL1 amiRNA* lines. If MEL enzymes are functioning redundantly with FATB in the export of fatty acids from the plastid, it is possible that FATB activity masks the effects of reduced *MEL1* transcript as FATB is known to be responsible for a large portion of epicuticular wax precursors (Bonaventure *et al.*, 2003). While there is a role for a thioesterase in many aspects of extracellular lipid biosynthesis, as outlined above, the data presented by this study does not resolve these alternate roles (see Chapter 5 for future directions). Preliminary data from experiments carried out after the completion of this thesis has shown that MEL1 is likely localized to the plastid (Alia Busuttil and Owen Rowland, personal communication). Plastid localization has also been seen in the related MKS2 enzyme from tomato (Yu *et al.*, 2010). This does not support MELs function in the roles of modifying acyl-chains for wax, cutin, or suberin biosynthesis following the export of long-chain fatty acids from the plastid, as all evidence thus far indicates that modification to these monomers takes place in the ER (Samuels *et al.*, 2008). However, it does indicate that MELs may be playing a role parallel to FATB in fatty acid synthesis, or in producing mid- to -long-chain methylketones, but these have not yet been identified in the *Arabidopsis* cuticle. MEL enzymes are likely still functioning in extracellular lipid biosynthesis as their gene expression patterns are so tightly correlated with other genes involved in surface lipid barriers.

Chapter 5: Conclusion and Future Directions

This work has demonstrated that the MEL family of enzymes possess thioesterase activity *in vitro* and when heterologously expressed in *E. coli*. *MEL1* and *MEL2* co-regulate with cuticle and suberin genes, respectively, and *MEL1, MEL2,* and *MEL4* are expressed in a tissue specific manner that suggests their involvement in extracellular lipid biosynthesis. In *MEL1* knockdown lines, there were no observable alterations to the cuticle composition. *MEL1* may, however, still function in cuticle biosynthesis, as these lines are not null mutants. Alternatively, *MEL1* could be functioning in the production of compounds currently unidentified in the cuticle matrix, such as methylketones, or redundantly with other lipid biosynthetic enzymes such as FATB. Future experiments are needed to fully elucidate the function of MEL1 and the other MEL family members.

5.1 Future experiments to determine the physiological role of *MEL* genes

In order to elucidate the *in vivo* function of the *MEL* family of genes, several experiments can be carried out. While there is no obvious phenotype when *MEL1* is knocked down, it is possible that knocking down *MEL2, MEL3,* or *MEL4* may produce a more distinct phenotype. Therefore amiRNA lines specific for *MEL2, MEL3,* and *MEL4* should be generated and screened for altered lipid composition. Specifically, the suberin composition in a *MEL2* knockdown line and the lipid associated with sporopollenin in a *MEL4* knockdown line should be examined. The decreased function of a thioesterase in the suberin or sporopollenin pathways may provide stronger phenotypes than in the cuticle. There also may be less potential redundancy with other thioesterases, such as MEL3, in these tissues. A hairpin RNA with less specificity for one specific *MEL*

transcript may knockdown the entire *MEL* family and any observed phenotype may give an indication of MEL protein function, even if it is pleiotropic. While losing specificity is a disadvantage to the hairpin RNA, it could be advantageous to knockdown *MEL3* in conjunction with the other *MEL*s.

The recent finding that MEL1 may be localized to the plastid leads to the hypothesis that MEL1 is working in parallel with FATB in the export of saturated fatty acids from the plastid. Crossing *MEL1 amiRNA-4* with *fatb* could provide valuable insight. If the *fatb* phenotype is unaltered by the loss of *MEL1,* then it is likely that *MEL1* is not functioning in terminating fatty acid synthesis. However, if a more dramatic phenotype is observed in the *mel1 fatb* double mutant, this would support *MEL1* and *FATB* being partially redundant. Similarly, over-expressing *MEL1* in the *fatb* mutant background could illustrate the same principle. If MEL1 is functionally redundant with *fatb* and is a long-chain thioesterase terminating fatty acid synthesis, then over-expressing *MEL1* in the *fatb* background could rescue or partially rescue the mutant phenotype (Bonaventure *et al.*, 2003). The same principle can be applied to examine if MEL1 is playing a regulatory role. The *wax1/shn1* mutant affecting an AP2-type transcription factor shows altered cuticle composition, but not completely altered regulation. Therefore, other mechanisms are likely involved in regulating genes involved in extracellular lipid biosynthesis (Kannangara *et al.*, 2007). Crossing *MEL1 amiRNA-4* with the *wax1/shn1* mutant may lead to a more severe phenotype if both of these potential aspects of regulation are being affected. In order to determine if *MEL1* is carrying out a regulatory role, real time RT-PCR could be used to detect if the transcript levels of various cutin and wax biosynthetic genes are altered by the decreased or increased

expression of *MEL1*. The lack of phenotype may be due to the fact that altering *MEL1* expression does not cause large changes to gene expression, but their mis-regulation may still be detectable by sensitive methods.

Cutin analysis by GC-MS should be carried out on the identified *MEL1* over-expression line to observe if any alterations to the cutin composition have occurred due to increased *MEL1* expression. If *MEL1* is influencing cutin biosynthesis, the over-expression line may provide crucial information about the role it may play in cuticle biosynthesis, even if amiRNA lines do not reduce transcript levels enough to see a phenotype. Cutin analysis by GC-MS of *MEL1 amiRNA-1* and *MEL1 amiRNA-4* should also be repeated with a larger amount of tissue to increase the ability to accurately detect the levels of the various compounds.

To get better insight into *MEL3* gene expression patterns, a larger portion of the genomic sequence upstream of the *MEL3* start codon should be used to drive expression of a reporter gene (e.g. GUS). The expression patterns observed with promoter GUS for *MEL1, MEL2,* and *MEL4* are consistent between individual transformants and matches endogenous transcriptional patterns measured by RT-PCR and DNA microarrays, but this consistency has not been seen with *MEL3* promoter:GUS lines (Schmid *et al.* 2005, Winter *et al.*, 2007). A larger portion of genomic sequence may possess promoter elements that were not present in the first construct and therefore a consistent gene expression pattern may be observed. This expression will allow us to determine in which cell types that *MEL3* is specifically expressed in or whether it is constitutively expressed in all cell-types. This may provide clues as to the physiological role of MEL1 in lipid biosynthesis.

5.2 Experiments to biochemically examine MEL enzymes

Biochemical assays are also needed to further elucidate the biological function of the MEL proteins. The expression of MEL1, MEL2, and MEL3 in *E. coli* led to the production of known methylketones and fatty acids (Figure 24; Figure 25). However their expression also lead to the production of several unidentified compounds. These unknown compounds should be identified by GC-MS. As the profile of unknown compounds is unique to each expressed MEL, identifying these compounds could help elucidate the different functions of each of these enzymes, especially in differentiating MEL3 from the other MEL proteins as MEL3 appears to be globally expressed.

It has been shown previously that when enzymes specific for very-long-chain fatty acyl-CoAs are expressed in *E. coli*, novel compounds are produced that do not necessarily represent the *in planta* substrate specificity (Doan *et al.*, 2009). This is likely due to the fact that very-long-chain-fatty acyl substrates are not present in *E. coli* and therefore the substrates available to the enzymes are limited to long-chain-fatty acyl-ACPs. The expression of lipid biosynthetic genes in yeast may be more physiologically relevant than expression in *E. coli* as yeast are capable of elongating fatty acids to very long chain lengths. The expression of MEL1, MEL2, MEL3, and MEL4 in yeast, as opposed to *E. coli,* could give further indications as to the physiological function of these enzymes. Analyzing the spent media from yeast for the presence of fatty acids or methylketones could support or refute the evidence observed in *E. coli.*

The observation that the MEL proteins accumulate to much higher levels in K27(DE3) cells then in BL21(DE3)pLysS is intriguing. This could be due simply to a

higher expression of T7 RNA polymerase (unknown at present), but it may in fact be linked to the *fadD* mutation in the K27 cells. The *fadD* mutation prevents *E. coli* from importing fatty acids from the media, allowing fatty acids to accumulate outside the cell. High levels of free fatty acids within the cell are typically toxic to organisms and by preventing the accumulation of fatty acids in the cell, it is possible the MEL proteins are able to accumulate to higher levels without causing lethality (Neal *et al.*, 1965; Wu *et al.*, 2006). Therefore all four MEL proteins and the mutant MEL1(D64A) should be purified from K27 cells to yield increased amounts of pure protein and then thioesterase activity assays carried out. With purer enzyme, a selection of substrates could be tested to observe if the MEL proteins preferentially hydrolyze one substrate over another. Many of the long-chain acyl-CoA substrates are available commercially; however, to test the ability of the MELs to hydrolyze β-ketoacyl-CoAs, very-long-chain acyl-CoAs, or acyl-ACPs would require substrate synthesis in the lab. Testing MELs for their activity toward long-chain fatty acyl-CoAs, very-long-chain fatty acyl-CoAs, long-chain β-ketoacyl-CoAs, very-long-chain β-ketoacyl-CoAs, long-chain fatty acyl-ACPs, and long-chain β-ketoacyl-ACPs could indicate a potential physiological function. Based on the preliminary data that MEL1 is localized in the plastid, it is likely that the native substrate is an acyl-ACP but this should be confirmed by comparing its kinetics with acyl-CoA substrates. Comparing the affinity of various MELs for various fatty-acyl substrates and β-ketoacyl substrates can distinguish if methylketone production is a non-biologically relevant byproduct of fatty-acyl thioesterase activity or if the synthesis of β-ketoacids is the primary function of the MEL proteins.

The characterization of the *MEL* gene family will identify the role of a previously uncharacterized family of thioesterases. The characterization of thioesterases in plants has thus far been minimal in spite of the multitude of physiological roles for thioesterases. Three *Arabidopsis* thioesterases have been characterized to date, FATA, FATB, and Acyl-CoA thioesterase 2, and one from tomato, MKS2 (Salas and Ohlrogge, 2002; Tilton *et al.*, 2004; Ben-Israel *et al.*, 2009; Yu *et al.*, 2010). Due to the general lack of knowledge surrounding plant thioesterases, characterizing this new family of acyl thioesterases greatly contributes to the understanding of lipid metabolism in plants. Elucidating how the MEL family contributes to extracellular lipid biosynthesis will allow for a better understanding of these pathways and help direct future research.

Appendix 1: Primer list

Primer Name	Primer Sequence
MEL1_BamHI_Fwd	AAAGGATCCATGCTTAAAGCTACCGGCACAG
MEL1_EcoRI_Rev	AAAGAATTCTCAATATTCGACAACGTGTTGAC
MEL2_BamHI_Fwd	AAAGGATCCATGTTTCAAGCTACCAGCAC
MEL2_EcoRI_Rev	AAAGAATTCTCAATCGACCAACTGTTGAC
MEL3_BamHI_Fwd	AAAGGATCCATGTTTCTTCAGGTTACCGGCA
MEL3_EcoRI_Rev	AAAGAATTCTCAAACGGCGTCGTCTTGG
FatB_Trunc_SacI_Fwd	AAGAGCTCTTACCTGACTGGAGCATGCTTCTTGC
FatB_HindIII_Rev	GCAAGCTTGGTAGTAGCAGATATAGTT
MEL1_D64A_Fwd	TTATGAATTAGCCCAATTTGGT
MEL1_D65A_Rev	CACCAAATTGGGCTAATTCATAA
MEL1_Antisense_Fwd	ATGCTTAAAGCTACCGGCACAGT
MEL1_Antisense_Rev	CATAATACGACTCACTATAGGTCAATATTCGACAACGTG
MEL1_sense_Fwd	CATAATACGACTCACTATAGGATGCTTAAAGCTACCGGC
MEL1_sense_Rev	TCAATATTCGACAACGTGTTGACG
MEL1_RT_Fwd	ATGCTTAAAGCTACCGGCACAGT
MEL1_RT_Rev	AACTGTCCACCTCTCCCGAC
MEL2_RT_Fwd	ATGTTTCAAGCTACCAGCACG
MEL2_RT_Rev	TATAGGTCATAAATTTTGTGATGCCC
MEL3_RT_Fwd	CGAAAACCCAGAAATGTTTCTTCAGG
MEL3_RT_Rev	TCGCTTTCACCACGAATTTGT
GAPC_Fwd	TCAGACTCGAGAAAGCTGCTAC
GAPC_Rev	GATCAAGTCGACCACACGG
MEL1_OE_XbaI_Fwd	AAATCTAGAATGCTTAAAGCTACCGGCACAG
MEL1_OE_SacI_Rev	AAAGAGCTCTCAATATTCGACAACGTGTTGAC
MEL1_Prom_SalI_Fwd	AAAGTCGACATGCATCGTTCACCATATCCAC
MEL1_Prom_BamHI_Rev	AAAGGATCCTGTGCCGGTAGCTTTAAGCAT
MEL2_Prom_SalI_Fwd	AAAGTCGACCACCTTCTCGTAATACAAAGTTTCTC
MEL2_Prom_BamHI_Rev	AAAGGATCCCGTGCTGGTAGCTTGAAACA
MEL3_Prom_SalI_Fwd	AAAGTCGACGAGCAAGATCCCATCTCCCTAAAC
MEL3_Prom_BamHI_Rev	AAAGGATCCAACCTGAAGAAACATTTCTGGGTTTTC
MEL4_Prom_SalI_Fwd	AAAGTCGACCATTTAGAGCGATCCCTTACTCATG
MEL4_Prom_BamHI_Rev	AAAGGATCCTGAAGTCGGAAACACCACAGACATA
MEL1_ami-A_I	GATTAGAGCGTATGTAAGACGGCTCTCTCTTTTGTATTCC
MEL1_ami-A_II	GAGCCGTCTTACATACGCTCTAATCAAAGAGAATCAATGA
MEL1_ami-A_III	GAGCAGTCTTACATAGGCTCTATTCACAGGTCGTGATATG
MEL1_ami-A_IV	GAATAGAGCCTATGTAAGACTGCTCTACATATATATTCCT
MEL1_ami-B_I	GATTGACCGAAATTAGAGCGTACTCTCTCTTTTGTATTCC
MEL1_ami-B_II	GAGTACGCTCTAATTTCGGTCAATCAAAGAGAATCAATGA
MEL1_ami-B_III	GAGTCCGCTCTAATTACGGTCATTCACAGGTCGTGATATG
MEL1_ami-B_IV	GAATGACCGTAATTAGAGCGGACTCTACATATATATTCCT
pRS300_A	CTGCAAGGCGATTAAGTTGGGTAAC

pRS300_B	GCGGATAACAATTTCACACAGGAAACAG
Ami_adapterA_XbaI	AAATCTAGACAAACACACGCTCGGACGC
Ami_adapterB_SacI	AAAGAGCTCCCCCATGGCGATGCCTTAA

Appendix 2: Vector maps of constructs

NOS terminator, term.; NOS promoter, Pr; 35S enhancer sequence, E6; Kanamycin resistance, KanR; BASTA resistance, BAR; Hygromycin resistance, HygR.

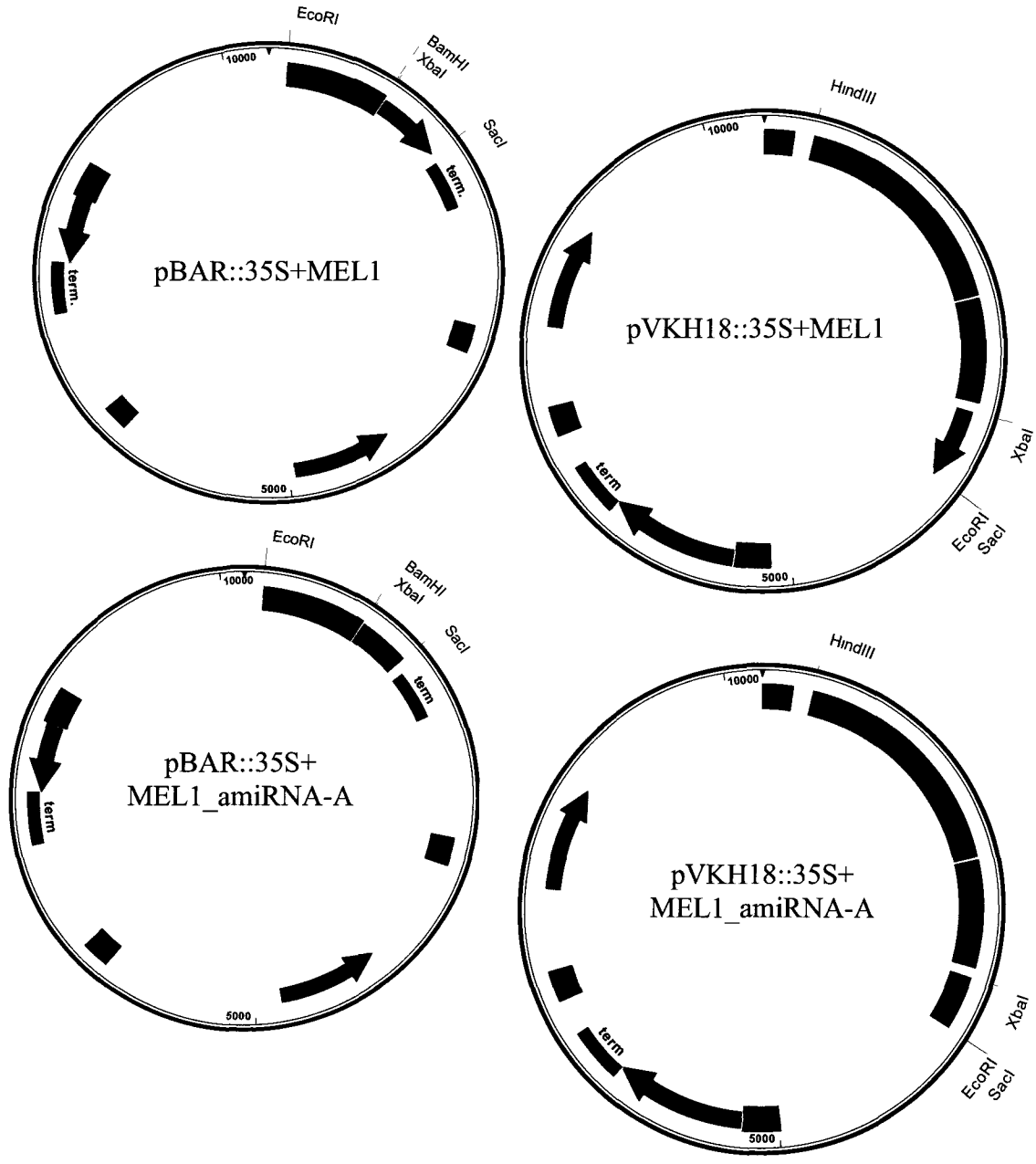

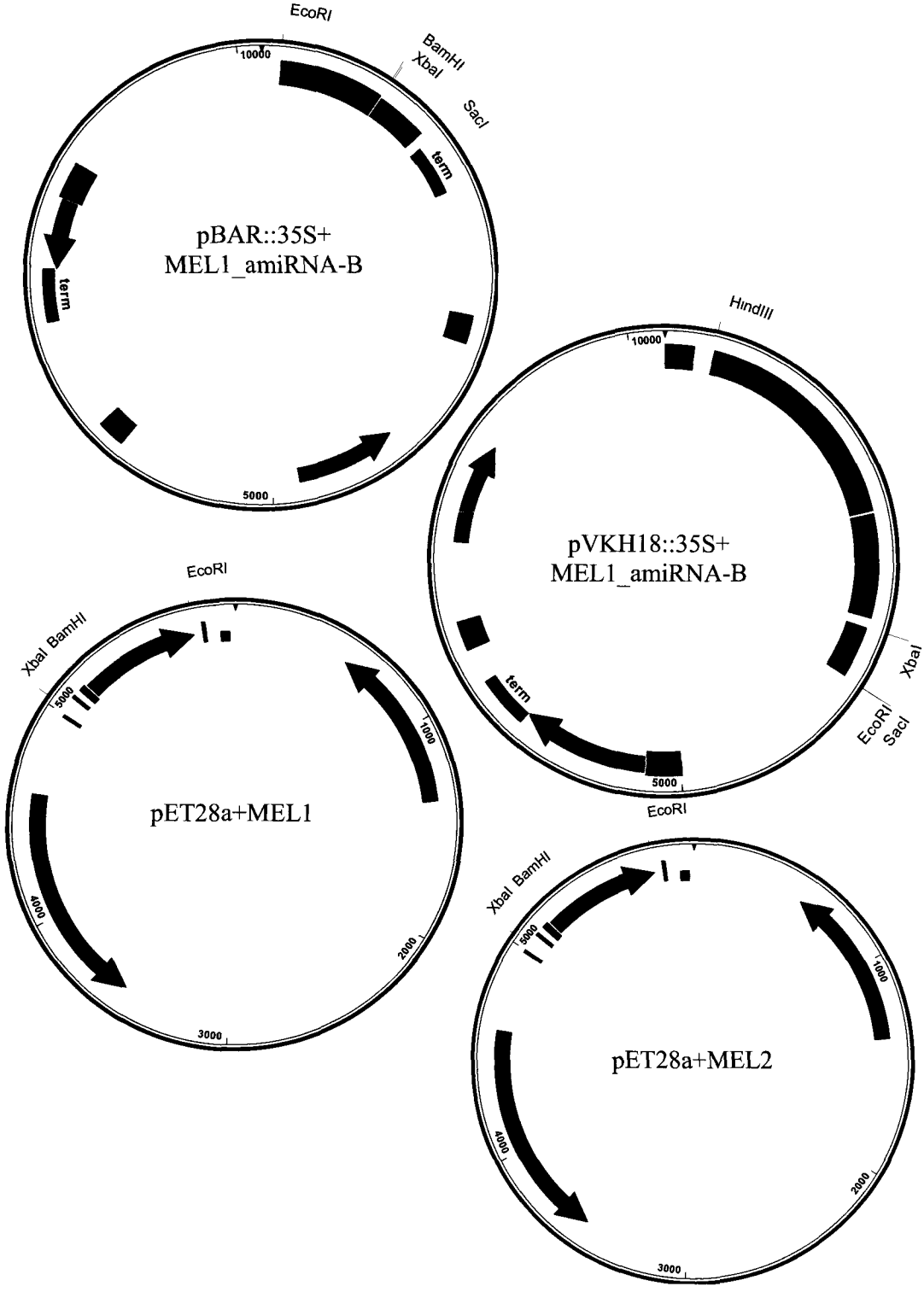
EcoRI
BamHI
XbaI
SacI
term
term
pBAR::35S+
MEL1_amiRNA-B
10000
5000
HindIII
pVKH18::35S+
MEL1_amiRNA-B
XbaI
EcoRI
SacI
EcoRI
XbaI BamHI
pET28a+MEL1
XbaI BamHI
pET28a+MEL2

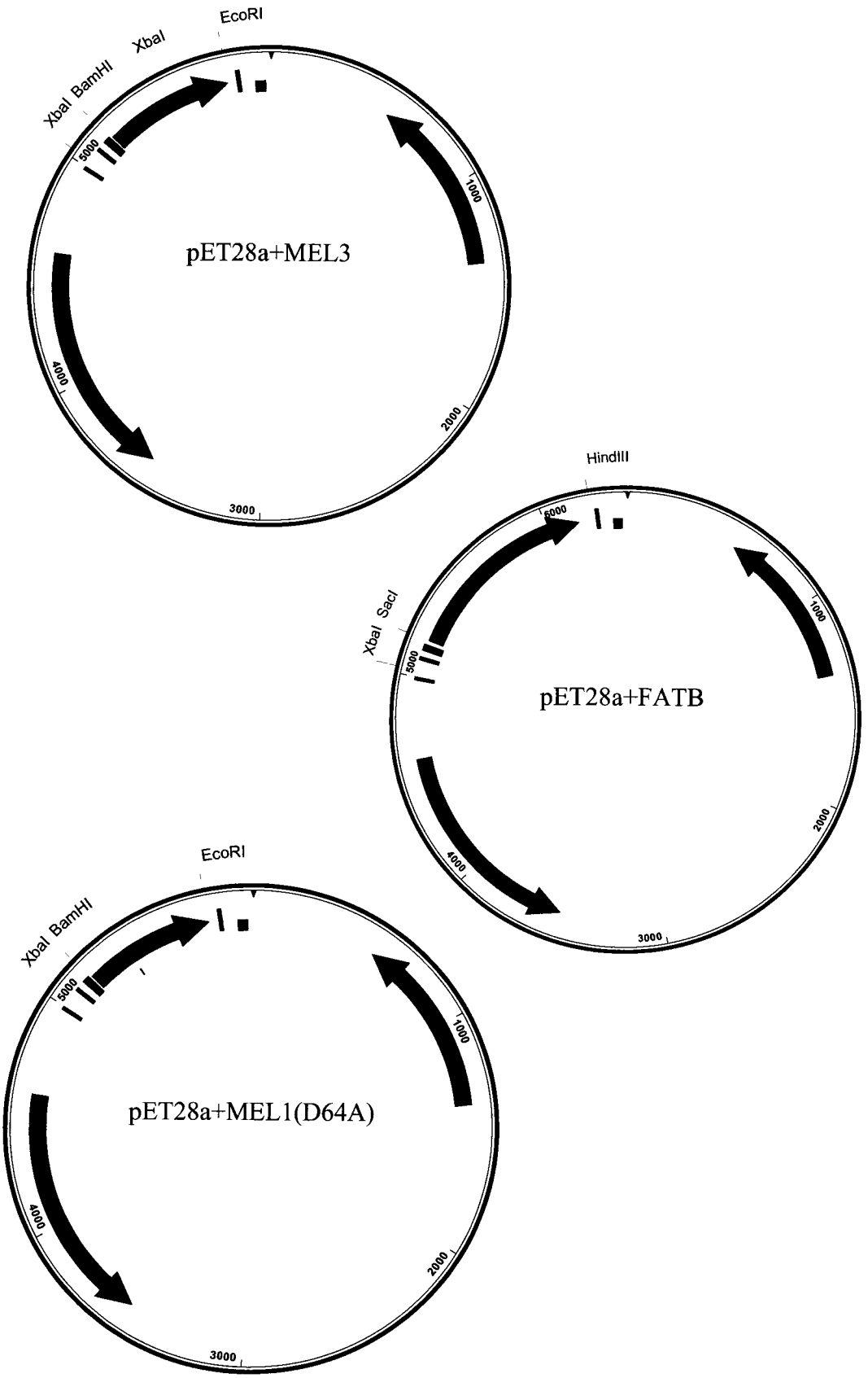
EcoRI
XbaI
XbaI BamHI
5000
1000
pET28a+MEL3
4000
2000
3000
HindIII
6000
XbaI SacI
5000
1000
pET28a+FATB
2000
4000
3000
EcoRI
XbaI BamHI
5000
1000
pET28a+MEL1(D64A)
4000
2000
3000

Appendix 3: Previously identified cuticle associated genes.

Gene Name	Locus	Function	Reference
CER1	At1g02205	Unknown function. Putative oxidoreductase, metalloenzyme.	Aarts *et al.*, 1995, Hannoufa *et al,* 1993, McNevin, *et al.*, 1993.
CER2	At4g24510	Unknown function. Putative acyltransferase	Lai *et al.*, 2007, Negruk *et al.*, 1996, Xia *et al.*, 1996, Xia *et al.*, 1997.
CER3 (WAX2/YRE/FLP)	At5g57800	Unknown function. Putative oxidoreductase, metalloenzyme	Ariizumi *et al.*, 2003, Chen *et al.*, 2003, Kurata *et al.*, 2003, Rowland *et al.*, 2007
CER4/FAR3	At4g33790	Alcohol forming fatty acyl-coenzyme A reductase	Rowland *et al.*, 2006
CER5 (WBC12)	At1g51500	ABC transporter	Pighin *et al.*, 2004, Rashotte *et al.*, 2001.
CER6 (CUT1/KCS6)	At1g68530	β-ketoacyl-coenzyme A synthase. (Condensing enzyme)	Fiebig *et al.*, 2000, Miller *et al.*, 1999, Lai *et al.*, 2007.
CER7 (RRP45)	At3g60500	Exosome subunit	Hooker *et al*, 2007.
CER8 (LACS1)	At2g47240	Long chain acyl-CoA synthetase	Lü, *et al.*, 2009. Weng *et al.*, 2010.
FATB	At1g08510	Acyl-ACP thioesterase	Mayer and Shanklin, 2005, Bonaventure *et al.*, 2003, Salas and Ohlrogge, 2002.
WSD1	At5g37300	Wax synthase/acyl-coenzyme A: diacylglycerol acyltransferase.	Li *et al.*, 2008.
MAH1	At1g57750	Cytochrome P450 hydroxylase	Greer *et al.*, 2007.
WBC11	At1g17840	ABC transporter	Bird *et al.*, 2007, Panikashvili *et al.*, 2007, Luo *et al.*, 2007.
KCS1	At1g01120	β-ketoacyl-coenzyme A synthase. (Condensing enzyme)	Todd *et al.*, 1999.

KCS2 (DAISY)	At1g04220	β-ketoacyl-coenzyme A synthase. (Condensing enzyme)	Franke *et al.*, 2009, Lee *et al.*, 2009a.
KCS20	At5g43760	β-ketoacyl-coenzyme A synthase. (Condensing enzyme)	Lee *et al.*, 2009a.
PAS2 (HCD)	At5g10480	3-hydroxy-acyl-CoA dehydratase	Bach *et al.*, 2008.
KCR1	At1g67730	β-ketoacyl-CoA reductase	Beaudoin *et al.*, 2009.
LACS2	At1g49430	Long chain acyl-CoA synthetase	Schnurr *et al.*, 2004, Lü, *et al.*, 2009, Weng *et al.*, 2010.
LTPG	At1g27950	Glycosylphosphatidylinositol -anchored lipid transfer protein	Lee *et al.*, 2009b, Debono *et al.*, 2009.
SHN1 (WIN1)	At1g15360	AP2-type transcription factor	Aharoni *et al.*, 2004, Kannangara *et al.*, 2007, Broun *et al.*, 2004.
SHN2	At5g25390	AP2-type transcription factor	Aharoni *et al.*, 2004.
SHN3	At5g11190	AP2-type transcription factor	Aharoni *et al.*, 2004.
MYB30	At3g28910	MYB transcription factor	Raffaele *et al.*, 2008.
MYB41	At4g28110	MYB transcription factor	Lippold *et al.*, 2009.
ATT1	At4g00360	Cytochrome P450 monooxygenase	Xiao *et al.*, 2004.
LCR	At2g45970	Cytochrome P450 monooxygenase	Wellesen *et al.*, 2001.
GPAT4	At1g01610	Glycerol-3-phosphate acyltransferase	Li *et al.*, 2007.
GPAT8	At4g00400	Glycerol-3-phosphate acyltransferase	Li *et al.*, 2007.
DCR	At5g23940	BAHD acyltransferase	Panikashvili *et al.*, 2009.

Appendix 4: Previously identified suberin associated genes.

Gene Name	Locus	Enzyme	Reference
GPAT5	At3g11430	Glycerol-3-phosphate acyltransferase	Beisson *et al.*, 2007.
CYP86A1	At5g58860	Fatty acid hydroxylase.	Li *et al.*, 2007. Höfer *et al.*, 2008.
CYP86B1	At5g23190	cytochrome P450	
KCS2 (DAISY)	At1g04220	β-ketoacyl-coenzyme A synthase. (Condensing enzyme)	Franke *et al.*, 2009, Lee *et al.*, 2009a.
KCS20	At5g43760	β-ketoacyl-coenzyme A synthase. (Condensing enzyme)	Lee *et al.*, 2009a.
FAR1	At5g22500	Alcohol forming fatty acyl-coenzyme A reductase	Domergue *et al.*, 2010.
FAR4	At3g44540	Alcohol forming fatty acyl-coenzyme A reductase	Domergue *et al.*, 2010.
FAR5	At3g44550	Alcohol forming fatty acyl-coenzyme A reductase	Domergue *et al.*, 2010.
AFST	At5g41040	Feruloyl-CoA transferase	Molina *et al.*, 2009, Gao *et al.*, 2009.
ESB1	At2g28670	Unknown function	Baxter *et al.*, 2009.
CER8 (LACS1)	At2g47240	Long chain acyl-CoA synthetase	Lü, *et al.*, 2009, Weng *et al.*, 2010, Li – Beisson *et al.*, 2010.
LACS2	At1g49430	Long chain acyl-CoA synthetase	Schnurr *et al.*, 2004, Lü, *et al.*, 2009, Weng *et al.*, 2010, Li-Beisson *et al*, 2010.

Appendix 5: Amino acid sequence alignment of the predicted MEL proteins with related single-domain Hotdog fold proteins.

Predicted Hotdog fold plant thioesterases from *Arabidopsis thaliana* (At) *Arabidopsis lyrata* (Al), *Chlamydomomas reinhardtii* (Cr), *Ricinus communis* (Rc), *Solanum habrochaites* (Sh), *Zea mays* (Zm), *Oryza sativa* (Os), *Vitis vinifera* (Vv), *Amborella trichopoda* (Atr), *Picea glauca* (Pg), *Humulus lupulus* (Hl), *Petunia integrifolia* (Pi), *Solanum lycopersicum* (Sl), *Lycopersicon hirsutum* (Lh), *Picea sitchensis* (Ps), *Selaginella moellendorfii* (Sm), and *Gossypium hirsutum* (Gh). In this alignment, conserved amino acids are highlighted in black while similar amino acids are highlighted in gray. The MEL proteins contain the conserved catalytic residues (Asp 64, Gly 67, and Val 69 in MEL1) observed in the 4-hydroxybenzoyl CoA thioesterase (4HBT) from Pseudomonas (Benning *et al.*, 1998). Across all sequences the catalytic aspartic acid, noted with *, has 100% conservation while the glycine and valine, noted with #, are conserved in 95% of sequences, including MELs. In 4HBT, a tyrosine residue is predicted to involved with nucleophilic attack, however, this predicted tyrosine is not conserved in plant thioesterases. It is possible that the tyrosine residue two amino acids downstream (noted with an @) may carryout this function. Nomenclature is as follows: species name_accession number.

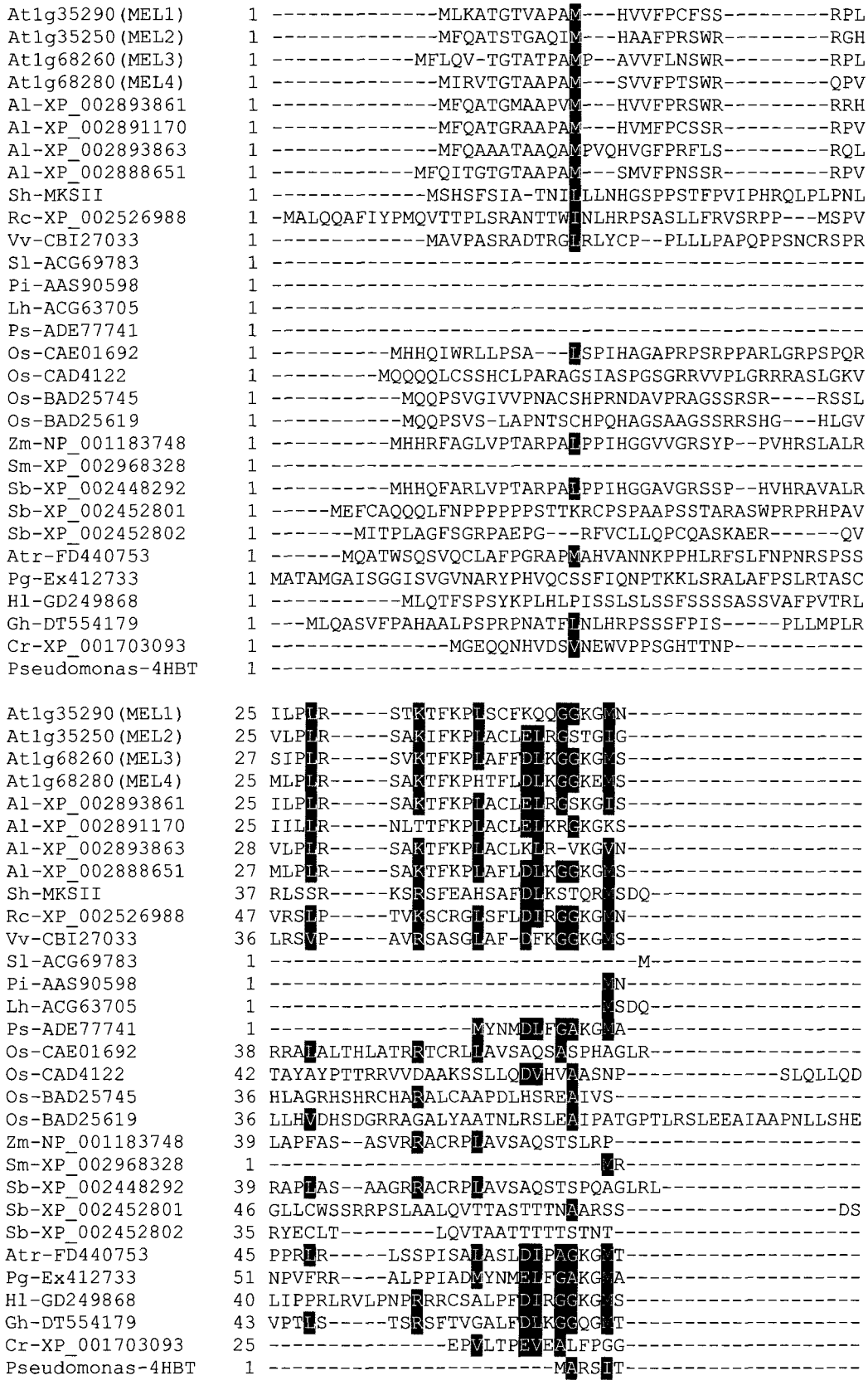
At1g35290(MEL1)
At1g35250(MEL2)
At1g68260(MEL3)
At1g68280(MEL4)
Al-XP_002893861
Al-XP_002891170
Al-XP_002893863
Al-XP_002888651
Sh-MKSII
Rc-XP_002526988
Vv-CBI27033
Sl-ACG69783
Pi-AAS90598
Lh-ACG63705
Ps-ADE77741
Os-CAE01692
Os-CAD4122
Os-BAD25745
Os-BAD25619
Zm-NP_001183748
Sm-XP_002968328
Sb-XP_002448292
Sb-XP_002452801
Sb-XP_002452802
Atr-FD440753
Pg-Ex412733
Hl-GD249868
Gh-DT554179
Cr-XP_001703093
Pseudomonas-4HBT

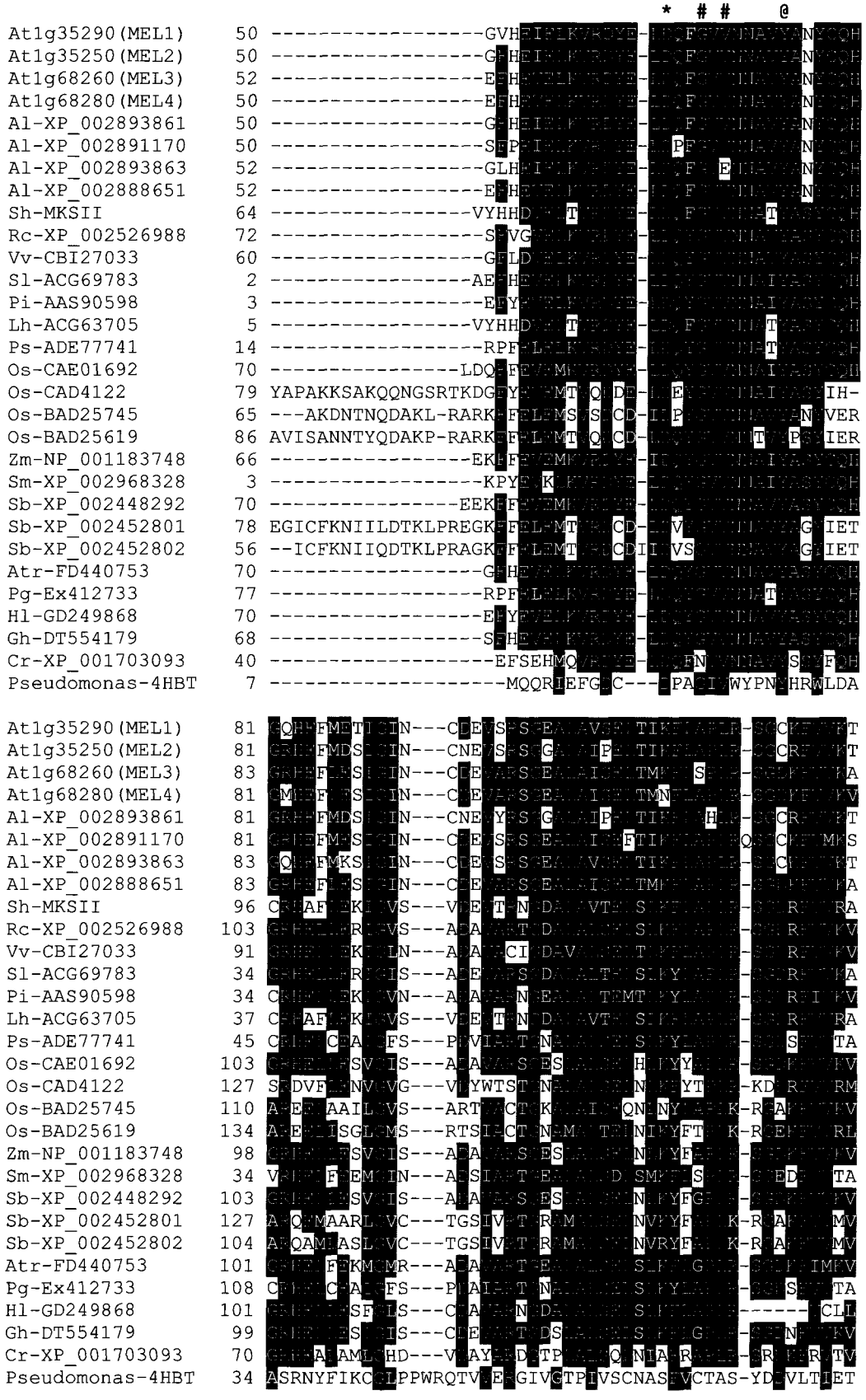
At1g35290(MEL1)
At1g35250(MEL2)
At1g68260(MEL3)
At1g68280(MEL4)
Al-XP_002893861
Al-XP_002891170
Al-XP_002893863
Al-XP_002888651
Sh-MKSII
Rc-XP_002526988
Vv-CBI27033
Sl-ACG69783
Pi-AAS90598
Lh-ACG63705
Ps-ADE77741
Os-CAE01692
Os-CAD4122
Os-BAD25745
Os-BAD25619
Zm-NP_001183748
Sm-XP_002968328
Sb-XP_002448292
Sb-XP_002452801
Sb-XP_002452802
Atr-FD440753
Pg-Ex412733
Hl-GD249868
Gh-DT554179
Cr-XP_001703093
Pseudomonas-4HBT

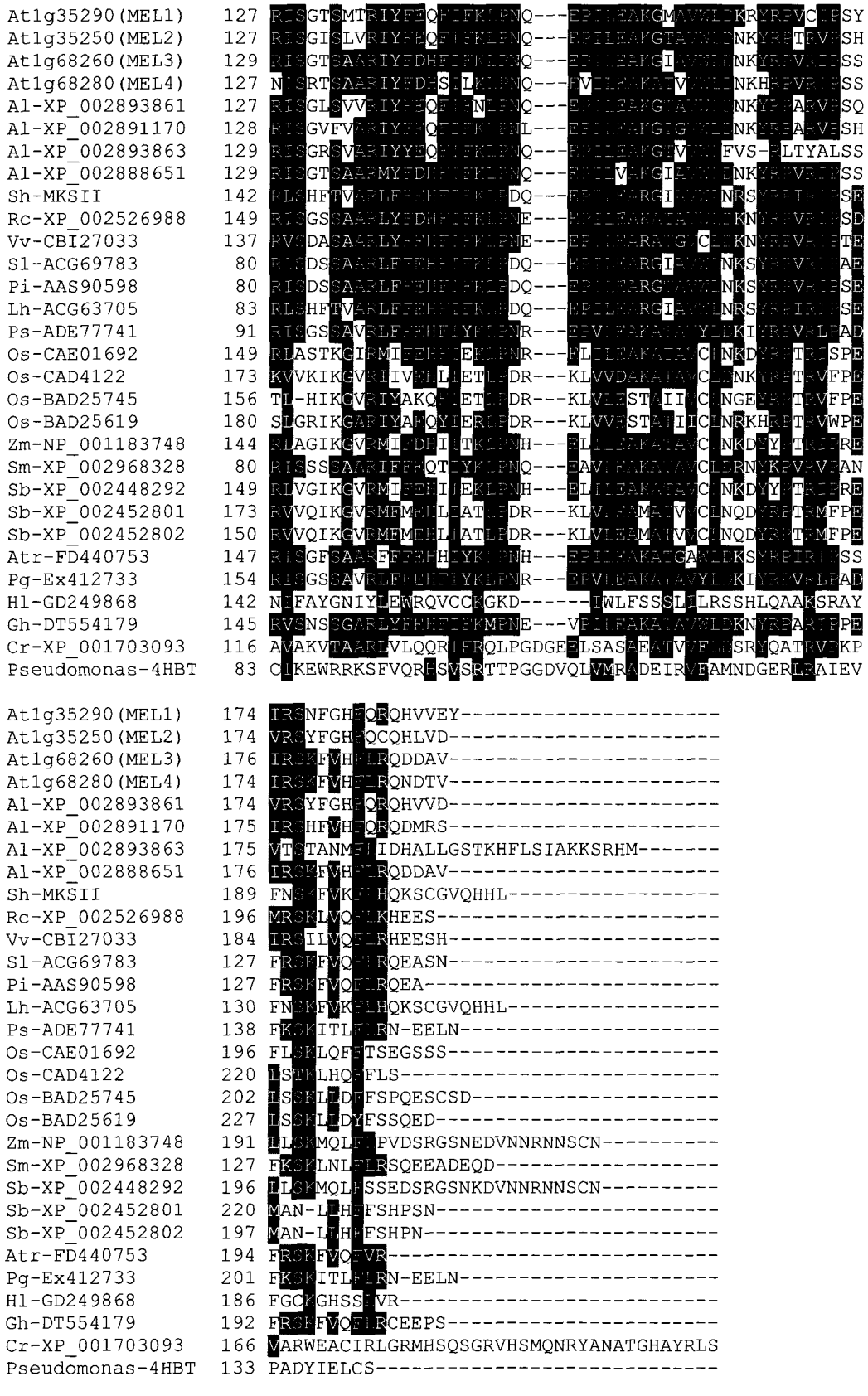
At1g35290(MEL1) 127
At1g35250(MEL2) 127
At1g68260(MEL3) 129
At1g68280(MEL4) 127
Al-XP_002893861 127
Al-XP_002891170 128
Al-XP_002893863 129
Al-XP_002888651 129
Sh-MKSII 142
Rc-XP_002526988 149
Vv-CBI27033 137
Sl-ACG69783 80
Pi-AAS90598 80
Lh-ACG63705 83
Ps-ADE77741 91
Os-CAE01692 149
Os-CAD4122 173
Os-BAD25745 156
Os-BAD25619 180
Zm-NP_001183748 144
Sm-XP_002968328 80
Sb-XP_002448292 149
Sb-XP_002452801 173
Sb-XP_002452802 150
Atr-FD440753 147
Pg-Ex412733 154
Hl-GD249868 142
Gh-DT554179 145
Cr-XP_001703093 116
Pseudomonas-4HBT 83
At1g35290(MEL1) 174
At1g35250(MEL2) 174
At1g68260(MEL3) 176
At1g68280(MEL4) 174
Al-XP_002893861 174
Al-XP_002891170 175
Al-XP_002893863 175
Al-XP_002888651 176
Sh-MKSII 189
Rc-XP_002526988 196
Vv-CBI27033 184
Sl-ACG69783 127
Pi-AAS90598 127
Lh-ACG63705 130
Ps-ADE77741 138
Os-CAE01692 196
Os-CAD4122 220
Os-BAD25745 202
Os-BAD25619 227
Zm-NP_001183748 191
Sm-XP_002968328 127
Sb-XP_002448292 196
Sb-XP_002452801 220
Sb-XP_002452802 197
Atr-FD440753 194
Pg-Ex412733 201
Hl-GD249868 186
Gh-DT554179 192
Cr-XP_001703093 166
Pseudomonas-4HBT 133

Appendix 6: Types of aliphatic compounds in the first and second generations of *MEL1 amiRNA* and *MEL1-35S.*

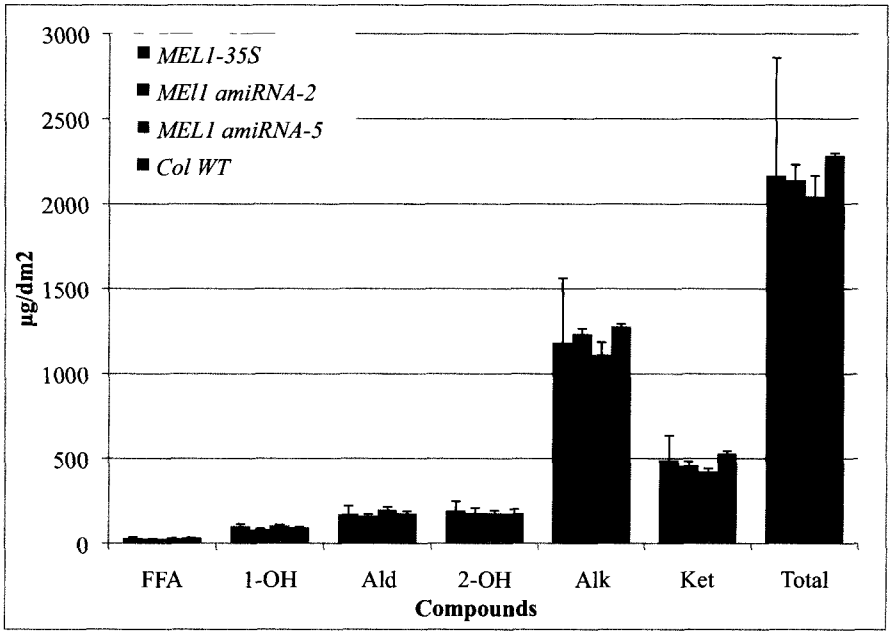

Figure Appendix 6A: Types of aliphatic compounds found in the cuticular waxes in the T2 generation as determined by GC-FID.

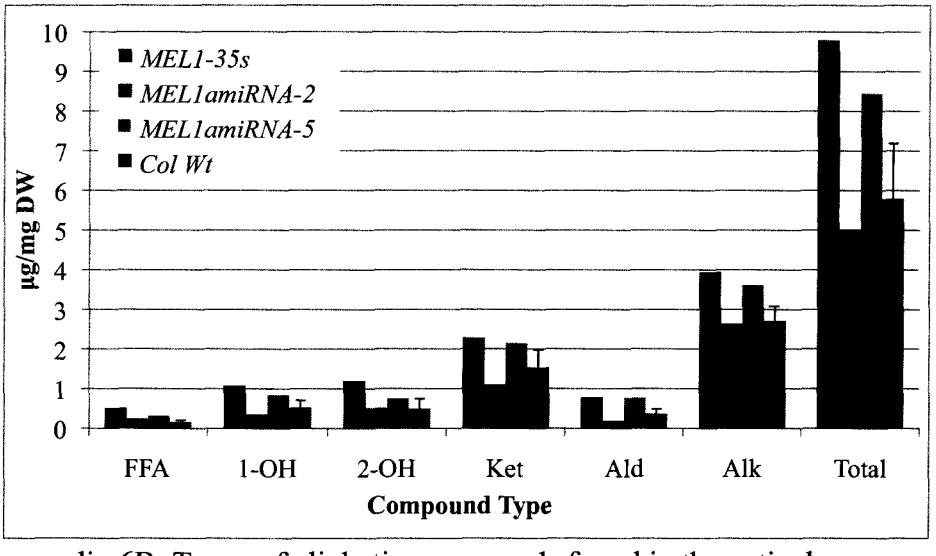

Figure Appendix 6B: Types of aliphatic compounds found in the cuticular waxes in the T1 generation of plants as determined by GC-FID.

References

1. Aarts, M. G. M., Keijzer, C. J., Stiekema, W. J., and Pereira, A. 1995. Molecular characterization of the *CER1* gene of *Arabidopsis* involved in epicuticular wax biosynthesis and pollen fertility. *Plant Cell.* 7: 2115-2127.
2. Aarts, M. G., Hodge, R., Kalantidis, K., Florack, D., Wilson, Z. A., Mulligan, B. J., Stiekema, W. J., Scott, R., and Pereira, A. 1997. The Arabidopsis MALE STERILITY 2 protein shares similarity with reductases in elongation/condensation complexes. *Plant Journal.* 12: 615-623.
3. Aharoni, A., Dixit, S., Jetter, R., Thoenes, E., van Arkel, G., and Pereira, A. 2004. The SHINE clade of AP2 domain transcription factors activates wax biosynthesis, alters cuticle properties, and confers drought tolerance when overexpressed in Arabidopsis. *Plant Cell.* 16: 2463-2480.
4. Ahlers, F., Thom, I., Lambert, J., Kuckuk, R., and Wiermann, R. 1999. ^{1}H NMR analysis of sporopollenin from *Typha Angustifolia*. *Phytochemistry.* 50: 1095-1098.
5. Ariizumi, T., Hatakeyama, K., Hinata, K., Sato, S., Kato, T., Tabata, S., and Toriyama, K. 2003. A novel male-sterile mutant of Arabidopsis thaliana, faceless pollen-1, produces pollen with a smooth surface and an acetolysis-sensitive exine. *Plant Molecular Biology.* 53: 107-116.
6. Arnold, K., Bordoli, L., Kopp, J., and Schwede, T. 2006. The SWISS-MODEL Workplace: A web-based environment for protein structure homology modeling. *Bioinformatics.* 22: 195-201.

7. Bach, L., Michaelson, L. V., Haslam, R., Bellec, Y., Gissot, L., Marion, J., Da costa, M., Boutin, J. P., Miquel, M., Tellier, F., Domergue, F., Markham, J. E., Beaudoin, F., Napier, J. A., and Faure, J. D. 2008. The very-long-chain hydroxy fatty acyl-CoA dehydratase PASTICCINO2 is essential and limiting for plant development. *PNAS.* 105: 14727-14731.

8. Batoko, H., Zheng, H.-Q., Hawes, C., and Moore, I. 2000. A Rab1 GTPase is required for transport between the endoplasmic reticulum and golgi apparatus and for normal golgi movement in plants. *The Plant Cell.* 12: 2201-2217.

9. Baxter, I., Hosmani, P. S., Rus, A., Lahner, B., Borevitz, J. O., Muthukumar, B., Mickelbart, M. V., Schreiber, L., Franke, R. B., and Salt, D. E. 2009. Root suberin forms an extracellular barrier that affects water relations and mineral nutrition in *Arabidopsis*. *PLoS Genetics.* 5: e1000492.

10. Beaudoin, F., Wu, X., Li, F., Haslam, R. P., Markham, J. E., Zheng, H., Napier, J. A., and Kunst, L. 2009. Functional characterization of the Arabidopsis beta-ketoacyl-coenzyme A reductases candidates of the fatty acid elongase. *Plant Physiology.* 150: 1174-1191.

11. Beisson, F., Li, Y., Bonaventure, G., Pollard, M., and Ohlrogge, J. B. 2007. The acyltransferase GPAT5 is required for the synthesis of suberin in seed coat and root of Arabidopsis. *Plant Cell.* 19: 351-368.

12. Ben-Israel, I., Yu, G., Austin, M. B., Bhuiyan, N., Auldridge, M., Nguyen, T, Schauvinhold, I., Noel, J. P., Pichersky, E., and Fridman, E. 2009. Multiple biochemical and morphological factors underlie the production of methylketones in tomato trichomes. *Plant Physiology.* 151: 1952-1964.

13. Beisson, F., Li, Y., Bonaventure, G., Pollard, M., and Ohlrogge, J. B. 2007. The Acyltransferase GPAT5 is required for the synthesis of suberin in seed coat and root of *Arabidopsis*. *The Plant Cell*. 19: 351-368.

14. Benning, M. M., Wesenberg, G., Liu, R., Taylor, K. L., Donaway-Mariano, D., and Holden, H. M. 1998. The three-dimensional structure of 4- hydroxybenzoyl-CoA thioesterase from *Pseudomonas* sp. Strain CBS-3. *Journal of Biological Chemistry*. 273: 33572-22579.

15. Benveniste, I., Tijet, N., Adas, F., Philipps, G., Salaün, J.P. and Durst, F. 1998. CYP86A1 from *Arabidopsis thaliana* encodes a cytochrome P450-dependent fatty acid omega-hydroxylase. *Biochemical and Biophysical Research Communications*. 243: 688-693.

16. Benveniste, I., Saito, T., Wang, Y., Kandel, S., Huang, H., Pinot, F., Kahn, R. A., Salaün, J.P., and Shimoji, M. 2006. Evolutionary relationship and substrate specificity of *Arabidopsis thaliana* fatty acid omega-hydroxylase. *Plant Science*. 170: 326-338.

17. Bernards, M. A. 2002. Demystifying suberin. *Canadian Journal of Botany*. 80: 227-240.

18. Bird, D., Beisson, F., Brigham, A., Shin, J., Greer, S., Jetter, R., Kunst, L., Wu, X., Yephremov, A., and Samuels, L. 2007. Characterization of Arabidopsis ABCG11/WBC11, an ATP binding cassette (ABC) transporter that is required for cuticular lipid secretion. *Plant Journal*. 52: 485-489.

19. Bonaventure, G., Salas, J. J., Pollard, M. R., and Ohlrogge, J. B. 2003. Disruption of the *FATB* gene in *Arabidopsis* demonstrates an essential role of saturated fatty acids in plant growth. *Plant Cell.* 15: 1020-1033.

20. Bonaventure, G., Beisson, F., Ohlrogge, J., and Pollard, M. 2004. Analysis of the aliphatic monomer composition of polyesters associated with *Arabidopsis* epidermis: occurrence of octadeca-cis-6, cis-9-diene-1, 18-dioate as the major component. *The Plant Journal.* 40: 920-930.

21. Broun P, Poindexter P, Osborne E, Jiang C-Z and Riechmann JL. 2004. WIN1, a transcriptional activator of epidermal wax accumulation in Arabidopsis. *Proceedings of the National Academy of Sciences of the United States of America.* 101: 4706–4711.

22. Buchanan, B. B., Gruissem, W., and Jones, R. 2000. Lipids. In *Biochemistry and Molecular Biology of Plants.* American Society of Plant Biologists. 456-527.

23. Cantu, D. C., Chen, Y., and Reilly, P. J. 2010a. ThYme: A database for thioester-active enzymes. *Nucleic Acids Research.* doi: 10.1093/nar/gkq1072.

24. Cantu, D. C., Chen, Y., and Reilly, P. J. 2010b. Thioesterases: A new perspective based on their primary and tertiary structures. *Protein Science.* 19: 1281-1295.

25. Cheesborough, T. M. and Kolattukudy, P. E. 1984. Alkane biosynthesis by decarbonylation of aldehydes catalyzed by a particulate preparation from *Pisum sativum*. *Proceedings of the National Academy of Sciences.* 81: 6613-6617.

26. Chen, X., Goodwin, S. M., Boroff, V. L., Liu, X., and Jenks, M. A. 2003. Cloning and characterization of the *WAX2* gene of *Arabidopsis* involved in cuticle membrane and wax production. *Plant Cell.* 15: 1170-1185.

27. Coen, E. S., Romero, J. M., Doyle, S., Elliot, R., Murphy, G., and Carpenter, R. 1990. *Floricaula*: A homeotic gene required for flower development in *Antirrhinum majus*. *Cell.* 63: 1311-1322.

28. Compagnon, V., Diehl, P., Benveniste, I., Meyer, D., Schaller, H., Schreiber, L, Franke, R., and Pinot, F. 2009. CYP86B1 Is Required for Very Long Chain ω-Hydroxyacid and α,ω-Dicarboxylic Acid Synthesis in Root and Seed Suberin Polyester. *Plant Physiology*. 150: 1831-1843.

29. Debono, A., Yeats, T. H., Rose, J. K., Bird, D., Jetter, R., Kunst, L., and Samuels, L. 2009. Arabidopsis LTPG is a glycosylphosphatidylinositol-anchored lipid transfer protein required for export of lipids to the plant surface. *Plant Cell.* 12: 1230-1238.

30. Desvergne, B. and Wahli, W. 1999. Peroxisome proliferator-activated receptors: nuclear control of metabolism. *Endocrine Reviews.* 20: 649-688.

31. Dillon, S. C., and Bateman, A. 2004. The hotdog fold: wrapping up a superfamily of thioesterases and dehydratases. *BMC Bioinformatics*. 5: 109.

32. Doan, T.T., Carlesson, A.S., Hamberg, M., Bülow, L., Stymne, S., & Olsson, P. 2009. Functional expression of five Arabidopsis fatty acyl-CoA reductase genes in Escherichia coli. *Journal of Plant Physiology*. 166: 787-796.

33. Domergue, F., Vishwanath, S. J., Joubès, J., Ono, J., Lee, J. A., Bourdon, M., Alhattab, R., Lowe, C., Pascal, S., Lessire, R., and Rowland O. 2010. Three Arabidopsis fatty acyl-Coenzyme A reductases, FAR1, FAR4, and FAR5, generate primary fatty alcohols associated with suberin deposition. *Plant Physiology*. 153: 1-16.

34. Dominguez, E., Mercado, J.A., Quesada, M.A., and Heredia, A. 1999. Pollen sporopollenin: degradation and structural elucidation. *Sexual Plant Reproduction.* 12: 171-178.

35. Elholm, M., Dam, I., Jorgensen, C., Krogsdam, A-M., Holst, D., Kratchmarova, I., Gottlicher, M., Berge, R., Flatmark, T., Knudsen, J., Mandrup, S., and Kristiansen, K. 2001. Acyl-CoA esters antagonize the effects of ligands on peroxisome proliferator-activated receptor α conformation, DNA binding, and interactions with Co-factors. *The Journal of Biological Chemistry.* 276: 21410-21416.

36. Ellman, G. L. 1958. A colorimetric method for determining low concentrations of mercatans. *Archives Biochemistry and Biophysics.* 75: 443-450.

37. Fehling, E., and Mukherjii, K. D. 1991. Acyl-CoA enlongase from a higher plant (*Lunaria annua*): metabolic intermediates of very-long-chain acyl-CoA products and substrate specificity. *Biochimica et Biophysica Acta.* 1082: 239-246.

38. Fiebig, A., Mayfield, J. A., Miley, N. L., Chau, S., Fischer, R. L., and Preuss, D. 2000. Alterations in *CER6*, a gene identical to *CUT1*, differentially affect long-chain lipid content on the surface of pollen and stems. *Plant Cell.* 12: 2001-2008.

39. Franke, R., Briesen, I., Wojciechowski, T., Faust, A., Yephremov, A., Nawrath, C., and Schreiber, L. 2005. Apoplastic polyesters in *Arabidopsis* surface tissues-A typical suberin and a particular cutin. *Phytochemistry.* 66: 2643-2658.

40. Franke, R. and Schreiber, L. 2007. Suberin-a biopolyester forming apoplastic plant interfaces. *Current Opinion in Plant Biology.* 10: 252-259.

41. Franke, R., Höfer, R., Briesen, I., Emsermann, M., Efremova, N., Yphremov, A., and Schreiber, L. 2009. The DAISY gene from *Arabidopsis* encodes a fatty acid

elongase condensing enzyme involved in the biosynthesis of aliphatic suberin in roots and the chalaza-micropyle region of seeds. *Plant Journal.* 57: 80-95.

42. Fridman, E., Wang, J., Iijima, Y., Froehlich, J. E., Gang, D. R., Ohlrogge, J., and Pichersky, E. 2005. Metabolic, genomic, and biochemical analyses of glandular trichomes from the wild tomato species *Lycopersicon hirsutum* identify a key enzyme in the biosynthesis of methylketones. *The Plant Cell.* 17: 1252-1267.
43. Fujita, Y., Matsuoka, H., and Hirooka, K. 2007. Regulation of fatty acid metabolism in bacteria. *Molecular Microbiology.* 66: 829-839.
44. Gao, J., Ajjawi, I., Manoli, A., Sawin, A., Xu, C., Froehlich, J.E., Last, R.L., and Benning, C. 2009. FATTY ACID DESATURASE4 of Arabidopsis encodes a protein distinct from characterized fatty acid desaturases. *Plant Journal.* 60: 832–839.
45. Graça, J. and Santos, S. 2007. Suberin: A Biopolyester of Plant's Skin. *Macromolecular Bioscience.* 7: 128-135.
46. Graça, J., and Lamosa, P. 2010. Linear and branched poly(ω-hydroxyacid) esters in plant cutins. *Journal of Agricultural and Food Chemistry.* 58: 9666-9674.
47. Greer, S., Wen, M., Bird, D., Wu, X., Samuels, L., Kunst, L., and Jetter, R. 2007. The cytochrome P450 enzyme CYP96A15 is the midchain alkane hydroxylase responsible for formation of secondary alcohols and ketones in stem cuticular wax of *Arabidopsis*. *Plant Physiology.* 145: 653-667.
48. Guilford, W. J., Schneider, D. M., Labovitz, J., and Opella, S. J. 1988. High resolution solid state ^{13}C NMR spectroscopy of Sporopollenins from different plant taxa. *Plant Physiology.* 86: 134-136.

49. Hannoufa, A., McNevin, J., and Lemieux, B. 1993. Epicuticular waxes of *eceriferum* mutants of *Arabidopsis thaliana*. *Phytochemistry*. 33: 851-855.

50. Hartmann, K., Peiter, E., Koch, K., Schubert, S., and Schreiber, L. Chemical composition and ultrastructure of broad bean (*Vicia faba* L.) nodule endodermis in comparison to the root endodermis. *Planta*. 215: 14-25.

51. Heckman, K.L. and Pease, L.R. 2007. Gene splicing and mutagenesis by PCR-driven overlap extension. *Nature Protocols*. 2: 924-932

52. Heredia, A. 2003. Biophysical and Biochemical characteristics of cutin, a plant barrier biopolymer. *Biochemcia et Biophysica Acta*. 1620: 1-7.

53. Hertz, R., Magehheim, J., Berman, I., and Bar-Tana, J. 1998. Fatty acyl-CoA thioesters are ligands of hepatic nuclear factor-4alpha. *Nature*. 392: 512-516.

54. Höfer, R., Briesen, I., Beck, M., Pinot, F., Schreiber, L., and Franke, R. 2008. The *Arabidopsis* cytochrome P450 CYP86A1 encodes a fatty acid omega-hydroxylase involved in suberin monomer biosynthesis. *Journal of Experimental Botany*. 59: 2347-2360.

55. Hooker, T. S., Miller, A. A., and Kunst., L. 2002. Significance of the expression of the CER6 condensing enzyme for cuticular wax production in Arabidopsis. *Plant Physiology*. 129: 1568-1580.

56. Hooker, T. S., Lam, P., Zheng, H., and Kunst, L. 2007. A core subunit of the RNA-processing/degrading exosome specifically influences cuticular wax biosynthesis in Arabidopsis. *Plant Cell*. 19: 904-913.

57. Hsieh, K., and Huang, A.H.C. 2007. Tapetosomes in *Brassica* tapetum accumulate endoplasmic reticulum-derived flavonoids and alkanes for delivery to the pollen surface. *The Plant Cell.* 19: 582-596.

58. Huijser, P., Klein, J., Lonnig, W. E., Meijer, H., Saedler, H., and Sommer, H. 1992. Bracteomania, an inflorescence anomaly, is caused by the loss of function of the MADS-box gene saquamosa in Antirrhinum majus. 1992. *EMBO.* 11: 1239-1249.

59. Hunt, M. C. and Alexson, S. E. 2002. The role Acyl-CoA thioesterases play in mediating intracellular lipid metabolism. *Progress in Lipid Research.* 41: 99-130.

60. Javelle, M., Vernoud, V., Depège-Fargeix, N., Arnould, C., Oursel, D., Domergue, F., Sarda, X., and Rogowsky, P. M. 2010. Over-expression of the epidermis-specific HD-ZIP IV transcription factor OCL1 in maize identified target genes involved in lipid metabolism and cuticle biosynthesis. *Plant Physiology.* 154: 273-286.

61. Jenks, M.A., Joly, R.J., Peters, P.J., Rich, P.J., Axtell, J.D., and Ashworth, E.A. 1994. Chemically induced cuticle mutation affecting epidermal conductance to water vapor and disease susceptibility in *Sorghum bicolor* (L.) Moench. *Plant Physiology.* 105: 1239-1245.

62. Jenks, M. A., Tuttle, H. A., Eigenbrode, S. D., and Feldmann, K. A. 1995. Leaf epicuticular waxes of the *Eceriferum* mutants in *Arabidopsis*. *Plant Physiology.* 108: 369-377.

63. Jones, J. M. and Gould, S. J. 2000. Identification of PTE2, a human peroxisomal long-chain acyl-CoA thioesterase. *Biochemical and Biophysical Research Communications.* 275: 233-240.

64. Kannangara, R., Branigan, C., Liu, Y., Penfield, T., Rao, V., Mouille, G., Höfte, H., Pauly, M., Riechmann, J. L., and Broun, P. 2007. The transcription factor WIN1/SHN1 regulates Cutin biosynthesis in *Arabidopsis thaliana*. *Plant Cell.* 19:1278-1294.

65. Keller, H., Dryer, C., Medin, J., Mahfoudi, A., Ozato, K., and Wahli, W. 1992. Fatty acids and retinoids control lipid metabolism through activation of peroxisome poliferator-activated receptor-retinoid X receptor heterodimers. *Proceedings of the National Academy of Sciences of the United States of America.* 90: 2160-2164.

66. Kerstiens, G. 1996. Signaling across the divide: a wider perspective of cuticular structure-function relationships. *Trends in Plant Science.* 1: 125-129.

67. Kiefer, F., Arnold, K., Künzli, M., Bordoli, L., and Schwede, T. 2009. The SWISS-MODEL Repository and associated resources. *Nucleic Acids Research.* 37: D387-392.

68. Kotaka, M., Kong, R., Wureshi, I., Ho, Q. S., Sun, H., Liew, C. W., Goh, L. P., Cheung, P., Mu, Y., Lescar, J., and Liang, Z-X. 2009. Structure and catalytic mechanism of the thioesterase CalE7 in Enediyne Biosynthesis. *The Journal of Biological Chemistry.* 284: 15739-15749.

69. Kolattukudy PE. 1987. Lipid-derived defensive polymers and waxes and their role in plant-microbe interaction. In *The Biochemistry of Plants,* ed. PK Stumpf, EE Conn, 9:291–314. New York: Academic.

70. Krauss P, Markstädter C and Riederer M. 1997. Attenuation of UV radiation by plant cuticles from woody species. *Plant, Cell and Environment.* 20: 1079-1085.

71. Kunst, L., and Samuels, A.L. 2003. Biosynthesis and secretion of plant cuticular wax. *Progress in Lipid Research*. 42: 51-80.

72. Kurata, T., Kawabata-Awai, C., Sakuradani, E., Shimizu, S., Okada, K., and Wada, T. 2003. The *YORE-YORE* gene regulates multiple aspects of epidermal cell differentiation in *Arabidopsis*. *Plant Journal*. 36: 55-66.

73. Lai, C., Kunst, L., and Jetter, R. 2007. Composition of alkyl esters in the cuticular wax on inflorescence stems of *Arabidopsis thaliana cer* mutants. *Plant Journal*. 50: 189-196.

74. Larkin, M. A., Blackshields, G., Brown, N. P., Chenna, R., McGettigan, P. A., McWilliams, H., Valentin, F., Wallace, I. M., Wilm, A., Lopez, R., Thompson, J. D., Gibson, T. J., and Higgins, D. G. 2007. ClustalW and ClustalX version 2. *Bioinformatics*. 23: 2947-2948.

75. Lee, S. B., Jung, S. J., Go, Y. S., Kim, H. U., Cho, H. J., Park, O. K., and Suh, M. C. 2009. The Arabidopsis 3-ketoacyl CoA synthase genes, KCS20 and KCS2/DAISY, are functionally redundant in cuticular wax and root suberin biosynthesis, but differentially controlled by osmotic stress. *Plant Journal*. 60: 462-475.

76. Lee, S. B., Go, Y. S., Bae, H. J., Park, J. H., Cho, S. H., Cho, H. J., Lee, D. S., Park, O. K., Hwang, I., and Suh, M. C. 2009. Disruption of glycosylphosphatidylinositol-anchored lipid transfer protein gene altered cuticular lipid composition, increased plastoglobules, and enhanced susceptibility to infection by the fungal pathogen *Alternaria brassicicola*. *Plant Physiology*. 150: 42-54.

77. Leesong, M, Henderson, B. S., Gilling, J. R., Schwab, J. M., and Smith, J. L. 1996. Structure of a dehydratase-isomerase from the bacterial pathway for biosynthesis of unsaturated fatty acids: two catalytic activities in one active site. *Structure*. 4: 253-264.

78. Li, F., Wu, X., Lam, P., Bird, D., Zheng, H., Samuels, L., Jetter, R., and Kunst, L. 2008. Identification of the wax ester synthase/acyl-coenzyme A: diacylglycerol acyltransferase WSD1 required for stem wax ester biosynthesis in *Arabidopsis*. *Plant Physiology*. 148: 97-107.

79. Li, Y., Beisson, F., Koo, A. J., Molina, I., Pollard, M., and Ohlrogge, J. 2007. Identification of acyltransferases required for cutin biosynthesis and production of cutin with suberin-like monomers. *Proceedings of the National Academy of Sciences of the United States of America*. 104: 18339-18244.

80. Li, Y.H., Beisson, F., Ohlrogge, J., and Pollard, M. 2007b. Monoacylglycerols are components of root waxes and can be produced in the aerial cuticle by ectopic expression of a suberin-associated acyltransferase. *Plant Physiology*. 144: 1267–1277.

81. Li-Beisson, Y., Shorrosh, B., Beisson, F., Andersson, M. X., Arondel, V., Bates, P. D., Baud, S., Bird, D., Debono, A., Durrett, T. P., Franke, R. B., Graham, I. A., Katayama, K., Kelly, A. A., Larson, T., Markham, J. E., Miquel, M., Molina, I., Nishida, I., Rowland, O., Samuels, L., Schmid, K. M., wada, H., Welti, R., Xu, C., Zallot, R., and Ohlrogge, J. 2010. Acyl-Lipid Metabolism. In *The Arabidopsis book*. American Society of Plant Biologists. 1-65.

82. Li-Beisson, Y., Pollard, M., Sauveplane, V., Pinot, F., Ohlrogge, J., and Beisson, F. 2010. Nanoridges that characterize the surface morphology of flowers require the synthesis of cutin polyester. *Proceedings of the National Academy of Sciences of the United States of America.* 106: 22008-22013.

83. Lippold, F., Sanchez, D. H., Musialak, M., Schlereth, A., Scheible, W. R., Hincha, D. K., and Udvardi, M.K. 2009. AtMyb41 regulates transcriptional and metabolic responses to osmotic stress in Arabidopsis. *Plant Physiology.* 149: 1761-1772.

84. Liu, D. and Post-Beittenmiller, D. 1995. Discovery of an epidermal stearoyl-acyl carrier protein thioesterase. Its potential role in wax biosynthesis. *The Journal of Biological Chemistry.* 270: 16962-16969.

85. Lopes, M.H., Gil, A.M., Silvestre, A.J.D., and Neto, C.P. 2000. Composition of suberin extracted upon gradual alkaline methanolysis of *Quercus suber* L. cork. *Journal of Agricultural and Food Chemistry.* 48: 383-391.

86. Lü, S., Song, T., Kosma, D. K., Parsons, E. P., Rowland, O., and Jenks, M. A. 2009. Arabidopsis *CER8* encodes LONG-CHAIN ACYL-COA SYNTHETASE 1 (LACS1) that has overlapping functions with LACS2 in plant wax and cutin synthesis. *Plant Journal.* 59: 553-564.

87. Lu, J. Y., Verkruyse, L. A., and Hofmann, S. L. 1996. Lipid thioesters derived from acylated proteins accumulate in infantile neuronal ceroid lipofuscinosis: correction of the defect in lymphoblasts by recombinat palmitoyl-protein thioesterase. *Proceedings of the National Academy of Sciences of the United States of America.* 93: 10046-10050.

88. Luo, B., Xue, X. Y., Hu, W. L., Wang, L. J., and Chen, X. Y. 2007. An ABC transporter gene of *Arabidopsis thaliana*, AtWBC11, is involved in cuticle development and prevention of organ fusion. *Plant and Cell Physiology.* 48: 1790-1802.

89. Marchler-Bauer, A, Anderson, J. B., Chitsaz, F., Derbyshire, M. K, DeWeese-Scott, C., Fong, J. H., Geer, L. Y., Geer, R. C., Gonzales, N. R., Gwadz, M., He, S., Hurwitz, D. I., Jackson, J. D., Ke, Z., Lanczycki, C. J., Liebert, C. A., Liu, C., Lu, F., Lu, S., Marchler, G. H., Mullokandov, M., Song, J. S., Tasneem, A., Thanki, N., Yamashita, R. A., Zhang, D., Zhang, N., and Bryant, S. H. 2009. CDD: specific function annotation with the Conserved Domain Database. *Nucleic Acids Research.* 37: 205-210.

90. Markstädter, C., Federle, W., Jeter, R., Riederer, M. and Holldobler, B. 2000. Chemical composition of the slippery epicuticular wax blooms on Maca- ranga (Euphorbiaceae) ant-plants. *Chemoecology.* 10: 33–40.

91. Martinez, M.A., Zaballa, M.-E., Schaeffer, F., Bellinzoni, M., Albanesi, D., Schujman, G.E., Vila, A.J., Alzari, P. M., and de Mendoza, D. 2010. A novel role of malonyl-ACP in lipid homeostasis. *Biochemistry.* 49: 3161-3167.

92. Mayer, K. M. and Shanklin, J. 2005. A structural model of the plant acyl-acyl carrier protein thioesterase FatB comprises two helix/4-stranded sheet domains, the N-terminal domain containing residues that affect specificity and the C-terminal domain containing catalytic residues. *Journal of Biological Chemistry.* 280: 3621-3627.

93. Mayer, K. M. and Shanklin, J. 2007. Identification of amino acid residues involved in substrate specificity of plant acyl-ACP thioesterases using a bioinformatics-guided approach. *BMC Plant Biology*. 7: 1.

94. McNevin, J. P., Woodward, W., Hannoufa, A., Feldmann, K. A., and Lemieux, B. 1993. Isolation and characterization of *eceriferum* (*cer*) mutants induced by T-DNA insertions in *Arabidopsis thaliana*. *Genome*. 36: 610-618.

95. Miller, A. A., Clemens, S., Zachgo, S., Giblin, E. M., Taylor, D. C., and Kunst, L. 1999. *CUT1*, an *Arabidopsis* gene required for cuticular wax biosynthesis and pollen fertility, encodes a very-long-chain fatty acid condensing enzyme. *Plant Cell*. 11: 825-838.

96. Miller, A. A., and Kunst, L. 1997. Very-long-chain fatty acid biosynthesis is controlled through the expression and specificity of the condensing enzyme. *The Plant Journal*. 12: 121-131.

97. Molina, I., Li-Beisson, Y., Beisson, F., Ohlrogge, J. B., and Pollard, M. 2009. Identification of an *Arabidopsis* feruloyl-coenzyme A transferase required for suberin biosynthesis. *Plant Physiology*. 151: 1317-1328.

98. Murakami, K., Ide, T., Nakazawa, T., Okazaki, T., Mochizuki, T., and Kadowaki, T. 2001. Fatty-acyl-CoA thioesters inhibit recruitment of steroid receptor co-activator 1 to α and γ isoforms of peroxisome-proliferator-activated receptors by competing with agonists. *Biochemical Journal*. 353: 231-238.

99. Nardini, M. and Dijkstra, B. W. 1999. α/β hydrolase fold enzymes: the family keeps growing. *Current Opinion in Structural Biology*. 9: 732-737.

100. Neal, A.L., Weinstock, J.O., and Lampen, J.O. 1965. Mechanisms of fatty acid toxicity for yeast. *Journal of Bacteriology*. 90: 126-131.

101. Negruk, V., Yang, P., Subramanian, M., McNevin, J. P., and Lemieux, B. 1996. Molecular cloning and characterization of the *CER2* gene of *Arabidopsis thaliana*. *Plant Journal*. 9: 137-145.

102. Ohlrogge, J.B. and Jaworski, J.G. 1997. Regulation of fatty acid synthesis. *Annual Review of Plant Physiology and Plant Molecular Biology*. 48: 109-136.

103. Ollis, D. L., Cheah, E. Cygler, M., Dijkstra, B., Frolow, F., Franken, S. M., Harel, M., Remington, S. J., Silman, I., Schrag, J., Sussman, J. L., Verschueren, K. H. G., and Goldman, A. 1992. The α/β hydrolase fold. *Protein Engineering*. 5: 197-211.

104. Ossowski, S., Fitz, J., Schwab, R., Riester, M., and Weigel, D. 2005. Personal communication. WMD2-Web MicroRNA Designer. http://wmd2.weigelworld.org.

105. Ossowski , S., Schwab, R., and Weigel, D. 2008. Gene silencing in plants using artificial microRNAs and other small RNAs. *The Plant Journal*. 53: 674-690.

106. Overath, P., Pauli, G., and Schairer, H. U. 1969. Fatty acid degradation in Escherichia coli. An inducible acyl-CoA synthetase, the mapping of old-mutations, and the isolation of regulatory mutants. *European Journal of Biochemistry*. 7: 559 – 574.

107. Panikashvili, D., Savaldi-Goldstein, S., Mandel, T., Yifhar, T., Franke, R. B., Höfer, R., Schreiber, L., Chory, J., and Aharoni, A. 2007. The Arabidopsis DESPERADO/AtWBC11 transporter is required for cutin and wax secretion. *Plant Physiology*. 145: 1345-1360.

108. Panikashvili, D., Shi, J. X., Schreiber, L., and Aharoni, A. 2009. The *Arabidopsis DCR* endoding a soluble BAHD acyltransferase is required for cutin polyester formation and seed hydration properties. *Plant Physiology*. 151: 1773-1789.

109. Peitsch, M. C. 1995. Protein modeling by E-mail. *Bio/Technology*. 13: 658-660.

110. Perera, M., Qin, W., Yandeau-Nelson, M., Fan, L., Dixon, P., and Nikolau, B.J. 2010. Biological origins of normal-chain hydrocarbons: a pathway model based on cuticular wax analyses of maize silks. *The Plant Journal*. 64: 618-632.

111. Pidugu, L. S., Maity, K., Ramaswamy, K., Surolia, N., and Suguna, K. Analysis of proteins with the 'hot dog' fold: prediction of function and identification of catalytic residues of hypothetical proteins. *BMC Structural Biology*. 9: 37.

112. Piffanelli, P., Ross, J. H. E., and Murphy, D. J. 1998. Biogenesis and function of the lipidic structures of pollen grains. *Sexual Plant Reproduction*. 11: 65-80.

113. Pighin, J. A., Zheng, H., Balakshin, L. J., Goodman, I. P., Western, T. L., Jetter, R., Kunst, L., and Samuels, A. L. 2004. Plant cuticular lipid export requires an ABC transporter. *Science*. 306: 702-704.

114. Pollard, M., Beisson, F., Li, Y., and Ohlrogge, J. B. 2008. Building lipid barriers: biosynthesis of cutin and suberin. *Trends in Plant Science*. 13: 236-246.

115. Post-Beittenmiller, D. 1996. Biochemistry and molecular biology of wax production in plants. *Annual Review of Plant Physiology and Plant Molecular Biology*. 47: 405-430.

116. Raffaele, S., Vailleau, F., Léger, A., Joubès, J., Miersch, O., Huard, C., Blée, E., Mongrand, S., Domergue, F., and Roby, D. 2008. A MYB transcription factor

regulates very-long-chain fatty acid biosynthesis for activation of the hypersensitive cell death response in *Arabidopsis*. *Plant Cell*. 20: 752-567.

117. Rashotte, A. M. Jenks, M. A., and Feldmann, K. A. 2001. Cuticular waxes on eceriferum mutants of *Arabidopsis thaliana*. *Phytochemistry*. 57: 115-123.

118. Rashotte, A. M., Jenks, M. A., Ross, A. S., and Feldmann, K. A. 2004. Novel *eceriferum* mutants in *Arabidopsis thaliana*. *Planta*. 219: 5-13.

119. Ray AK, Chen Z, and Stark RE. 1998. Chemical depolymerization studies of the molecular architecture of lime fruit cuticle. *Phytochemistry*. 49: 65-70.

120. Ray AK and Stark RE. 1998. Isolation and molecular structure of an oligomer produced enzymatically from the cuticle of lime fruit. *Phytochemistry*. 48: 1313-1320.

121. Riederer, M. and Schreiber, L. 2001. Protecting against water loss: analysis of the barrier properties of plant cuticles. *Journal of Experimental Botany*. 52: 2023-2032.

122. Rowland, O., Zheng, H., Hepworth, S. R., Lam, P., Jetter, R., and Kunst, L. 2006. *CER4* encodes an alcohol-forming fatty acyl-Coenzyme A reductases involved in cuticular wax production in *Arabidopsis*. *Plant Physiology*. 142: 866-877.

123. Rowland, O., Lee, R., Franke, R., Schreiber, L., and Kunst, L. 2007. The *cer3* wax biosynthetic gene from *Arabidopsis thaliana* is allelic to *WAX2/YRE/FLP1*. *FEBS Letters*. 581: 3538-3544.

124. Salas, J. J. and Ohlrogge, J. B. 2002. Characterization of substrate specificity of plant FatA and FatB acyl-ACP thioesterases. *Archives of Biochemistry and Biophysics*. 403: 25-34.

125. Samach, A., Kohalmi, S. E., Motte, P., Datla, R., and Haughn, G. W. 1997. Divergence of function and regulation of class B floral organ identity genes. *The Plant Cell*. 9: 559-570.

126. Samuels, L., Kunst, L., and Jetter, R. 2008. Sealing Plant Surfaces: Cuticular Wax Formation by Epidermal Cells. *Annual Review of Plant Biology*. 59: 683-707.

127. Schirmer, A., Rude, M. A., Li, X., Popova, E., and del Cardayre, S. B. 2010. Microbial biosynthesis of alkanes. *Science*. 329: 559-562.

128. Schleberger, C., Sachelaru, P., Brandsch, R., and Schulz, G. E. 2007. Structure and action of a C-C bond cleaving alpha/beta-hydrolase involved in nicotine degradation. *Journal of Molecular Biology*. 367: 409-418.

129. Schmid, M., Davison, T. S., Henz, S. R., Pape, U.J., Demar, M., Vingron, M., Schölkopf, B., Weigel, D., and Lohmann, J. U. 2005. A gene expression map of *Arabidopsis thaliana* development. *Nature Genetics*. 37: 501-506.

130. Schneider-Belhaddad and Kolattukudy, P. 2000. Solubilization, Partial Purification, and Characterization of a Fatty Aldehyde Decarbonylase from a Higher Plant, *Pisum sativum*. *Archives of Biochemistry and Biophysics*. 377: 341-349.

131. Schnurr, J., Shockey, J.M., de Boer, G.-J., and Browse, J. 2002. Fatty acid export from the chloroplast. Molecular characterization of a major plastidial acyl-coenzyme A synthetase from *Arabidopsis*. *Plant Physiology*. 129: 1700-1709.

132. Schnurr, J., Shockey, J., and Browse, J. 2004. The acyl-CoA synthetase encoded by LACS2 is essential for normal cuticle development in Arabidopsis. *Plant Cell*. 16: 629-642.

133. Schujman, G. E., Guerin, M., Buschiazzo, A., Schaeffer, F., Llarrull, L. I., Reh, G., Vila, A. J., Pedro, M. A., and de Mendoza, D. 2006. Structural basis of lipid biosynthesis regulation in gram-positive bacteria. *The EMBO Journal*. 25: 4074-4083.

134. Shockey, J. M., Fulda, M. S., and Browse, J. A. 2002. Arabidopsis contains nine long-chain acyl-coenzyme A synthetase genes that participate in fatty acid and glycerolipid metabolism. *Plant Physiology*. 129: 1710-1722.

135. Sieber, P., Schorderet, M., Ryser, U., Buchala, A., Kolattukudy, P., Metraux, J.-P., and Nawrath, C. 2000. Transgenic *Arabidopsis* plants expressing a fungal cutinase show alterations in the structure and properties of the cuticle and postgenital organ fusions. *Plant Cell*. 12: 721-738.

136. Somerville, S. C. and Ogren, W. L. 1982. Isolation of photorespiratory mutants of *Arabidopsis*. *In* RB Hallick, NH Chua, eds, Methods in Chloroplast Molecular Biology. Elsevier, New York, 129-139.

137. Suh, M. C., Samuels, L., Jetter, R., Kunst, L., Pollard, M., Ohlrogge, J., and Beisson, F. 2005. Cuticular lipid composition, surface structure, and gene expression in *Arabidopsis* stem epidermis. *Plant Physiology*. 139: 1649-1665

138. Thoden, J. B., Zhuang, Z., Dunaway-Mariano, D., and Holden, H.M. 2003. The structure of 4-hydroxybenzoyl-CoA thioesterase from Arthrobacter sp. strain SU. *Journal of Biological Chemistry*. 278: 43709-43716.

139. Tilton, G.B., Shockey, J.M., and Browse, J. 2004. Biochemical and molecular characterization of ACH2, an acyl-CoA thioesterase from *Arabidopsis thaliana*. *The Journal of Biological Chemistry*. 279: 7487-7494.

140. Todd, J., Post-Beittenmiller, D., and Jaworski, J. G. 1999. KCS1 encodes a fatty acid elongase 3-ketoacyl-CoA synthase affecting wax biosynthesis in *Arabidopsis thaliana*. *Plant Journal*. 17: 119-130.

141. Toufighi, K., Brady, S. M., Autsin, R., Ly, E., and Provart, N. J. 2005. The botany array resource: e-Northerns, expression angling and promoter analyses. *The Plant Journal*. 43: 153-163.

142. Vioque, J. and Kolattukudy, P. E. 1997. Resolution and purification of an aldehyde-generating and an alcohol-generating fatty acyl-coA reductase from Pea Leaves (*Pisum sativum* L.). *Archives of biochemistry and biophysics*. 340: 64-72.

143. von Wettstein-Knowles P. 1982. Elongase and epicuticular wax biosynthesis. *Physiologie Végétale*. 20: 797–809.

144. Wang, X. and Kolattukudy, P. E. 1995. Solubilization and purification of aldehyde-generating fatty acyl-CoA reductase from geen alga *Botryococcus braunii*. *FEBS Letters*. 370: 15-18.

145. Wei, J., Kang, H., and Cohen, D. 2009. Thioesterase superfamily member 2 (Them2)/acyl-CoA thioesterase 13 (Acot13): a homotetrameric hotdog fold thioesterase with selectivity for long-chain fatty acyl-CoAs. *Biochemical Journal*. 421: 311-322.

146. Wellesen, K., Durst, F., Pinot, F., Benveniste, I., Nettesheim, K., Wisman, E., Steiner-Lange, S., Saedler, H., and Yephremov, A. 2001. Functional analysis of the *LACERATA* gene of *Arabidopsis* provides evidence for different roles of fatty acid omega-hydroxylation in development. *Proceedings of the National Academy of Sciences of the United States of America*. 98: 9694-9699.

147. Weng, H., Molina, I., Schockey, J., and Browse, J. 2010. Organ fusion and defective cuticle function in a lacs1lacs2 double mutant of *Arabidopsis*. *Planta*. 231: 1089-1100.

148. Winter, D., Vinegar, B., Nahal, H., Ammar, R., Wilson, G.V. and Provart, N. J. 2007. An "Electronic Fluorescent Pictograph" browser for exploring and analyzing large-scale biological data sets. *PLoS ONE*. 2: e718.

149. Wu, J.T., Chiang, Y.R., Huang, W.Y., and Jan, W.N. 2006. Cytotoxic effects of free fatty acids on phytoplankton algae and cyanobacteria. *Aquatic Toxicology*. 80: 338-345.

150. Xia Y., Nikolau, B. J., and Schnable, P. S. 1996. Cloning and characterization of *CER2*, an *Arabidopsis* gene that affects cuticular wax accumulation. *Plant Cell*. 8: 1291-1304.

151. Xia Y., Nikolau, B. J., and Schnable, P. S. 1997. Developmental and hormonal regulation of the *Arabidopsis* CER2 gene that codes for a nuclear-localized protein required for the normal accumulation of cuticular waxes. *Plant Physiology*. 115: 925-937.

152. Xiao, F., Goodwin, S. M., Xiao, Y., Sun, Z., Baker, D., Tang, X., Jenks, M. A., and Zhou, J-M. 2004. *Arabidopsis* CYB86A2 represses *Pseudomonas syringae* type III genes and is required for cuticle development. *The EMBO Journal*. 23: 2903-2913.

153. Yu, G., Nguyen, T.T.H, Guo, Y., Schauvinhold, I., Auldridge, M.E., Bhuiyn, N., Ben-Israel, I., Iijima, Y., Fridman, E., Noel, J. P., and Pichersky, E. 2010. Enzymatic functions of wild tomato methylketone synthases 1 and 2. *Plant Physiology*. 154: 67-77.

154. Zhang, X., Henriques, R., Lin, S., Niu, Q., and Chua, N. 2006. *Arabidopsis*-mediated transformation of *Arabidopsis thaliana* using the floral dip method. *Nature Protocols*. 1: 641-646.

155. Zhuang, Z., Gartemann, K-H., Eichenlaub, R., and Dunaway-Mariano, D. 2003. Characterization of the 4-hydrozybenzoyl-coenzyme A thioesterase from *Arthrobacter* sp. Strain SU. *Applied and Environmental Microbiology*. 69: 2707-2711.

156. Zhuang, Z., Song, F., Zhao, H., Li, L., Cao, J., Eisenstein, E., Herzberg, O., and Dunaway-Mariano, D. 2008. Divergence of function in the hot dog fold enzyme superfamily: the bacterial thioesterase YciA. *Biochemistry*. 47: 2789-2796.